Understanding the Differential Effects of Dexamethasone on the Metabolism of Healthy and Diseased Articular Cartilage

by

Rebecca M. Black

B.S. Molecular and Cellular Biology
Johns Hopkins University, 2017

Submitted to the Department of Biological Engineering in Partial Fulfillment of the Requirements for the Degree of Doctor of Philosophy in Biological Engineering at the Massachusetts Institute of Technology, May 2022

Author: .....
Rebecca M. Black
Department of Biological Engineering
May 6th, 2022

Certified by: .....
Alan J. Grodzinsky
Professor of Biological, Electrical, and Mechanical Engineering
Thesis Supervisor

Accepted by: .....
Katharina Ribbeck
Professor of Biological Engineering
Graduate Program Committee Chair

Thesis Committee

Alan J. Grodzinsky
Thesis Advisor
Professor of Biological, Electrical, and Mechanical Engineering
Massachusetts Institute of Technology

Dr. Forest M. White
Thesis Committee Chair
Professor of Biological Engineering
Massachusetts Institute of Technology

Dr. Christopher H. Evans
Committee Member
Professor of Orthopedics
Mayo Clinic, Minnesota

Dr. Patrik Önnerfjord
External Reader
Associate Professor of Rheumatology and Molecular Skeletal Biology
Lund University, Lund, Sweden

Understanding the Differential Effects of Dexamethasone on the Metabolism of Healthy and Diseased Articular Cartilage

by

Rebecca M. Black

Submitted to the Department of Biological Engineering on May 6th, 2022
in Partial Fulfillment of the Requirements for the Degree of Doctor of Philosophy
in Biological Engineering at the Massachusetts Institute of Technology

Abstract

The glucocorticoid drug Dexamethasone (Dex) has been proposed as a potential therapeutic to treat or prevent post-traumatic osteoarthritis (PTOA), a disease affecting millions of Americans without a disease-modifying drug. However, current reports on Dex efficacy often disagree on the effects of Dex on cartilage tissue homeostasis.

The first part of this thesis uses proteomic analyses of a bovine *ex vivo* cartilage explant monoculture model of PTOA progression to identify inflammation-induced catabolic processes associated with disease progression that were attenuated by the addition of Dex. Some of the matrix fragments and inflammatory cytokines appear to be novel, promising disease biomarker candidates. Dex had an imperfect rescue effect on the observed dysregulation of anabolic and chondroprotective processes.

The second part of this thesis expands the *ex vivo* cartilage explant monoculture PTOA model to use human donor knee cartilage. Proteins released into the media were clustered by the kinetics of their release over three weeks. This analysis further details the classification of biomarker candidates by their timing of release from cartilage, which was compared to the timing of proteins reported to be in patient synovial fluids after traumatic joint injuries. Experiments here revealed that Dex restored the kinetics of release to many matrix components.

The final part of this work combines both healthy human ankle cartilage and bone in a novel osteochondral PTOA model that incorporates disease-relevant tissue crosstalk. Across seven human donors, proteomic analysis of culture media and cartilage tissue revealed that catabolic disease effects such as matrix breakdown and sGAG loss were attenuated by Dex, as well as the dysregulation of bone metabolism with disease but not Dex treatment. Regression analysis was used to find disease-specific peptide biomarkers by regressing individual peptide abundances against sGAG loss. Regressing protein abundances against Dex rescue effects on sGAG loss then identified an association of pro-inflammatory humoral proteins and apolipoproteins that were associated with lower donor-specific Dex efficacy.

Taken together, these results demonstrate the anti-catabolic effects of Dex in human cartilage and osteochondral PTOA model systems, with only minor off-target effects on anabolic processes and identify methods of better predicting disease and Dex responses.

Thesis Supervisor: Alan J. Grodzinsky
Title: Professor of Biological, Electrical, and Mechanical Engineering

Acknowledgements

It would take this entire thesis to properly thank Alan Grodzinsky for the guidance, support, and fun he has brough to my graduate school journey. There was not a single meeting we had where I didn't leave the room with a smile on my face, excited for my next experiments, no matter what mood I had been in going into his office. He is truly a model for what a scientific and personal mentor should be, and I attribute all of my success to having his kind, unquestionable support behind me every step of the way.

I would like to thank Forest White for being my thesis chair, and for all of his scientific input. From discussing class choices to the nuances of mass spectrometry data, he brought as much levity and laughter with his infectious smile to our conversations as he did scientific insight.

Chris Evans has been a part of our lab's work on Dex for over a decade, and I would like to thank him for being on my thesis committee and all of his invaluable contributions with his clinical perspective.

I would also like to thank Patrik Önnerfjord for graciously hosting me in his lab to learn mass spectrometry techniques and work directly with his lab members on these studies. He has provided countless hours of feedback and guidance that have resulted in several successful papers that have pushed the boundaries of the field, and been a kind and supportive mentor along the way. It is an honor to have him as a collaborator and an external reader on my thesis.

Everyone in the Grodzinsky lab were some of the best coworkers and friends I could have asked for during my scientific journey. Lisa Flaman taught me the basics of human cartilage culture and I have been so lucky to call such a steadfast and thoughtful woman my friend for these past five years. Brianne Connizzo was always a thoughtful ear with whom to troubleshoot difficult experiments and think through the nuances of cellular behavior. Yamini Krishnan and Brett Geiger taught me a variety of skills and were excellent examples of how to put together careful experiments and see projects through to completion. Hannah Szapary has provided so many hours of fun, exciting discussions about science and has been a joy to work with in lab. I would like to thank Garima Dwivedi as well for scientific input and carefully designing such exciting experiments that I am grateful to be a part of. Han-Hwa and Eliot are truly the backbone of the lab, ready to answer any technical question I have and help when things inevitably go wrong. Linda Bragman has been a wonderful resource to work with through any number of logistical questions. My work has built upon work by past and present lab members, and I am so thankful to them all for creating such a supportive, collaborative, and thoughtful space in which to pursue the cutting edge of orthopedic research.

I would like to thank everyone I worked with during my time at Lund University, particularly Elin Folkesson, Martin Rydén, Staffan Larsson, Karin Lindblom, and André Struglics. You welcomed an American tourist with open arms and taught me so much, not only about the research you do, but about Sweden and its culture. I felt so welcomed my entire visit, and it was a pleasure to work beside you in lab.

It was amazing to find a PhD program that brought me close to home, and I would like to thank my parents and sibling for the unconditional love and support they have brought over the last five years. The world has changed so much and grad school is always full of unique stresses, but home has always been a place of comfort to settle and relax.

To my best friends, Sydney and Alli, and the rest of our quarantine pod – Yash, Jake, Jeremiah, Josh, and Allegra – I have been so lucky to have friends like you by my side to lift me up and stand by me. Your love and support means the world to me, in ways I will never truly be able to thank you for. There are so many other friends who have been part of my journey in our Biological Engineering department as well as outside of MIT – Bianca, Jelle, Krista, Blake, Mike, Anna, Diana, Willie, Caitlin, Wilhelm, Thomas, and so many more – you have brought so much joy and happiness to my life, and every brunch and coffee and evening of laughter we spent together has been so precious to me.

I would like to dedicate this thesis to Ella Mae Bosse Borgstedte and Elizabeth Mildred Sackmann Black. They believed in the value of women in higher education long before it was the norm, and the legacy they left behind is an inspiration to this day.

Table of Contents

List of Figures and Tables

Chapter 1. Introduction

1.1 The case for corticosteroids

Glucocorticoids (GCs), a family of steroid hormones, have been used since the 1950s for treating pain and inflammation in both rheumatoid arthritis (RA) and osteoarthritis (OA), diseases associated with cartilage degeneration and joint inflammation [1,2]. In the early twentieth century, new treatments for RA using extracts of animal adrenal cortical tissue led to the need for greater quantities of synthetic steroids. By the 1960s, rapid advances in chemical synthesis of GCs resulted first in synthetic cortisone, then hydrocortisone, fluorohydrocortisone, prednisone, prednisolone, triamcinolone, methylprednisolone and, finally, dexamethasone, the latter acknowledged to be the most potent member of the GC family [3].

Although the beneficial effects of GCs are now cited as well-known and accepted, there remains much controversy in the field about their prescription for patients. Harmful side effects from systemic delivery of GCs were recognized early on, leading to the pioneering development of intra-articular (i.a.) injection for steroid therapy in the 1950s [4]. However, even with i.a. delivery of GCs, their mechanism of action in both diseased and healthy joints is not well understood. GCs can affect a variety of cellular pathways, suppressing inflammation with sometimes-unknown off-target effects [5]. Even among the most recent clinical trials, there are conflicting results over their safety and efficacy, often due to low-quality evidence on their effects or different methodologies used [6,7].

The greatest concern over GCs in the context of arthritis treatment is their potential for catabolic effects on cartilage. While several clinical studies show significant short-term reduction in pain

after treatment with GCs, others reveal that with repeated i.a. injections at typically high clinical doses, GCs can lose their analgesic effects [6,8,9]. In addition, a recent report suggested that repeated i.a. injections every 3 months over a 2-year period caused certain macroscopic changes in cartilage, e.g., a loss of knee cartilage volume and thickness as measured by MRI [10]. Animal and in vitro studies have also raised critically important issues regarding dose and duration of repeated injections. The oft-cited study of Mankin *et al.* reported a significant loss of cartilage sGAG and suppressed matrix biosynthesis following daily intramuscular injections of cortisone into rabbits at 4.5 mg/kg over a 9-week study duration [11]. In contrast, Gibson *et al.* injected prednisolone (3.5 mg/kg) into mature monkey knees only once, twice or six times over a 12-week period and reported essentially no changes in injected knees compared to controls, and Samuels *et al.* surveyed many studies and found no evidence that GCs accelerate joint deterioration [7,12]. Was the difference in cartilage response associated with the animal species, dose, number of injections, or choice of GC? Even after so many decades of clinical use of GCs, questions remain as to what mechanisms GCs act on cartilage and surrounding joint tissues, and under what dosing regimens GCs remain safe for patient use [8,13].

While the most commonly used GCs today include prednisolone, triamcinolone, betamethasone and dexamethasone, they are reported to have differential effectiveness at different doses from one another, further complicating our ability to compare and interpret treatment protocols and mechanisms of action. Therefore, for the purposes of this thesis, we will focus on the effects of only one member of the GC family, dexamethasone (Dex). This narrower focus enables a comparison of studies on the effects of a single GC across different biological systems, from isolated cells to intact organ culture explants, animal studies *in vivo*, and human clinical trials.

The controversy over Dex begins at the level of clinical trials. Two recent trials studying changes in pain post-knee arthroplasty surgery used the same Dex dose, but only one found a significant reduction in pain after Dex administration [14,15]. Unlike other GCs, no clinical trial has been completed that assesses the effects of Dex on cartilage structure or function; however, several recent studies have shown that Dex may have chondroprotective effects on cartilage in the context of post-traumatic osteoarthritis (PTOA) using *in vitro* human cartilage explant models [16–18]. These results present the possibility of repurposing and using Dex as a disease-modifying drug (DMOAD) in contexts such as PTOA, where the anti-inflammatory and chondroprotective effects of Dex may prevent the progression of the disease. However, more studies must be done to clarify the timing and dosage appropriate to obtain these effects *in vivo*.

While these possibilities are exciting, caution must be taken until possible chondrotoxic effects of Dex are better understood. Several studies using healthy human chondrocytes report that even low doses of Dex cause cell death and reduce cell proliferation, suggesting potential cytotoxic and catabolic side effects. However, the observed effects of Dex depends greatly on dose, model, duration of treatment and context (e.g., isolated cells versus intact cartilage). Thus, study conclusions often differ greatly, complicating the discussion of the safety and efficacy of this drug. It is particularly important to understand appropriate use in human disease due to the variety of reported side effects of GC treatment, including hypertension, adrenal gland suppression, psychological disturbances, Cushing's syndrome, osteoporosis, and susceptibility to infections as a result of immunosuppression [19,20].

1.2 Dex and animal models of arthritis

Studies in animals, summarized in **Table 1.1**, suggest promise for Dex as a potent preventative measure against arthritis progression but, conversely, suggest that it may damage healthy cartilage at certain doses and durations. In a collagen-induced mouse model of RA, Rauchhaus *et al*. found that daily intravenous injections of free Dex at a concentration 1.6 mg/kg, or a single injection of liposomal-encapsulated Dex from 0.4 to 4 mg/kg, both reduced the frequency of arthritis occurrence and lowered its severity [21]. However, the persistent anti-inflammatory effects gained by single-dose liposomal encapsulation hint at the importance of drug delivery. Islander *et al.* used a mouse postmenopausal OA model and found that daily 125 μg intraperitoneal injections of Dex protected against arthritis and joint destruction [22]. In two rat meniscal transection OA models, one using daily oral gavage treatments with Dex at 0.1 mg/kg starting 11 days after surgery and another with weekly 20 μg i.a. injection of Dex, treatment decreased animal pain response in the affected paw, lowered inflammatory signaling and macrophage infiltration, and partially rescued proteoglycan (PG) loss in the joint cartilage [23,24]. A similar rat study using adjuvant-induced arthritis (AA) treated with 0.15 mg/kg daily Dex via oral gavage starting 13 days after AA induction found less swelling in the paws of rats treated with Dex [25]. This same study showed that there was also a significant overlap in genes downstream of inflammatory mediators regulated by Dex and the network of genes affected by the development of AA, but did not explore the identity of these genes or how they may provide protection to cartilage. Daily treatment with a lower dose of Dex injected intraperitoneally caused chondrocyte apoptosis in the paws of mice with arthritis induced by collagen II injection, but did reduce inflammation [26]. Rabbits injected intra-articularly with 0.5 mg/kg Dex once before and every three days after a surgery-induced PTOA model showed protection of articular cartilage at three weeks after surgery, with Mankin

scores equal to the control rabbits [27]. Heard *et al.* then used the same rabbit surgical model with a single i.a. Dex injection at the time of surgery (0.5 mg/kg) and showed significant improvement of histological grading of cartilage and synovium 9 weeks post-surgery [28]. They noted that this was due to improvement in safranin-O staining of GAGs, while Dex treatment did not influence the medial structure grade. Malfait *et al.* credited such a protective effect of Dex on inhibition of GAG loss to protection against aggrecan proteolysis in cartilage matrix, demonstrated in their rat model of OA using i.a. injections of TNFα followed by 16 hours of intravenous infusion of 0.001-1 mg/mL Dex in saline [29]. Even in animal models, however, there are discrepancies in the results of Dex: Huhtakangas *et al.* also found that i.a. Dex did not have a difference in histological knee grades for mice with zymosan-induced arthritis [30]. The duration of treatment can also have significant effects on the assessment of Dex safety: mice with OA induced by a meniscal destabilization given 5 mg/kg Dex i.a. for 4, 8, or 12 weeks had increasing severity of structural damage and chondrocyte apoptosis the longer they were exposed to Dex [31].

The most in-depth analysis of cartilage structure after Dex treatment in an animal model was performed by Jaffré *et al.*, who used quantitative ultrasound measurements and picrosirius red staining to interrogate the surface and internal structure of the cartilage after inducing synovitis and significant loss of cartilage sGAG in young rats with injections of zymosan [32]. Daily 0.1 mg/kg i.a. injections of Dex prevented knee swelling and histological changes such as loss of hypertrophic cells and surface alterations seen with toluidine blue staining, and maintained proteoglycan content at control levels. Using ultrasound measurements, they demonstrated that Dex returned the integrated reflection coefficient of the OA-challenged cartilage to control levels after 14 days, suggesting that the Dex restored the microarchitecture and smoothness of the

superficial layer after zymosan challenge. After two weeks of Dex treatment, however, the internal collagen network of the cartilage was markedly changed, with thinner and more disperse collagen fibers, a greater change than the effect of arthritis induction alone.

While Dex appears to provide protection against cartilage degradation, the results of Jaffré et al. suggest that there may be some dysregulation of the internal structure of cartilage organization, particularly in developing cartilage. It is also important to note the degenerative side effects of long-term daily Dex treatment: it is well established that extended high doses of Dex can retard growth, which was verified by Jaffré et al. with significantly lower knee sizes and weights in their Dex-treated rats. The rabbits in the study by Huebner *et al.* had extensive damage to their organs after Dex treatment; their lungs, livers, and kidneys all appeared fibrotic and had large necrotic areas, suggesting serious systemic side effects to drug treatment [27]. Rauchhaus *et al.* reported other systemic side effects in their mouse model, with reductions in body weight and lymphocyte count, neutrophilia, and transient reduction in serum corticosterone levels [21]. Two injections of 0.12 or 0.24 mg Dex reduced the growth of rat fetuses (an unsurprising finding given the well-established effect of GCs stunting growth in developing children) and caused the cartilage within the fetuses to have lower collagen content and reduced chondrocyte biosynthetic activity [33,34]. Taken together, these findings suggest the need for approaches to single injection for sustained low-dose intra-cartilage delivery of GCs, thereby minimizing unwanted exposure to other tissues.

1.3 Dex and healthy, non-arthritic animal models

The results from animal models demonstrate that there is clearly a need to better understand the appropriate dosage and duration of treatment to prevent local and systemic side effects, especially

when considering how the potential detrimental effects of Dex can extend to healthy cartilage. In models of OA, Dex can maintain the proteoglycan content of cartilage, but in healthy animals, Dex has been shown to damage cartilage and chondrocytes depending on dose and frequency of treatment. In a long-term study by Glade *et al.,* daily intra-muscular injections of Dex at 0.5 to 5.0 mg/100 kg into 6 month old pony weanlings for up to 11 months caused massive degeneration of the still-developing injected joints, with articular lesions, fibrous scars, and large necrotic areas of both cartilage and bone [35]. These results were attributed to a suppression of cartilage metabolism during the first 8 months of treatment, measured by ^{35}S-methionine incorporation and lactate dehydrogenase (LDH) activity. Li *et al.* reported a loss of cartilage sGAG content and increased MMP synthesis in the cartilage of rats injected i.a. twice a week for two months with 0.5 mg/kg Dex [36]. In a small animal model but with a much higher Dex dose, rats treated with 3.33 mg/kg Dex by systemic intramuscular injection for 5 weeks (1 mg per week) showed reduced size of the rough endoplasmic reticulum and Golgi complex within articular chondrocytes, hypothesized to cause a reduction in protein synthesis [37]. Dex treatment resulted in an increased number of dead cells, attributed to its effect on lysosomal function as well as disrupting cell metabolism via reducing mitochondrial size. Annefeld and Erne also found a suppression of cartilage metabolism with a similar dose of intramuscular Dex (3 mg/kg), as well as higher rates of cell death within the cartilage after only three weeks [38]. While it is difficult to extrapolate the doses used in animal models to what is appropriate for human patients, it is apparent that in some ways the effects of Dex may be chondroprotective under arthritic stresses, but lead to catabolic degeneration and a loss of viability in healthy tissue as the dose and duration increase.

Using animal models, chondrocyte death and matrix degradation are two of the most commonly reported outcome measures for determining the beneficial or harmful effects of Dex. However, there are many processes affecting these readouts that these studies do not always capture: Dex regulates many intracellular processes affecting cell viability, and regulates both the production of ECM proteins as well as the proteases responsible for organizing and breaking down the matrix. Some of the most well-studied processes are summarized in **Figure 1.1**. The complex nature of the interactions of these effects complicates interpretation of the effect of Dex on cartilage tissue, and necessitates using *in vitro* cartilage explant and chondrocyte studies to interrogate the mechanistic effects of Dex.

1.4 Cartilage explant models of arthritis

While there are no clinical data on the specific effects of Dex on cartilage in human patients, several studies have been performed on cartilage explants *in vitro* using tissue from human donors, listed in **Table 1.2**. Li *et al.* (2015) demonstrated in an IL-1-challenge of full-thickness near-normal human cartilage disks that culture with 100 nM Dex continuously over a 17-day treatment rescued glycosaminoglycan (GAG) loss and maintained more viable cells within the cartilage, relevant to potential PTOA prevention. Dex also rescued the cytokine-induced decrease in sGAG synthesis in this disease model, though not up to control levels. These results showed beneficial effects of Dex on cartilage metabolism and ECM synthesis in a diseased state, the opposite of what was seen following long-term Dex treatment of healthy developing animal models [35]. Using human tissue in an 8-day TNFα + IL-6 challenge of normal human knee explants (+/- a single injurious compressive impact injury relevant to PTOA), Lu *et al.* also found that continuous Dex treatment rescued GAG loss [16]. Interestingly, in the same TNFα/IL-6 model, Dex greatly

decreased the secreted levels of MMP1 and MMP13, which correlated with decreases in fragments of extracellular matrix components released to the media, such as aggrecan, cartilage oligomeric matrix protein, and collagen III neoepitopes [17]. In a co-culture model using human cartilage and synovial tissue from surgical discards, 100 nM Dex attenuated MMP and CCL2 release while increasing IL-8 release, but did not affect GAG loss [39].

Animal cartilage explant models corroborate some of the findings of human tissue, and offer some additional mechanistic understanding of how the effects of Dex on arthritis progression are propagated at the transcriptional level. Dex returned GAG loss and sulfate incorporation to control levels in two studies of TNFα-treated bovine cartilage at Dex concentrations as low as 1 nM [16,40]. The reduction in GAG loss was suggested to be due to a suppressive effect of Dex on the activity of remodeling proteases like aggrecanases through routes not limited to transcription alone, particularly in the case of ADAMTS-4 and -5, where mRNA transcripts remained elevated even after Dex exposure. A similar finding was reported by Busschers *et al.* using equine cartilage, where the addition of 100 nM or 1 μM Dex did not reduce the increase in ADAMTS-5 transcription after IL-1β challenge and levels of ADAMTS-4 mRNA transcripts were still elevated from control, though decreased from IL-1β alone [41]. This same study reported no change in GAG loss into the medium or GAG content of articular and nasal cartilage explants after 72 hours of exposure to Dex, different from the findings of Lu *et al.* with bovine cartilage, and from studies using human cartilage [16]. Whether this is due to a difference in species, the inflammatory cytokines used to model arthritis, or the length of culture remains to be answered.

In a 24-day IL-1-challenge of bovine cartilage explants, Dex maintained cell viability as measured by fluorescein diacetate and propidium iodide staining, consistent with a previous report of rescue of cell viability following mechanical impact injury using 100 μM [18,42]. PCR results in the same study showed that after four days of IL-1 treatment, Dex greatly decreased the transcription of IL-6, ADAMTS-4, ADAMTS-5, MMP-3, and MMP-13 compared to IL-1 alone without Dex, while also rescuing some expression of aggrecan and collagen II, though not up to control levels. It is of note that these results contradict the findings of Lu *et al.* on the effect of Dex on ADAMTS-4 and -5 transcription, though this discrepancy may be due to the different inflammatory cytokines used to stimulate cartilage breakdown and subsequent transcriptional pathways being activated [16]. In another experiment with IL-1 and plasminogen challenge on rabbit cartilage, Saito *et al.* also found a decrease in the release of MMP-1 and MMP-3 into the culture media at Dex concentrations as low as 1 nM. In addition, they showed some rescue of hydroxyproline release, a marker for collagen degradation [43]. In a whole-joint *ex vivo* porcine model of a traumatic mechanical joint injury, Dex was further shown to reduce the expression of catabolic genes including ADAMTS-4, MMP-13, IL-1β, and TNFα [44].

Taken together, these results support the hypothesis that Dex helps to prevent the degradation of extracellular matrix components by inhibiting the increase in transcription or activity of matrix-degrading factors brought on during the progression of arthritis, and by restoring some level of expression of the matrix molecules themselves, processes highlighted in **Figure 1.1**. However, there are still some discrepancies among the results of these experiments. While Li *et al.* reported a decrease in IL-6 expression in IL-1-challenged bovine explants, Lu *et al.* did not see a change in IL-6 transcription with the addition of Dex to TNFα-challenged tissue [16,18]. In a study of equine

cartilage explants subjected to treatment with IL-1 and the protease activated protein C (APC), 1 μM Dex did rescue hydroxyproline loss and decreased MMP-1, MMP-3, and MMP-13 transcription, However, Dex + APC treatment increased GAG release above the levels of IL-1/APC alone [45]. This discrepancy may be due to the combined treatment with a protease as opposed to cytokines alone, as in the other models. Alternatively, the GAG loss may be overestimated due to the analysis being based on GAG loss per wet weight of cartilage, a calculation that yields an exponentially increasing result for a linearly increasing loss of GAG.

1.5 Non-arthritic cartilage explant models

Experiments treating healthy cartilage with Dex in the absence of an arthritic context have shown disagreements in the effects of Dex on extracellular matrix (ECM) composition and tissue metabolism, summarized in **Table 1.3**. Two separate experiments with normal juvenile bovine explants treated with 100 nM Dex and one with equine cartilage explants treated with 100 nM or 1 μM Dex showed no change in the concentration of GAG per wet weight of the explants [16,46]. The two bovine experiments reported no change in the release of GAGs into the culture medium, while equine cartilage explants showed a slightly increased amount of GAG loss and a corresponding increase in transcript levels of the protease ADAMTS-5 [41]. However, Siengdee *et al.* found that a dose of 1.27 mM, four orders of magnitude greater than that used by the three previously mentioned studies, caused porcine cartilage explants to lose less GAG content to the media and maintain higher levels of Safranin-O staining, indicative of greater concentrations of GAGs in the cartilage matrix [47].

The effect of Dex on the structure of the cartilage matrix may be dependent on the developmental state of the tissue, as Bian *et al.* observed an increase in the equilibrium modulus and dynamic modulus of Dex-treated juvenile bovine cartilage, but not in adult bovine or canine cartilage, an effect that may be due to Dex causing more rapid differentiation of immature chondrocytes and subsequent changes to the extracellular matrix. In the same experiment, treated juvenile explants had greater concentrations of orthohydroxyproline (analogous to total collagen concentration) per wet weight after Dex exposure, while adult explants did not [46].

How the metabolism of healthy cartilage responds to Dex exposure is also unclear based on the current literature. Lu *et al.* showed no change in the rate of ^{35}S-sulfate incorporation at low doses of Dex; only at doses above 100 nM, the ^{35}S-sulfate incorporation significantly increased from the control [16]. The exact opposite effect, however, was seen in a tilapia gill cartilage explant model, where any exposure to Dex, as low as 250 pM, significantly decreased the level of ^{35}S-sulfate uptake, suggesting a decrease in metabolic activity and ECM synthesis [48]. Due to the variety of transcriptional changes caused by glucocorticoids, it is unsurprising that there would be effects on the rates of protein synthesis within the tissue, even if the direction of the effect reported in the literature is inconsistent, perhaps across different species or types of cartilage used. Siengdee *et al.* hypothesized that Dex treatment would lead to some level of cell death within the matrix, which they confirmed with histological sections revealing clusters of clumped chondrocytes, indicative of cell death [47]. While Datuin *et al.* did not report effects on cell viability within the tissue, Dex doses above 250 nM significantly decreased the level of ^{3}H-thymidine incorporation, associated with decreased cell proliferation [48].

Cartilage explant models of arthritis show potentially protective effects of Dex on ECM due to the downregulation of MMPs, and the structure of healthy cartilage seems to be maintained under Dex exposure. However, the results on cell behavior and metabolism within native tissue leave open the possibility that there may be negative effects of the drug on resident chondrocytes themselves, especially at higher doses. A number of studies have been performed on chondrocytes isolated from tissue to interrogate the mechanisms of Dex action in both arthritic and healthy contexts, with many conflicting results in different models and Dex doses, as described below.

1.6 Dex and chondrocyte studies of arthritis and inflammation

Human chondrocytes isolated from patients with arthritis or cultured with inflammatory cytokines offer a model system in which the pathways affected by Dex treatment can be examined in more detail, and the studies using this model system are listed in **Table 1.4**. However, in keeping with the animal and explant studies, it is difficult to draw specific conclusions because publications often report conflicting results. A broad transcriptomics analysis of human OA chondrocytes treated with 1 μM Dex demonstrated its effects on reducing inflammatory factors and matrix proteinases, with mixed effects on genes associated with the regulation of oxidative stress [49]. Stöve *et al.* isolated primary chondrocytes from the cartilage of OA patients taken at the time of knee joint replacement surgery, cultured them in alginate beads with 0.1 ng/mL IL-1β. They found that addition of Dex (100 nM-10 μM) lowered the PG content of the culture and decreased the transcription of aggrecan and MMP-3, supporting the hypothesis that Dex does not protect cartilage by increasing synthesis of ECM components, but instead by preventing the synthesis of matrix-degrading factors [50]. In another study of chondrocytes and cartilage from human donors with no joint disease, culture with IL-1 stimulated increased transcription of biologically active

monocyte chemoattractant protein-1 (MCP-1). Treatment with Dex decreased MCP-1 synthesis, suggesting the ability to prevent monocyte infiltration and thus progression of cartilage degradation [51]. However, certain chondrocyte models reveal that Dex may pose a risk to the viability of the cells themselves. 63 μM Dex was shown to significantly increase the rate of apoptosis in chondrocytes isolated from knee cartilage of OA joint replacement patients by decreasing ERK signaling [52]. This Dex dose was quite high, but other examples in the literature discussed below show similar effects at doses orders of magnitude lower.

Some studies with human chondrocytes have been performed to elucidate the effect of Dex on inflammatory pathways, though the entire picture still remains unclear. 1-100 nM Dex reduced IL-17 induced nitric oxide (NO) synthesis, inhibiting the production of IL-6 and iNOS transcription, suggesting a potential pathway for the anti-inflammatory effects of Dex in cartilage tissue [53]. 100 nM Dex was found to decrease the transcription of the soluble IL-1 receptor antagonist (IL-1Ra) after IL-6 exposure with human primary chondrocytes, indicating that IL-1Ra production is not a method by which Dex could protect cartilage from damaging inflammatory factors [54]. A phosphoproteomics study using primary human chondrocytes treated with IL-1 and 100 nM Dex showed a decrease in the phosphorylation of JNK1 and -2 linked to the anti-catabolic effects of Dex, suggesting a major role for JNK in regulating cartilage breakdown upon inflammatory challenge [55]. The anti-inflammatory effects of Dex have also been attributed to its ability to reduce the production of the (mostly) pro-inflammatory prostaglandin E_2 (PGE_2): in human chondrocytes isolated from patients with OA and mouse chondrocytes stimulated with IL-1β, the addition of 1 μM Dex reduced the synthesis of microsomal prostaglandin E synthase-1, a terminal synthesizer of PGE_2 [56].

Several studies of animal chondrocytes subjected to arthritic-like conditions, listed in **Table 1.4**, are consistent with some of the findings from human cells. IL-1-challenged chondrocytes from equine and bovine joint cartilage also showed decreased expression levels of MMP3, MMP13, and MMP1 when treated with 100 nM Dex [41,57,58]. However, Dex had similar effects on the family of tissue inhibitors of metalloproteinases (TIMPs), decreasing their expression levels, further supporting the hypothesis that Dex may cause dysregulation of matrix organization beyond the scope of MMPs alone. This dose of Dex did not rescue GAG loss in response to IL-1β stimulation of equine chondrocytes, but did rescue collagen II loss in a model using IL-1α-challenged bovine chondrocytes cultured in agarose gels [58,59]. Similar to the results of Glade *et al.* and Datuin *et al.*, Sadowski and Steinmeyer found that Dex treatment (100 nM to 50 μM) depressed total protein synthesis by up to 40% in bovine chondrocytes stimulated with IL-1, though cell viability was not affected by Dex [35,48,57]. Roach *et al.* also reported that Dex did not change the anti-proliferative effect of IL-1 treatment, and that treating the chondrocytes with Dex alone resulted in the same inhibition of proliferation as inflammatory cytokines [59].

Dex has also been demonstrated to regulate the transcription of cyclooxygenase II (COX2), an inflammation-induced enzyme that produces prostaglandins, in arthritic contexts. 100 nM Dex prevented the transcription of COX2 in primary human chondrocytes after IL-1β exposure, as well as prevented the production of PGE_2, which has been a palliative target for RA treatment for years [60–62]. However, inhibition of COX2 likely does not produce a straightforward anti-inflammatory response, as some prostaglandins produced by COX2 can have anti-inflammatory

effects, and even PGE_2 has been shown to be involved in the resolution of inflammation as well as its induction in an RA mouse model [63].

1.7 Non-arthritic chondrocyte cultures: effects on viability and proliferation

As shown in **Table 1.5**, most studies with human chondrocytes show an apoptotic effect of Dex on isolated cells in a non-arthritic context, which Liu *et al.* attributed to the induction of autophagy by Dex [64–67]. In this model, a downstream effect of Dex is to increase the production of reactive oxygen species (ROS) which trigger an autophagic response, proposed by Huang *et al.* to be regulated by ROS-induced increased p38 phosphorylation, leading to cell death [67]. However, Shen *et al.* proposed that oxidative stress due to increased ROS production was the cause of chondrocyte death, and autophagy served to protect the cells from this stress. The discrepancy could be due to the difference in their Dex concentration used, where Liu *et al.* was two orders of magnitude higher than Shen *et al.*, but the complex interplays between these pathways, highlighted in **Figure 1.1**, still remain to be clarified.

In contrast to these studies, Dragoo *et al.* (2012) did not find any changes in the amount of cell death, even at the incredibly high dose of 1.5 mM Dex [68]. Stueber *et al.* reported no change in cell viability as well, though their experiment only tested the effects of the drug for an hour, when Song *et al.* reported viability changes only after 72 hours of treatment [69,70]. Dragoo *et al.* reported their results after one week of treatment, however, so the discrepancy with that experiment still remains [68].

Mushtaq *et al.* were the only group to use isolated animal chondrocytes that reported the effects of Dex on apoptosis, and found no change after 20 days of Dex treatment [71]. It is of note that these cells were a chondrogenic teratocarcinoma cell line instead of primary chondrocytes, which may have influenced their behavior. All three groups that used animal chondrocytes, however, reported a reduction in the rate of cell proliferation after Dex exposure, suggesting that even if Dex did not kill the cells, it made them more quiescent [72–74]. It is unclear why so many chondrocyte models report an apoptotic effect that is not reflected in tissue explant cultures. This may be due to a lower effective concentration in explants, as the drug must diffuse through the dense cartilage depending on the duration of treatment, or a different homeostatic state of the cells themselves in a whole tissue versus cell monolayer. Chondrocytes in monolayer culture experience an entirely different set of external stimuli compared to those suspended in a native 3D pericellular matrix, both through biological and mechanical signaling [75]. This could lead to a lack of external survival signals received by the monolayer chondrocytes after Dex exposure, rendering them unable to prevent apoptosis.

The relationship between Dex, autophagy, and cell death is further complicated by a recent study that reported on the effects of Dex on senescence in rat knee chondrocytes. Xue *et al.* found that a range of 0.25-128 μM Dex activated autophagy and senescence in chondrocytes, and that senescence increased after inhibiting autophagy with an mTOR inhibitor, potentially demonstrating that Dex-induced autophagy serves to protect chondrocytes from senescence [76]. Senescence has been identified as a correlative factor for OA progression, so understanding the relationship of the dose of Dex and its activation of autophagy, apoptosis, and senescence will be critical to understanding how to safely use it in patients.

1.8 Non-arthritic chondrocyte cultures: other affected pathways

Changes in the synthesis of ECM components at the cellular level alone do not seem to explain the effect of Dex on cartilage as a whole. As shown in **Table 1.6**, collagen II synthesis either decreased or did not significantly change after Dex treatment [58,70,77]. Song *et al.* found that Dex decreased the synthesis of aggrecan in healthy human chondrocytes. Dex-induced suppression of aggrecan and collagen II synthesis was confirmed by Li *et al.* using human chondrocytes isolated from un-abraded regions of arthroplasty knee discards, who also found that Dex caused mitochondrial disfunction and increased ROS levels [36]. James *et al.* used a RNA microarray to assay the entire transcriptome of chondrocytes after Dex treatment, and found that ECM genes as a whole were highly enriched in the Dex-treated group, though aggrecan and collagen II were not in the list of the most enriched ECM genes, which included many other collagen-associated genes, including fibronectin, matrilin, and laminin.

In healthy cartilage explant models, it was unclear whether Dex increased, decreased, or did not affect the GAG content of the cartilage, while the results from isolated cells suggest a complicated interplay between the regulation of ECM-remodeling factors by Dex. In one study, MMP13, MMP1, and MMP3 were all shown to be significantly downregulated after Dex exposure but another showed that several members of the ADAMTS family were among the most highly enriched ECM genes after Dex treatment [58,77]. Adding to the discussion of the dysregulation of matrix organization by Dex, Hinek *et al.* reported that 100 nM Dex caused rabbit chondrocytes to deposit more elastic fibers in a more disorganized network [78]. The relationship of the effects of Dex on aggrecan and metalloproteinase expression and the resulting effects on cartilage tissue

structure as a whole have not yet been elucidated, but is integral to understanding the results of studies such as the disperse collagen networks of Jaffré *et al.*, as well as the safety of Dex for long-term joint treatment [32].

Several other pathways relevant to normal cartilage function have been found to be affected by Dex in isolated experiments. The results of the transcriptome screen done by James *et al.* identified the "metabolism" gene set as the most highly enriched in Dex-treated cells compared to control, though no single metabolic pathway stood out as being upregulated as a whole; glutathione S-transferases and aldehyde dehydrogenases, involved in several metabolic pathways, were some of the most notable individual genes [77]. One study with a non-arthritic embryonic mouse chondrocyte model found that SOX9, a transcription factor that activates chondrocyte differentiation, was upregulated after 100 nM Dex treatment for 48 hours [79,80]. In the study by Song *et al.* with adult human chondrocytes, however, the opposite effect was observed, which suggests that the effects of Dex could be dependent on the developmental state of the cells, just as with the differences noted by Bian *et al.* with juvenile versus adult bovine tissue, different types of cartilage used, or possibly a difference between species [46,70].

One troubling finding reported an increase in calcium pyrophosphate dihydrate (CPPD) crystal deposition in porcine chondrocytes caused by 96 hours of 10 nM to 1 μM Dex exposure hours as a result of the upregulation of transglutaminase activity. CPPD crystals are suspected to contribute to joint damage in osteoarthritis; thus, while Dex may help preserve the PG and collagen structure of arthritic cartilage, it may also initiate other cell-mediated processes that become detrimental to joints [81].

1.9 Discussion

The results of studies using Dex both in vivo and in vitro are highly dependent on the model system, dosage, and duration of Dex exposure. Understanding appropriate doses for glucocorticoids, in general, is vital to performing and comparing the results of clinical trials. For example, two separate trials studied the symptomatic benefits of triamcinolone (TA) on patients with knee OA (Kellgren-Lawrence grades 2 or 3); while Conaghan *et al.* found beneficial effects at 12 weeks using a single 32 mg dose of i.a. extended-release TA, McAlindon *et al.* used 40 mg i.a. injections of TA every three months for two years, and reported a significant increase in cartilage volume loss [6,10]. It is difficult to assess whether the differences in these outcomes are due to total dose, duration of treatment, or both.

Biological processes in cartilage that have been identified as being affected by Dex are highlighted in **Figure 1.1**. While the results of studies on ECM synthesis in healthy isolated chondrocytes are inconsistent, chronic administration of Dex at high doses was shown in some *in vivo* studies to have catabolic effects on initially healthy tissue [35,37,38,58,70,77]. However, Dex may offer protection against the degenerative effects of arthritic diseases on ECM structure. At the tissue and cell level Dex was shown to inhibit the production of matrix-degrading factors, rescuing matrix breakdown in arthritic contexts [16–18]. While ECM content may be maintained, there may still be disruption of the matrix structure itself due to the dysregulation of cell-mediated remodeling factors, the effects of which on cartilage tissue in the long-term remain to be studied [32]. One of the greatest challenges in comparing the results of various studies is the variety of model systems being used: isolated chondrocytes versus cartilage explant organ culture, or co-culture of different

joint tissues, versus animal models and human clinical trials. While chondrocyte monoculture is useful for easier interrogation of molecular pathways, this approach cannot recapitulate the complex interactions of cells within their native 3D tissue matrix or between the different tissues of the joint. Even cultures incorporating chondrocytes suspended in a hydrogel to recapitulate the earliest stages of a 3D neo-tissue environment do not capture the same processes as that occur in native tissues due to the differences in the composition of the ECM, which complicates conclusions drawn about ECM synthesis and remodeling [82].

The overall effects of Dex on cellular metabolism and viability remain unclear, as there are reports of both high and low doses of Dex either reducing or maintaining cell viability. Dex was shown to protect cartilage viability in an IL-1 challenge of bovine cartilage explants, but many studies using isolated chondrocytes report significant losses of cell viability after Dex exposure [18,64–66,70]. One mechanism that may underlie loss of cell viability is the dysregulation of metabolism triggered by Dex, leading to upregulation of ROS within the chondrocytes. This process can trigger an autophagic response, and there currently exist conflicting reports in the literature on whether autophagy is the cause of chondrocyte apoptosis after Dex exposure or protective against ROS-induced apoptosis in OA, and the answer likely depends on the dose of Dex used [65]. ROS generation has been linked to catabolic effects in OA, so the dose-dependent balance of ROS and autophagy in whole cartilage under arthritic conditions must be better understood [83]. This, as well as the increase in CPPD crystal formation after Dex treatment reported by Fahey *et al.,* could worsen the progression of the disease, and more work must be done with human tissue to determine the extent of the risk [81]. Autophagy is suppressed in arthritic contexts, so the pro-autophagic

response of Dex may serve to restore healthy homeostatic mechanisms and protect cartilage tissue [84].

Dex and other corticosteroids also affect energy metabolism of tissues including cartilage: 10 μM cortisol was shown to decrease glucose uptake by chondrocytes isolated from patients with OA, with or without interleukin-1 beta (IL-1β) stimulation [85,86], and Dex has been shown to modulate glucose levels systemically as well as locally within tissues by stimulating gluconeogenesis [85,87]. Glucose metabolism is shifted towards glycolysis in early OA, which can lead to the production of more damaging ROS due to increased ATP production. If Dex stimulates gluconeogenesis in cartilage under disease stress, this may help to alleviate the oxidative stress on chondrocytes, but also potentially disrupt energy production required for anabolic responses. Systems-level analyses of the Dex effect on cartilage energy metabolism, both for the glucose processing pathway and others important to cartilage function, are necessary to fully understand its effects on cartilage tissue and possible off-target effects. Side effects of Dex may also be ameliorated by combination treatments with other drugs such as antioxidants that combat its effects on metabolism, a combination that has already shown, *in vivo*, to improve the therapeutic capacity of Dex alone [88]. Pro-anabolic drugs like insulin growth factor-1 (IGF-1) have also been shown to rescue human ankle cartilage biosynthesis, suggesting it may also be a candidate for combination treatment with Dex to complement the anti-catabolic effects of the steroid [18,89].

Studies with isolated cells seem to agree that that Dex can reduce proliferation, which was also seen with higher Dex doses in cartilage tissue [48]. The anti-proliferative effect of Dex would be of great concern when treating young patients, as cartilage development could be disturbed upon

Dex exposure [48,72–74]. Importantly, it is not known under what conditions and doses Dex drives cells towards quiescence, senescence, or apoptosis. It has been shown *in vitro* and *in vivo* that Dex exposure activates the p53/p21 pathway in tenocytes, a driving pathway towards senescence, though the effects of Dex on this pathway in cartilage are still unknown [90]. If Dex-induced reduction in proliferation as measured by ^{3}H-thymidine incorporation is a result of a shift towards senescence, it could negatively affect the ability of cartilage tissue to respond to future challenges.

One aspect of Dex treatment that has not been well-explored in the literature is the duration of specific cell and tissue responses after a given exposure to Dex. Some studies have been performed with other GCs, such as that of Behrens *et al.* using rabbits injected every week with 25 mg hydrocortisone for nine weeks [91]. 26 weeks after hydrocortisone injections were stopped, metabolic rates increased towards normal along with an increase in cell proliferation, which was attributed to cells replicating to replace those killed by the multiple high-dose steroid injections, and the remaining cells restoring a more normal biosynthetic capacity. However, the extent to which the disrupted remodeling of the ECM can be rescued after such aggressive steroid treatment has not yet been explored, so it is unknown how the effects of the disruption of tissue remodeling factors may last, and whether this could render the tissue more prone to disease in the future.

A question that must be discussed when studying any aspect of arthritis *in vitro* is whether the results would be different in a model of the entire joint, taking into account the cross-talk between cartilage, joint capsule synovium, bone, and immune cells [92]. The disease-modifying potential of Dex does not depend only on its effects on cartilage, but on the state of the joint as a whole. Dex was shown to reduce the transcription of some inflammatory cytokines in cartilage explants

under arthritic stress, which would protect not only cartilage viability but potentially reduce inflammatory reactions of the surrounding joint tissues [16]. As mentioned above, Dex reduces the production of MCP-1 in chondrocytes, reducing the potential for macrophage infiltration in RA, a possible mechanism of reducing RA disease progression [93]. Dex also reduces cytokine expression by macrophages in an inflammatory environment, providing a potential protective mechanism against cytokine-induced damage in RA [94]. The ROS-producing effect of Dex, while linked to apoptosis in chondrocytes, serves to increase the T-cell suppressive capacity of anti-inflammatory macrophages, which has been associated with reducing the severity of RA in a mouse model [95,96]. The synovium also secretes a large quantity of inflammatory cytokines immediately following a traumatic joint injury, a process which Dex was shown to suppress in a rabbit model of post-traumatic OA, contributing to its apparent chondroprotective action [27]. In vitro human cartilage-bone-synovium co-culture models of PTOA have highlighted the potential of Dex in reducing cytokine release by synovium explants, and thereby inhibiting proteolytic aggrecan-GAG loss from cartilage [97,98]. Dex also inhibits the production of cyclooxygenase-2 (COX-2) in the synovium in response to IL-1, a non-disease modifying process that has been used in several drugs on the market for treating OA and RA symptoms [99–101].

One of the most serious side effects of chronic GC treatment in humans is bone loss, which also occurs during arthritis progression [102–104]. After Dex treatment, healthy bone metabolism is affected, leading to changes in remodeling and eventual bone density loss and a reduction in load potential [105]. It is unclear whether Dex worsens the progression of osteoporosis in arthritic animal models, but it is nonetheless worth exercising caution when considering the balance of side effects versus potential therapeutic gains [22,103,106]. Dex also has been shown to stunt growth

of developing bone and cartilage, explaining the effects of growth retardation and osteopenia seen in children treated with extended doses [34,107]. The joint space is surrounded by fibrous synovial joint capsule, which contains synoviocytes and inflammatory cells that communicate with cartilage and bone during OA development and contribute to joint damage through inflammation [108,109].

Therapeutic treatment for musculoskeletal injuries, broadly encompassing cartilage, bone, synovial joint capsule, and muscle tissue, are of great interest on Earth as well as in space. The potential chondroprotective effects of Dex could potentially be applied before or during spaceflight missions, whether for astronauts stationed on the International Space Station (ISS) or for future travelers as commercial spaceflight is becoming more of a reality. In space, the lack of gravity and high radiation can contribute to musculoskeletal atrophy, including structural changes to the intervertebral disk, and these conditions may also affect cartilage homeostasis and its ability to respond to disease [110,111]. Currently, astronauts on mission on the ISS exercise frequently to combat bone and muscle degeneration in space, and perform many mission activities that put them at higher risk of a musculoskeletal injuries that could contribute to PTOA or OA progression [112–116]. Drugs that can prevent disease progression after an injury like Dex have potential application in these conditions, but any differences in their response in the environment of space have not yet been studied.

Finally, given the need for low dose treatment without use of multiple i.a. injections, improved drug delivery techniques are critically important for therapeutic treatment of OA/PTOA. Developing tools such as nanocarriers or functionalized protein carriers to aid in delivery of Dex to the cartilage tissue specifically will allow the drug to be given in single injection low-dose

modalities, which may prevent its negative effects on cartilage tissue as well as systemic side effects. Methods of modulating the anti-inflammatory effects of Dex and targeting the drug to specific tissues are currently being explored with positively charged protein or carbohydrate carriers [117–120], microspheres [121,122], biomaterial carriers designed to reside long-term in the joint space [123,124], and methods of controlling release based on near-infrared light exposure, temperature, and ROS levels [125–127].

1.10 Thesis outline

The objective of this thesis was to use systems-level analyses to understand the effects of dexamethasone on cartilage homeostasis and metabolism using bovine and human models of post-traumatic osteoarthritis that investigate disease and drug effects on cartilage alone, as well as in co-culture systems with bone and synovial joint capsule.

In Chapter 2, the release of proteins from bovine knee cartilage explants in an *ex vivo* model of post-traumatic osteoarthritis was followed, and proteins upregulated with injury and cytokine treatment identified as potential disease biomarkers. The effects of Dex on these disease responses, including the suppression of catabolism and dysregulation of immune signaling, were explored.

In Chapter 3, proteomic data from bovine and human cartilage models of post-traumatic osteoarthritis were clustered based on the kinetics of their release from cartilage under disease stress and with Dex treatment. Early disease biomarkers were identified and Dex was shown to restore most proteins to their control kinetic behavior.

In Chapter 4, post-traumatic osteoarthritis progression was studied in a novel *ex vivo* human osteochondral model system from healthy donors, and cartilage and bone homeostasis were

quantified at the biochemical and proteomic level. Protein biomarkers of donor-specific Dex anti-catabolic responses were identified.

In Chapter 5, the major findings of all studies are summarized and future directions are discussed.

Acknowledgements: This work was supported by the NIH/NCATS Grant UG3/UH3 TR00218.

* sections of this introduction appeared in Black & Grodzinsky, Dexamethasone: chondroprotective corticosteroid or catabolic killer?, *European Cells and Materials* 2019; 38:246-263

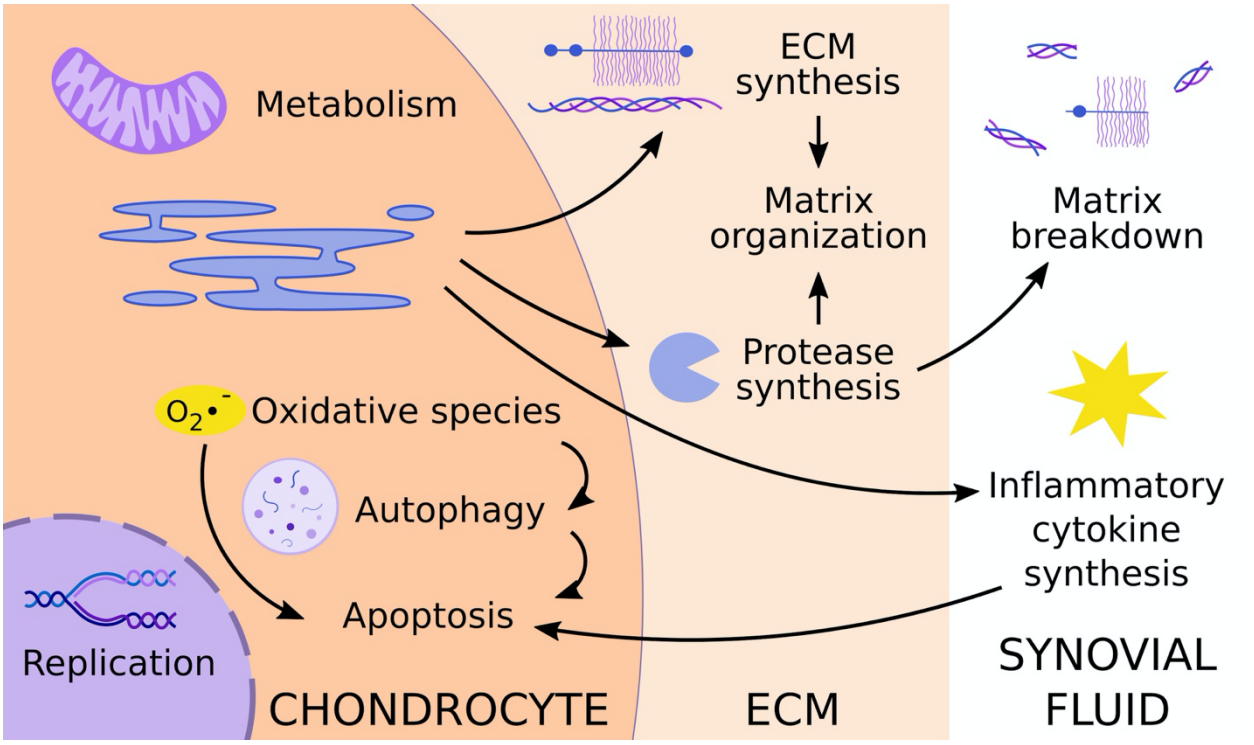

Figure 1.1. Biological processes identified as being affected by Dex either in healthy or diseased cartilage in studies using in vivo models, cartilage explants, or chondrocyte monoculture. Dex has been shown to affect matrix organization at the level of both ECM and protease synthesis, though studies often disagree on the specific up- or downregulation of ECM specific components. There is a general consensus that, under arthritic stresses, Dex prevents the upregulation of protease synthesis, which can prevent matrix loss. However, at higher doses in healthy cartilage, it is suggested that Dex may increase the rate of matrix degradation or the organization of the matrix itself. This could be due to effects on matrix components and proteases, or due to intracellular effects on metabolism and the production of reactive oxygen species that activate autophagy and lead to significant cell death. Data from studies in vitro have suggested that Dex maintains cell viability under arthritic stress, which could be linked to a Dex-induced reduction in inflammatory cytokine synthesis. Alternatively, the metabolic processes that Dex dysregulates in healthy tissue could serve to rescue changes in those processes after the initiation of arthritis. While the induction of autophagy in healthy tissue could lead to chondrocyte death and subsequent matrix breakdown, autophagy has been shown to be suppressed in arthritic contexts, so Dex could serve to rescue these cellular processes in a diseased state. It remains to be seen whether Dex inhibits proliferation under arthritic stress and what role this might play in disease progression, and whether the phenomenon of Dex-induced reduction of proliferation in healthy cartilage is due to cells becoming quiescent or senescent. Each possibility would have a significantly different biological outcome on cartilage exposed to Dex for an extended period of time.

Authors	Year	Animal model	Arthritis model	Dex dose	Duration	Frequency and route of administration	Observed effect
Huebner *et al.*	2014	Rabbit	Yes	0.5 mg/kg	3 wk	Once/3 days, i.a.	+
Heard *et al.*	2015	Rabbit	Yes	0.5 mg/kg	48 h-9 wk	Once, i.a.	+/-
Chen *et al.*	2021	Mouse	Yes	5 mg/kg	4-12 wk	3/wk, i.a.	-
Celvin *et al.*	2020	Mouse	Yes	0.25 mg/kg	14 d	Daily, i.p.	+/-
Islander *et al.*	2010	Mouse	Yes	~5 mg/kg	~25 d	Daily, i.p.	+
Rauchhaus *et al.*	2009	Mouse	Yes	0.4 - 4 mg/kg	7 d	Once, i.v.	+/-
Bai *et al.*	2021	Rat	Yes	0.02 mg	6 wk	1/wk, i.a.	+
Huhtakangas *et al.*	2021	Rat	Yes	0.1 mg/kg	8 d	Once, i.a.	=
Wang *et al.*	2017	Rat	Yes	0.15 mg/kg	7 d	Daily, oral gavage	+
Malfait *et al.*	2009	Rat	Yes	1 mg/kg *or* 0.001 - 1 mg/mL	16 h	Once, oral gavage *or* i.v. infusion	+
Ashraf *et al.*	2011	Rat	Yes	0.1 mg/kg	24 d	Daily, oral gavage	+
Jaffré *et al.*	2003	Rat	Yes	0.1 mg/kg	5-21 d	Daily, i.a.	+/-
Li *et al.*	2022	Rat	No	0.5 mg/kg	8 wk	2/wk, i.a.	-
Annefeld and Erne	1987	Rat	No	3 mg/kg	3 wk	1/wk, i.m.	-
Podbielski and Raiss	1985	Rat	No	3.3 mg/kg	3-5 wk	1/wk, i.m.	-
Glade *et al.*	1983	Horse	No	0.005 mg/kg	3-11 mo	Daily, i.m.	-

Table 1.1. Dex studies in animal models summarizing model used, Dex dosage and duration, frequency and administration route of Dex treatment, and overall observed effect. i.a.: intra-articular injection. i.p.: intra-peritoneal injection. i.v.: intravenous injection. i.m.: intra-muscular injection. (+) indicates a positive effect on cartilage and/or arthritis progression, (-) indicates a negative effect, (+/-) indicates some positive results alongside negative side effects, and (=) indicates no change from vehicle.

Authors	Year	Tissue type	Disease stimulus	Dex dose	Duration	Observed effect
Chan *et al.*	2022	Human	Synovial co-culture	100 nM	7 d	+
Arabiyat *et al.*	2020	Bovine	TNFα, 25 ng/mL	100 nM	6 d	+
Genemaras *et al.**	2018	Porcine	Mechanical impact	4 mg	8 hr	+
Wang *et al.*	2017	Human	TNFα, 100 ng/mL + IL-6, 50 ng/mL	100 nM	21 d	+
Li *et al.*	2015	Human	IL-1α, 1 ng/mL	100 nM	24 d	+
		Bovine	IL-1α, 1 ng/mL	100 nM	24 d	+/=
Lu *et al.*	2011	Human	TNFα, 100 ng/mL ± IL-6, 50 ng/mL	10 nM	6 d	+
		Bovine	TNFα, 25 ng/mL ± IL-6, 50 ng/mL	10 nM	6 d	+
Busschers *et al.*	2010	Equine	IL-1β, 5 ng/mL	100 nM-1 μM	72 h	+/=
Garvican *et al.*	2010	Equine	IL-1, 10 ng/mL + APC, 10 μg/mL	1 - 100 μM	4 d	+/-
Saito *et al.*	1999	Rabbit	IL-1α, 1 ng/mL + plasminogen, 100 μg/mL	0.1 - 100 nM	7 d	+

Table 1.2. Dex studies using explants from human or animal cartilage in models of arthritis. Summary of Dex concentration, duration of culture, stimulus used to model arthritic conditions, and observed effect on measurements associated with arthritis progression. APC: activated protein C. (+) indicates a rescue of arthritis-induced effects, (+/=) indicates rescue of only some effects, and (+/-) indicates rescue of some effects while worsening others. *Genemaras *et al.* used a whole joint harvested post-mortem.

Authors	Year	Tissue type	Dex dose	Duration	Observed effect
Siengdee *et al.*	2015	Porcine	1.25 - 5 mM	2 wk	-
Lu *et al.*	2011	Bovine	10 nM	6 d	=
Bian *et al.*	2010	Bovine	0.1 µM	4 wk	+/=
Busschers *et al.*	2010	Equine	100 nM-1 µM	72 h	-
Datuin *et al.*	2001	Tilapia	0.25 nM - 2.5 µM	Not reported	-

Table 1.3. Dex studies using cartilage explants in non-arthritic model systems. Summary of Dex concentration, duration of culture, and overall observed effect on cartilage. (=) indicates no change in measured outcomes, (+/=) indicates some healthy effects and some outcomes that did not change, and (-) indicates adverse effects on the cartilage tissue.

Authors	Year	Cell type	Cytokine treatment	Dex dose	Duration
Pemmari *et al.*	2020	Human, OA	N/A	1 μM	24 h
Tuure *et al.*	2019	Human, OA	N/A	1 μM	90 min – 24 h
		Mouse	IL-1β, 100 pg/mL	1 μM	90 min – 24 h
Wang *et al.*	2017	Human	IL-1, 10 ng/mL	100 nM	30 min
Tu *et al.*	2013	Human, OA	N/A	63 μM	48 h
Stöve *et al.*	2002	Human, OA	IL-1β, 0.1 ng/mL	100nM-10 μM	1 wk
Palmer *et al.*	2002	Human, OA	IL-1β, 10 ng/mL *or* IL-6, 100 ng/mL	100 nM	18 h
Shalom-Barak *et al.*	1998	Human	IL-17, 10 ng/mL	1-100 nM	48 hr
Villiger *et al.*	1992	Human	IL-1, 10 ng/mL	100 nM	5 h
Roach *et al.*	2016	Bovine	IL-1α, 10 ng/mL	100 nM	35 d
Busschers *et al.*	2010	Equine	IL-1β, 5 ng/mL	100 nM-1 μM	24 h
Richardson and Dodge	2003	Horse	IL-1β, 10 ng/mL *or* TNFα, 25 ng/mL	10 nM-1 μM	24 h
Sadowski and Steinmeyer	2001	Bovine	IL-1α, 0.5 ng/mL	100 nM-50 μM	48 h

Table 1.4. Dex studies using chondrocytes isolated from arthritic patients and/or cultured with inflammatory cytokines. Summary of cell source (OA: from patient with symptomatic OA), inflammatory cytokines used to model arthritic conditions, Dex concentration, and duration of culture.

Authors	Year	Cell type	Dex dose	Duration	Effect on viability
Huang *at al.*	2018	Human	1 μM	24 h	-
Shen *et al.*	2015	Human	1 μM, 10 μM	24 h	-
Liu *et al.*	2014	Human	100 μM	72 h	-
Zaman *et al.*	2014	Human	1 μM	24-72 h	-
Song *et al.*	2012	Human	20-200 μM	24 h-1 w	-
Stueber *et al.*	2014	Human	10 μM-1 mM	1 h	=
Dragoo *et al.*	2012	Human	1.5 mM	1 w	=

Authors	Year	Cell type	Dex dose	Duration	Effect on proliferation
Mushtaq *et al.*	2002	Mouse	10 nM-1 μM	20 d	-
Miyazaki *et al.*	2000	Rat	0.1 nM-100 μM	36 h	-
Hainque *et al.*	1987	Rabbit	10 nM-100 μM	24 h-2 w	-
Maor and Silbermann	1986	Mouse	1 μM	24 h	-

Table 1.5. Results on cell viability and proliferation after Dex treatment on primary chondrocytes in non-arthritic model systems. (-) denotes a decrease and (=) denotes no change from control.

Authors	Year	Cell type	Dex dose	Duration	Effect on RNA expression
Li *et al.*	2022	Human	250, 500, 1000 nM	48 h	-collagen II, -ACAN, +MMP13, +MMP3, +ADAMTS4, +ADAMTS5
Song *et al.*	2012	Human	20 - 200 μM	24 h-1 wk	- ACAN, - collagen II
James *et al.*	2007	Mouse	100 nM	24 h	+ ECM genes
Richardson and Dodge	2003	Equine	10 nM - 1 μM	24 h	- collagen II, - MMP13, - MMP1, - MMP3, + fibronectin

Table 1.6. ECM-related gene expression of primary chondrocytes after Dex exposure. (+) denotes an increase, (-) denotes a decrease, and (=) denotes no change from control. James *et al.* used an ECM gene set from the GSEA database [128].

Chapter 2. Proteomic Analysis Reveals Dexamethasone Rescues Matrix Breakdown but not Anabolic Dysregulation in a Cartilage Injury Model

Rebecca Mae Black[a,1], Yang Wang[a,1], André Struglics[b], Pilar Lorenzo[c], Viveka Tillgren[c], Martin Rydén[b], Alan J. Grodzinsky[a,d,e], Patrik Önnerfjord[c]

[a]Department of Biological Engineering, Massachusetts Institute of Technology, Cambridge, MA, USA
[b]Orthopaedics, Department of Clinical Sciences Lund, Faculty of Medicine, Lund University, Lund, Sweden
[c]Rheumatology and Molecular Skeletal Biology, Department of Clinical Sciences Lund, Faculty of Medicine, Lund University, Lund, Sweden
[d]Department of Mechanical Engineering, Massachusetts Institute of Technology, Cambridge, MA, USA
[e]Department of Electrical Engineering and Computer Science, Massachusetts Institute of Technology, Cambridge, MA, USA

[1]contributed equally to the manuscript

Published in Osteoarthritis and Cartilage Open 2020; 2(4):100099. The full text and supplemental material can be found at https://doi.org/10.1016/j.ocarto.2020.100099.

Abstract:

Objectives: In this exploratory study, we used discovery proteomics to follow the release of proteins from bovine knee articular cartilage in response to mechanical injury and cytokine treatment. We also studied the effect of the glucocorticoid Dexamethasone (Dex) on these responses.

Design: Bovine cartilage explants were treated with either cytokines alone (10 ng/ml TNFα, 20 ng/ml IL-6, 100 ng/ml sIL-6R), a single compressive mechanical injury, cytokines and injury, or no treatment, and cultured in serum-free DMEM supplemented with 1% ITS for 22 days. All samples were incubated with or without addition of 100 nM Dex. Mass spectrometry and western blot analyses were performed on medium samples for the identification and quantification of released proteins.

Results: We identified 500 unique proteins present in all three biological replicates. Many proteins involved in the catabolic response of cartilage degradation had increased release after inflammatory stress. Dex rescued many of these catabolic effects. The release of some proteins involved in anabolic and chondroprotective processes was inconsistent, indicating differential effects on processes that may protect cartilage from injury. Dex restored only a small fraction of these to the control state, while others had their effects exacerbated by Dex exposure.

Conclusions: We identified proteins that were released upon cytokine treatment which could be potential biomarkers of the inflammatory contribution to cartilage degradation. We also demonstrated the imperfect rescue of Dex on the effects of cartilage degradation, with many catabolic factors being reduced, while other anabolic or chondroprotective processes were not.

2.1 Introduction

While glucocorticoids have been used for over 50 years to treat osteoarthritis (OA) pain, the prescription of glucocorticoids remains controversial because of potentially harmful side effects to multiple joint tissues, especially cartilage. One glucocorticoid, Dexamethasone (Dex) has been demonstrated to rescue the loss of aggrecan and collagen constituents as well as chondrocyte viability in human and bovine cartilage explant models of inflammatory tissue injury and post-traumatic OA (PTOA) [16,18], suggesting the possibility of Dex as a disease-modifying drug. However, literature covering the effects of Dex on cartilage reveals conflicting results on the drug's safety profile [129]. Importantly, the anti-catabolic versus pro-catabolic effects of Dex on the cartilage extracellular matrisome, as well as the fate of intracellular proteins in the presence of tissue injury, remain unexplored. The goals of the present study are to utilize a discovery proteomics approach to quantify the loss of extracellular and intracellular proteins from cartilage explants subjected to inflammatory cytokine challenge and impact mechanical injury, and to determine whether Dex protects against or exacerbates the response.

Li *et al.* [18] demonstrated in an interleukin-1 (IL-1) challenge of full-thickness near-normal human cartilage explants that culture with 100 nM Dex continuously over a 17-day treatment rescued sulfated glycosaminoglycan (sGAG) loss and maintained more viable cells, relevant to potential PTOA prevention. Dex also rescued the cytokine-induced decrease in sGAG synthesis in this disease model, though not reaching control levels. These results showed beneficial effects of Dex on cartilage metabolism and extracellular matrix (ECM) synthesis in a model of early PTOA. Using human tissue in a tumor necrosis factor alpha (TNFα), interleukin-6 (IL-6), and single compressive injury challenge of normal human knee explants, Lu *et al.* [16] found that continuous

Dex treatment rescued sGAG loss. In a similar cytokine model, a targeted proteomics approach identified increased levels of ECM components released to the media, including aggrecan, cartilage oligomeric matrix protein (COMP), and collagen III, compared to untreated explants [130].

At the same time, deleterious effects of Dex on cartilage tissue have been reported. Several studies using isolated human chondrocytes showed that even low doses of Dex can cause cell death and reduce cell proliferation, suggesting potential cytotoxic and catabolic side effects. However, the observed effects of Dex depends greatly on dose, model, duration of treatment and context (*e.g.*, isolated cells *versus* intact cartilage). Thus, study conclusions often differ greatly, even when studying intact cartilage explants, complicating the discussion of safety and efficacy of Dex [129].

These disparate results on cartilage tissue response to Dex have typically focused on select few matrix macromolecules without the benefit of a more encompassing view that could be provided by a systems-level analysis of changes to cartilage. Thus, the specific objectives of the present study are to (1) use a global discovery proteomics approach to quantify the effects of inflammation and mechanical impact injury on cartilage explants, and (2) study the effects of Dex in the presence and absence of inflammatory and injurious mechanical challenges. We believe this approach can lead to an increased understanding of the potential benefits of a glucocorticoid such as Dex, as well as the identification of biomarkers of cartilage degradation in the presence and absence of such treatments.

2.2 Materials and Methods

2.2.1 Explant harvest and culture

Cartilage disks (3 mm x 1 mm thick including the intact superficial zone) were harvested from the femoropatellar grooves of 1-2-week-old bovines (Research '87, Boylston, MA) as described [18], **Figure 2.1**. One knee joint from each of three different animals were used. After harvesting, explant disks were pre-equilibrated for two days in serum-free medium (low-glucose phenol-red free Dulbecco's Modified Eagle's Medium (DMEM), ThermoFisher Scientific) supplemented with 10 mM HEPES buffer (Gibco), 2 mM L-Glutamine (Gibco), 0.1 mM nonessential amino acids (Sigma), 0.4 mM proline (Sigma), 20 µg/ml ascorbic acid (Sigma), 100 units/ml penicillin G, 100 µg/ml streptomycin, and 0.25 µg/ml amphotericin B (Sigma), and 1% insulin-transferrin-selenium (10 µg/ml, 5.5 µg/ml, and 5 ng/ml, respectively; Sigma).

2.2.2 Explant treatments

After pre-equilibration, samples were treated for 22 days as in **Figure 2.1**: no treatment (N), mechanical injury at day 0 (a single unconfined compression at 50% final strain, 100%/s strain rate, followed by immediate release at the same rate [131]; treatment I); cytokines (10 ng/ml recombinant human TNFα, 20 ng/ml recombinant human IL-6 and 100 ng/ml sIL-6R (R&D Systems); treatment C); injury+cytokines (treatment IC), with all four treatment groups additionally receiving 100 nM Dex (treatments D, ID, CD, and ICD, respectively). Medium changes were carried out every two days and collected medium was stored at -80°C until analysis.

2.2.3 Mass spectrometry preparation and identification

Culture medium (50 µL) from days 4, 8, 12, 16, and 20 (**Figure 2.1**) was prepared for mass spectrometry (MS) analysis as described [130]. Discovery MS was performed on medium samples using a quadrupole Orbitrap benchtop mass spectrometer (Q-Exactive, Thermo Scientific). Identification was performed using the UniProt Bos Taurus database (UP_000009136, 2017-10) with Proteome Discoverer 2.2 (Thermo Scientific). The protein false discovery rate (FDR) was 0.01. Label-free protein abundance quantification was obtained by summing peak area intensities from multiple unique peptides for each protein.

2.2.4 Data analysis

Proteins identified in all three animals were filtered, keeping only proteins identified and quantified in at least 5% of samples. Assuming that missing values were due to low abundance, missing values were imputed using quantities equal to half the lowest identified abundance for each protein. Abundance data were $\log_2$-transformed and principle component analysis (PCA) was performed on treatments N, I, C, and IC using the "prcomp" function in the R-package factoextra, with ‘center’ and ‘scale’ set to true to z-score values. Pairwise comparisons between treatments were performed on the summed peptide abundance over all five timepoints. Statistical analysis was performed using the R package limma, comparing $\log_2$-fold changes within each animal [132]. *P*-values were obtained using empirical Bayes statistics. Adjusted *p*-values were calculated using the Benjamini-Hochberg method with a *q*-value of 0.05.

2.2.5 Grouping of shared protein responses

Proteins were classified into three groups based on their response to treatments C and IC compared to control. The grouping criteria were: (I) decreased release in treatments C and/or IC, (II)

increased release by treatment C alone, or (III) increased release in IC with or without increased release in C. Proteins were selected if they had a differential effect from the control (p<0.05) and were present in at least three timepoints for one treatment condition across all three animals. Grouping criteria were based on patterns identified with hierarchical clustering of proteins with differential release from control, and validated against the raw, non-imputed data by two operators (AS, PÖ).

2.2.6 Enrichment analysis

Because of limitations in the annotation of the bovine proteome, we translated bovine accession numbers into human equivalents using blastp protein searches [133]. Enrichment analysis was performed by searching the Gene Ontology (GO) and STRING databases for biological process, molecular function, and Kyoto Encyclopedia of Genes and Genomes (KEGG) pathways [134–136]. Protein subcellular localization was determined via UniProt annotation [137]. *P*-values for intra- and extracellular groupings were determined through bootstrapping with all differentially expressed proteins as background and 10,000 repeats to generate estimated distributions [138].

2.2.7 Biochemical and Western blot analysis of aggrecan and cartilage oligomeric matrix protein (COMP) fragments

The amount of sGAG released to the culture medium over the 22-day culture was determined using the 1,9-dimethylmethylene blue assay (DMMB) [139]. The same samples were deglycosylated with chondroitinase ABC, keratanase and keratanase II as described [140], with the exception that keratanase II incubation was done for 3 hours with 0.01 mU/µg sGAG. Deglycosylated samples were precipitated and electrophoresed as described [141], separated by sodium dodecyl sulfate-

polyacrylamide gel electrophoresis (SDS-PAGE) and transferred to polyvinylidene difluoride (PVDF) membranes. Immunoreactions were performed using anti-ARGS aggrecan neoepitope antibodies [142] or anti-G3 aggrecan polyclonal antibodies (all tested for specificity [143],) and immunobands were visualized with secondary horse anti-mouse peroxidase-conjugated antibodies using enhanced chemiluminescence (ECL).

The breakdown of COMP was analyzed as described [144,145]. Twenty microliters of culture media were taken every second day from a separate set of bovine explant cultures (treatments N and IC, in the presence and absence of the combination of 100 nM Dex and continuous dynamic compression (10% strain amplitude, described previously [131])). Samples were separated by SDS-PAGE, transferred to a nylon membranes and incubated with rabbit anti-bovine COMP polyclonal antiserum [145]. Immunobands were visualized with secondary peroxidase-conjugated antibodies using ECL. Purified bovine COMP [145] was used as a reference.

2.3 Results

MS analysis identified 671 proteins; 500 proteins were found in all three animals (**Figure 2.2A**). The raw data are available via ProteomeXchange with identifier PXD020756 [146]. After filtering as described in Methods, the data set was reduced to 456 proteins. PCA clustering on log_2-transformed abundance data (**Figure 2.2B**) revealed cytokine treatment as the major determinant of medium composition: one cluster is seen for control and injury (N, I) and another cluster for samples treated by cytokines with and without injury (C, IC). Mechanical injury only (treatment I) had a marginal effect on this cytokine-dependent clustering. Therefore, treatment I was excluded

from the grouping criteria because of the low number of proteins significantly affected by that treatment and its similarity to control.

2.3.1 Comparison between explant treatments

Pairwise comparison between treatments showed a major effect of treatments C and IC: 175 proteins (149 up, 26 down) and 115 proteins (94 up, 21 down) respectively, were observed to have a difference from control. 195 proteins in total had a differential effect of treatments C and IC versus control, and 88 proteins had a differential effect of Dex on control, cytokines, or injury+cytokines (FDR = 0.05). After filtering for proteins present in at least one consistent treatment condition across all three animals, there were a resulting 188 proteins differentially released by treatments C or IC (**Figure 2.3**).

2.3.2 Protein selection into similar signal-response groups

The 188 filtered proteins were classified into three response groups (**Table 2.1**), illustrating treatment effects as well as the effects of Dex intervention. Compared to control, 156 proteins (83% of the 188 selected proteins) had increased release in conditions C and IC, while 32 proteins (17%) were decreased. We selected one representative protein from each response group with a clear representation of that group's trend to illustrate treatment effects in the presence and absence of Dex: type II collagen (COL2A1), phosphoglycerate kinase 1 (PGK1), and collagenase-3 (MMP-13) (**Figure 2.4A-C**). We further categorized the most highly enriched GO annotations for biological process and molecular function. Groups I and III had a high proportion of extracellular proteins (67% and 51% (p<0.0001), respectively, versus 42% for the entire population of 188

proteins). Group II was enriched (p<0.0001) for intracellular proteins (78% versus 47% in the entire population), while consisting of only 4% extracellular proteins.

2.3.3 Protein network analysis

STRING network analysis revealed two small network interaction clusters for proteins in Group I (**Figure 2.5A**): ECM-related proteins including collagens II and IX, and a cluster enriched for protein metabolism and IGF transport and uptake. The network map for Group II (**Figure 2.5B**) consisted of one large, highly interconnected cluster enriched for immune and RNA-metabolizing proteins, as well as a diverse subset of proteins involved in metabolic processes, including glycolysis, redox homeostasis, endoplasmic reticulum function, and protein synthesis. The pathways enriched in the largest cluster of Group III were ECM organization and the immune system, with a distinct cluster of histone proteins (**Figure 2.5C**).

2.3.4 Dexamethasone treatment

The effects of Dex on the release of the 188 selected proteins to the medium is shown in **Table 2.1**. Compared to treatments without Dex, 34 proteins (18%) had significantly decreased signal in the presence of Dex, while 11 proteins (5.4%) had increased signal. In the largest protein group (III), 31 of the 92 proteins (34%) showed reduced release following Dex treatment. A small number of proteins experienced an effect in every condition with Dex compared to that condition without Dex (**Table 2.1**), exemplified by connective tissue growth factor (CTGF) in **Figure 2.4D**.

2.3.5 Release of aggrecan and COMP fragments

Cytokine and injury treatments had no effect on the release of aggrecan fragments by proteomic analysis, but were evaluated in parallel by the DMMB assay for sGAG release (**Figure 2.6A**). Treatments C and IC caused a 2- to 3-fold increase in sGAG release compared to controls; this release was significantly reduced by addition of Dex. Western blot analysis supported these findings indicated by the release of aggrecanase-generated ARGS-CS2 fragments (**Figure 2.6B**), and by the release of smaller aggrecanase generated G3-CS2 fragments [143] upon treatment with cytokines and injury+cytokines (**Figure 2.7**). The release of these aggrecan fragments was rescued by treatment with Dex.

While our MS analyses of COMP release in the present study indicated no clear treatment effects (**Figure 2.4E**), Western blots indicated a dramatic increase in COMP degradation manifested by the release of smaller COMP fragments after addition of injury+cytokines and a partial amelioration of COMP fragment release upon Dex treatment (**Figure 2.8**).

2.4 Discussion

This study incorporates a global discovery approach to characterize the effects of inflammation and mechanical injury on cartilage explants, including the role of therapeutic intervention with Dex. This glucocorticoid treatment has been used with intra-articular injection for treatment of arthritic or post-surgery knee pain [147,148] with sometimes disappointing results [14], due in part to rapid clearance from the joint space before penetration into cartilage [119,149,150]. In some clinical trials with glucocorticoids, very high, frequent doses were used, leading to adverse effects

such as a reported decrease in cartilage volume without any reduction in knee pain [10]. However, *ex vivo* explant studies have shown that sustained low doses of Dex can rescue sGAG loss, reduce proteolytic enzyme synthesis, and maintain chondrocyte viability under inflammatory cytokine challenge [18].

The present study is based on label-free protein quantification allowing a semi-quantitative estimation of relative protein abundances. Cytokine treatment, in particular, exhibits a large effect on proteins released into the explant culture media, while treating with mechanical injury alone has a small effect, as demonstrated by the overlap of the two treatments in PCA space (**Figure 2.2B**).

2.4.1 Catabolic processes are activated under arthritic stress:

After an acute joint injury, the progression of PTOA is initiated by an early response characterized by the production of inflammatory factors and proteases, including MMPs, in reaction to inflammatory stress and chondrocyte death [151]. The transport into cartilage of inflammatory factors released from the synovium is thought to be further enhanced by microdamage to the cartilage surface caused by mechanical impact [152]. Together, these changes lead to progressive degeneration of the ECM which can cascade into irreversible matrix loss and PTOA [153].

In our model, we confirmed the PTOA-like effects of IL-6 and TNFα on bovine cartilage explants by examining the release of sGAGs over the three-week course of the experiment (**Figure 2.6A**).

We found an increased cumulative release of sGAG into the culture media upon cytokine treatment, consistent with previously published data from a similar experiment [16]. The sGAG release is associated mainly with proteolysis of aggrecan, as confirmed by release of ARGS-CS2 and G3-CS2 fragments (**Figure 2.6B**).

2.4.2 Groups II and III demonstrate cartilage catabolic response to inflammatory and mechanical stress

Group III, proteins with increased release after exposure to inflammatory cytokines with or without applied injury, best represents the catabolic response of cartilage to PTOA stress. This group is the largest and represented by MMP-13 (**Figure 2.4C**), an active protease in the breakdown of a range of cartilage proteins in OA [154]. Protein categories in Group III include proteases and protease inhibitors (ex. MMP-1, -3, -9, -13, plasma protease C1 inhibitor, plasminogen activator inhibitor 1, and serpin H1) signaling (ex. C-C motif chemokine 5, ephrin-A1, inhibin, and transforming growth factor beta-2 (TGFβ-2),) and ECM (ex. collagen VI, fibrillin-2, fibronectin, tenascin). These results suggest that Group III proteins are those actively released from the cartilage after the induction of PTOA: the degradation products of cleaved ECM components and the proteases, protease inhibitors, and other signaling factors associated with catabolic responses.

Inflammatory stress also disrupts intracellular processes and leads directly to chondrocyte death [18]. The dysregulation of chondrocyte homeostasis under disease stress can be observed within Group II proteins, whose release was increased by exposure to inflammatory cytokines alone and consist of majority intracellular proteins. The protein representing this group is PGK1, (**Figure**

2.4B), a major enzyme in the glycolytic pathway. It is notable that many of the proteins in this group are involved in cellular metabolism (ex. glyceraldehyde-3-phosphate dehydrogenase, L-lactate dehydrogenase, PGK1, phosphoglycerate mutase 1), endoplasmic reticulum processing (ex. 78 kDa glucose-regulated protein, protein disulfide-isomerase A6, calreticulin), or ribosomes (ex. ribosomal proteins L10A, L12, P0, and P2). The biological reason for the increased release of these proteins may be due to transcriptional or translational changes in response to cytokine treatment, or a result of cell death causing these highly abundant intracellular proteins to be released from necrotic cells.

2.4.3 Dexamethasone rescues some catabolic processes

The increased release of one third of the proteins in Group III was partially or completely rescued by Dex, including all four MMPs in this group. This finding agrees with literature supporting the observations that Dex inhibits the production of MMPs under arthritic stresses and prevents ECM breakdown as measured by sGAG loss and histological staining [129]. This effect of Dex was specific to the proteins in Group III from treatments CD or ICD: the proteins involved in ECM organization (including fibrillin, versican, five MMPs, TGF-β, and plasma protease C1 inhibitor) that Dex reduced from Group III were not affected by Dex alone, except a slight increase in MMP-13 release. However, Dex did not rescue the increased release of most of the proteins in Group II. Dex has been shown to protect against inflammatory cytokine-induced chondrocyte death [18], but many Group II proteins had high release at the earliest timepoint which was not prevented by Dex, suggesting that Dex may not prevent an early cellular response to inflammatory cytokines. This result may also be influenced by changes in protein synthesis. It has been hypothesized that

Dex suppresses cartilage metabolism, but whether these effects are propagated through changes in protein synthesis has not yet been explored [129].

2.4.4 Some anabolic processes are inhibited by PTOA stress

As catabolic processes continue in diseased cartilage, chondrocytes begin to produce chondroprotective and anabolic factors that initiate reparative processes to reverse proteolytic and inflammatory damage [151]. Group I represents proteins exhibiting decreased release after C or IC treatment, many of which would contribute to protective and anabolic responses, represented by collagen II, the most abundant collagen in cartilage (**Figure 2.4A**). Collagen IX has a similar pattern of release. It is likely that the reduced release of these proteins is due to decrease in their synthesis. With decreased release, the major effect on their release from cartilage would not be proteolysis or the increased permeability of degrading ECM. In a previous study using injury+cytokine-treated human knee cartilage, the release of the C-terminal pro-peptide of collagen II, a synthesis marker, was decreased [130]. The decrease in the synthesis of these proteins could be related to early suppression of fibrillogenesis of collagen II, which associates with collagens IX and XI to form thin collagen fibrils [155].

The release of lysyl oxidase (LOX), an enzyme that regulates fibrillogenesis and collagen synthesis [156,157], was also inhibited by cytokine addition. Another member of Group I, chondromodulin (CNMD) maintains cartilage homeostasis by preventing hypertrophic differentiation and remodeling to bone [158]. The release of some proteins may be affected by the developmental state of the tissue used in our model: chordin-like-2 (CHRDL2,) which inhibits chondrocyte

mineralization, and the signaling protein collagen triple helix repeat containing-1 (CTHRC1), have been found to be increased in human osteoarthritic cartilage, chondrocytes, or synovial fluid in other studies [159–161]. However, CHRDL2 is also expressed in differentiating chondrocytes, and CTHRC1 is expressed in developing growth plate cartilage [162], so the effect on their release may be associated with the juvenile tissue used in this study and not a protective response.

Certain proteins identified in Group III also reveal an increase in some chondroprotective processes. For example, the glycoprotein osteoprotegerin (TNFRSF11B) can suppress osteoclastogenesis and bone resorption [163,164]. Thrombospondin-2 (THBS2) is a chondrogenic growth factor, and chondrogenesis has been suggested as protective against OA progression [165,166]. In contrast to collagen II and IX, collagen VI, a major component of the pericellular matrix [167], showed increased release after IC treatment. Overall, it appears that some chondroprotective and anabolic processes may be activated after cartilage experiences injury or inflammation, while others are inhibited, possibly reducing the ability of the cartilage to resist subsequent damage to the matrix.

2.4.5 The effect of Dex on anabolic and chondroprotective factors is inconsistent

Dex does not reverse the effect of inflammatory cytokines for many proteins in Group I. For example, the release of LOX and testican-1 (SPOCK1, a member of the SPARC family) was rescued up to or above control levels, but the release of SPARC was not affected by Dex, suggesting that the actions of Dex on cartilage under arthritic stress do not result in a perfect rescue. This is also reflected in the behavior of collagens II and IX, as Dex did not rescue or further

decreased their release (which was attributed to a decrease in synthesis). Previous studies on the effects of Dex on collagen synthesis have often reported conflicting results [129].

2.4.6 Dex induces the release of proteins not present in any other condition

Highly relevant to the consideration of Dex as a PTOA disease-modifying drug are "side effects" of Dex: Dex causes a significant increase in the release of some proteins in all treatment conditions, such as CTGF (**Figure 4D**). CTGF is directly activated by glucocorticoids in its upstream promoter region, and is involved in a complex signaling network involving TGF-β signaling and joint homeostasis [168,169]. Dex is widely accepted to inhibit MMP production and/or activity [129], possibly in our model by stimulating the production of protease inhibitors such as SPOCK1, a pro-MMP2 inhibitor found in cartilage [170], and alpha-1-antiproteinase (SERPINA1), a broad protease inhibitor [171]. Our observation that Dex affects such proteins even without disease stress suggests that there may be some dysregulation in the maintenance of the cartilage matrix in healthy cartilage exposed to Dex during treatment. The effects and side effects of Dex will be affected by its concentration in the cartilage tissue: in this experiment, we used the low dose of 100 nM Dex, which has been shown to be effective in ameliorating sGAG loss in immature bovine tissue under inflammatory stress [16]. This dose is orders of magnitude lower than typical clinical injections, but novel targeted delivery methods can achieve a low, sustained dose in cartilage, removing the need for repeated high-dose injections of Dex to achieve clinical efficacy [119,149].

2.4.7 Study limitations

Proteomics is a powerful tool to measure changes in global protein expression at a high level and identify changes to entire pathways, but has some limitations. This analysis utilized data from a small number (48) of single-peptide identifications, which are less reliable for quantitation than proteins with more peptide coverage, but kept for analysis because of their identification at a FDR of 0.01 and their presence in at least 5% of samples. An MS approach summing peptide abundances reflects total protein level and is less sensitive to small changes in cleavage events, such as with COMP and aggrecan. Our proteomics results do not reveal a clear effect on treatment with cytokines; in contrast, the western blots show clear proteolytic cleavage (COMP: **Figure 2.4E**, **Figure 2.8**; aggrecan: **Figure 2.6B**, **Figure 2.7**). Some limitations could be circumvented by using an enzyme other than trypsin, though every enzyme will experience limitations based on its cleavage sites. While adult human cartilage may show some differences in the process of cartilage breakdown, this bovine model has been well-established as a model of PTOA progression in a more accessible and repeatable way than human cartilage. Three animals is a low number of replicates for robust statistical analysis, though somewhat offset by the repeatability of this bovine model. Future repeats and validation will strengthen the identified trends. Some observations here may be due to the early developmental state of the cartilage. Ongoing studies using adult human cartilage explants will be compared to the bovine results, and investigate the effects of bone and synovial responses to inflammation and crosstalk with cartilage such as the development of OA-related osteoporosis or Dex side effects [98].

2.5 Conclusions

In this exploratory study, we used a discovery proteomics approach to follow the release of proteins in response to mechanical damage and cytokine treatment of bovine knee articular cartilage. We

also investigated the effect of a low, continual dose of the glucocorticoid Dex. The majority of differentially expressed proteins were increased upon treatment but some proteins, including the fibrillar collagens II and IX, were reduced. A large number of the proteins with increased release after disease treatment had reduced release in the presence of Dex. These disease-induced proteins could be potential biomarkers of the inflammatory contribution to cartilage degradation and demonstrate the protective effect of Dex against matrix breakdown and protease release. Analyzing proteins released from the cartilage also allowed some insight into the dysregulation of anabolic processes after disease induction: the release of some anabolic factors was increased after cytokine exposure, suggesting attempts to protect against and repair catabolic effects, while many other anabolic factors had their release suppressed by cytokine exposure. Dex treatment had mixed effects on these changes, highlighting the need for further experiments to explore the effect of Dex on intracellular processes in tissue models of OA. The design of this study will allow for further exploration of regulation of protein release kinetics after disease or Dex treatment.

Acknowledgements

Supported by grants NIH-NIAMS AR060331 and NIH-NCATS UG3/UH3 TR002186 (AJG), A*STAR (Singapore) Fellowship and Poitras Pre-doctoral Fellowship (YW), the Swedish Research Council (2014−3303), the Swedish Rheumatism Association (AS and PÖ), the Krapperup Foundation (PÖ), the Alfred Österlund Foundation (AS, PÖ), the Greta & Johan Kock and Crafoord Foundations (AS, PÖ). We thank Takehiko Nakamura (Seikagaku, Japan) for the kind gift of keratanase and keratanase II, Sanjay Kumar and Michael Pratta (GSK, Collegeville, PA, USA) for the kind gift of the neoepitope monoclonal OA-1 antibody against ARGS-aggrecan. We are grateful to statistician Dr. Aleksandra Turkiewicz for input and discussions regarding study design and data analysis.

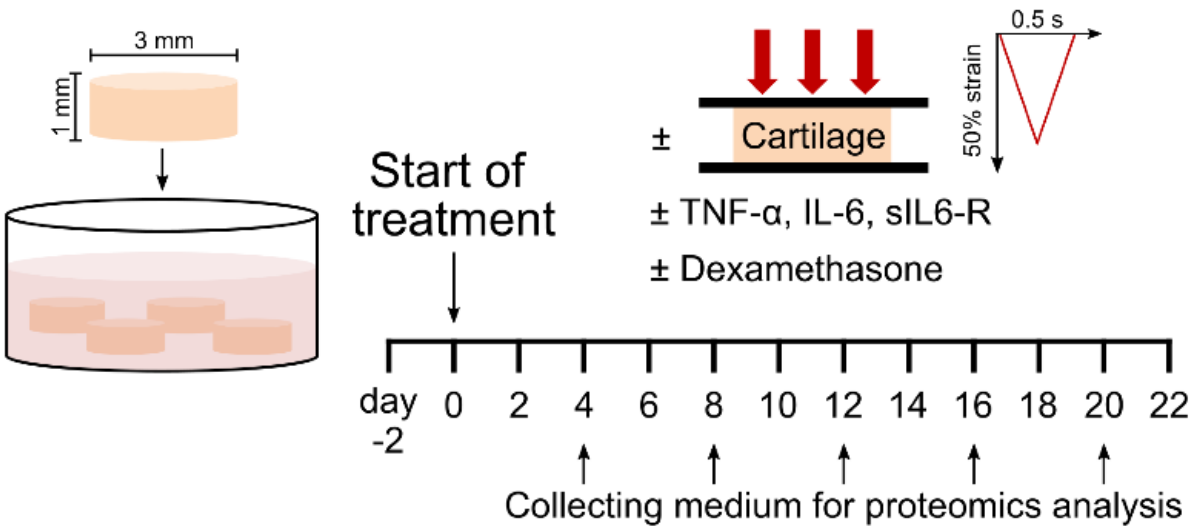

Treatment conditions:

N = no treatment	D = Dex alone
I = mechanical injury	ID = injury + Dex
C = cytokines	CD = cytokines + Dex
IC = injury + cytokines	ICD = injury + cytokines + Dex

Figure 2.1. Experimental setup. Bovine articular cartilage explants (3 mm x 1 mm cylinders including the superficial zone, 4 per well) were cultured for three weeks according to the following treatment conditions: (N) untreated controls; (I) a single applied mechanical impact injury (50% final strain at a strain rate of 100%/s, followed by immediate release at the same rate); (C), addition of cytokines: TNFα, IL-6 and sIL-6R (10 ng/ml, 20 ng/ml, and 100 ng/ml, respectively) (IC), applied injury plus addition of cytokines; (D), untreated control + Dex (100 nM); (ID), applied injury + Dex; (CD), cytokines + Dex; or (ICD), applied injury + cytokines + Dex. Culture medium was changed every two days, and three biological replicates (animals) were used for all treatment conditions.

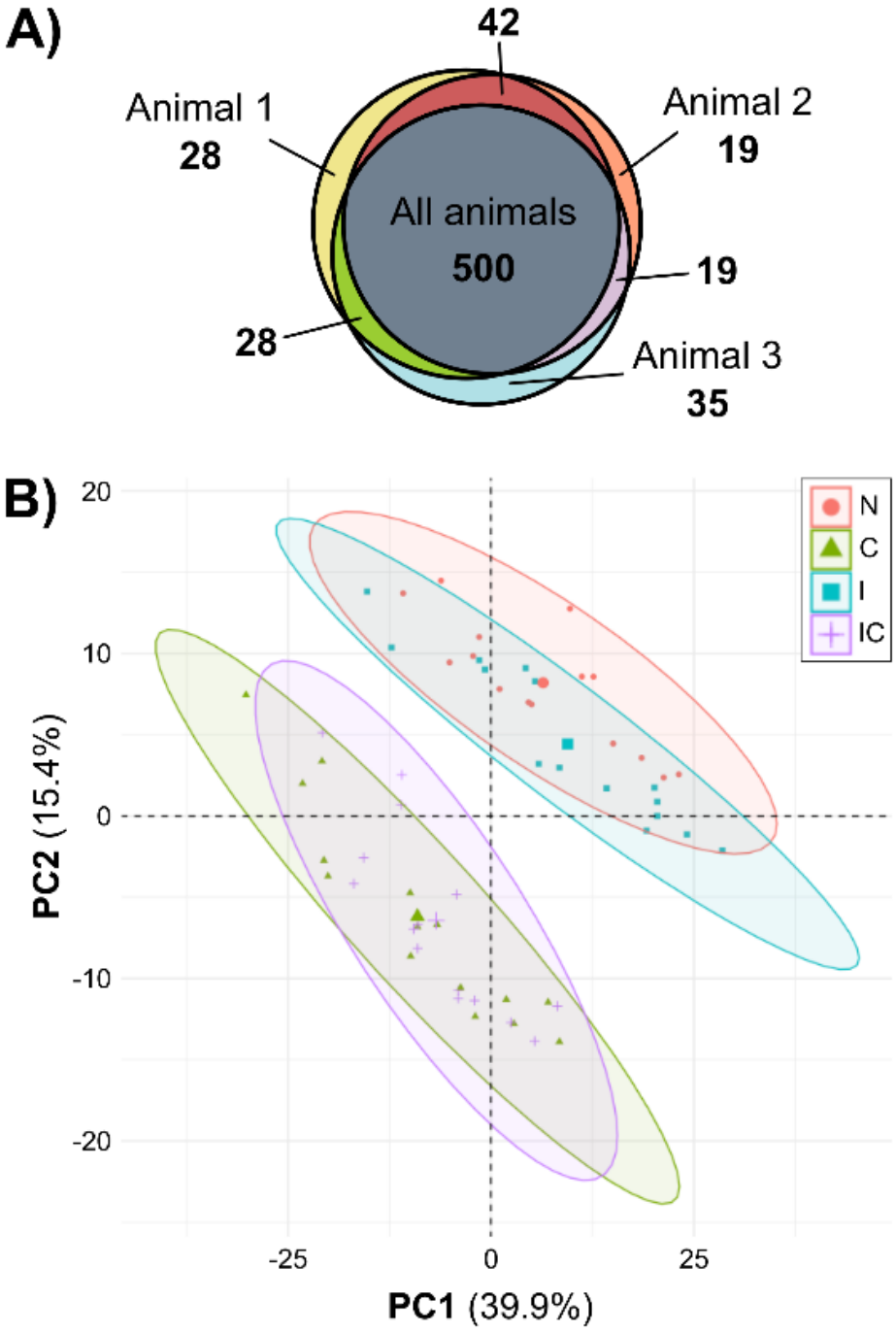

Figure 2.2. Proteomic overview of the three biological replicates. (A) A Venn diagram reveals a large overlap of MS-identified proteins between biological replicates. 500 proteins were found in medium samples from all three animals, and few proteins were found in only one or two animals. **(B)** Principle component analysis (PCA) was performed using abundance values for 456 filtered proteins obtained from MS analysis of cartilage explant medium samples taken on day 4, 8, 12, 16, and 20 of culture from the treatment groups control (N), injury (I), cytokines (C), and injury+cytokines (IC). The data clearly separate into two clusters, one with treatments N and I, and the second with treatments C and IC. Percentages on axes represent percent variance explained by that principal component. The large symbol within each cluster represents the cluster centroid.

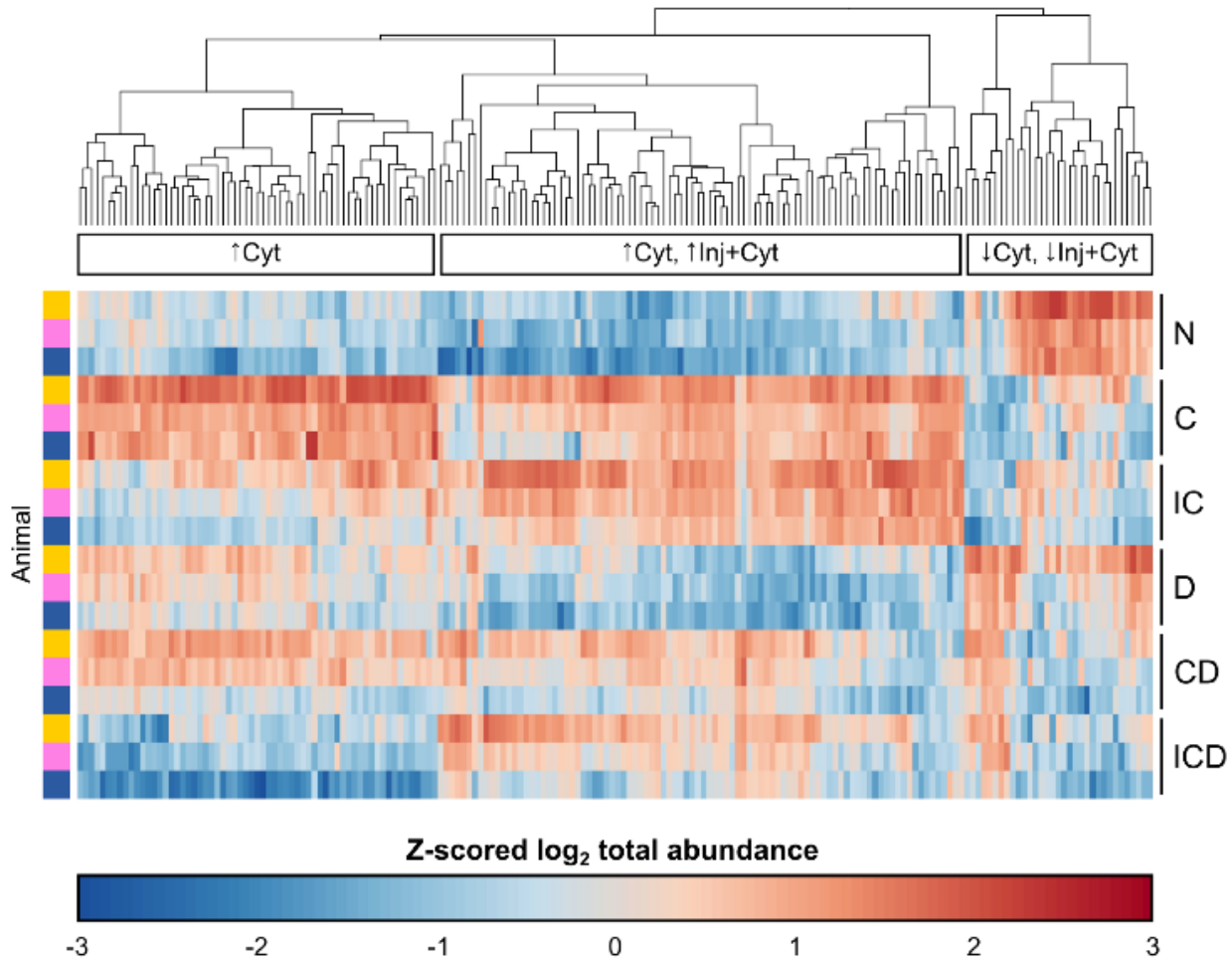

Figure 2.3. Heatmap of proteins significantly affected by disease treatment. Treatment effects were evaluated by pairwise comparisons of MS abundance data (log_2 summed ratios with imputation of missing values, FDR = 0.05) of different disease treatments within each animal replicate. Proteins were selected that had a differential effect of C or IC treatments and that were present in at least three time points across at least one consistent treatment condition between all three biological replicates (to avoid biases from imputing missing values), resulting in 188 selected proteins. The raw abundance value for each filtered protein was summed over all timepoints and log_2-transformed. For visualization, the log_2-transformed values were normalized via z-scoring across all treatment conditions, excluding injury alone and injury with Dex: control (N), cytokine (C), injury+cytokines (IC), Dex (D), cytokines+Dex (CD), and injury+cytokines+Dex (ICD). Proteins are plotted on the horizontal axis, and ordered based on their hierarchical clustering (Euclidian distance) across all six selected treatment conditions. Each individual replicate is plotted on the vertical axis, ordered by treatment condition and then by animal. The clustering reveals three major patterns of protein release: increased release by cytokines alone (↑Cyt), an increase by both cytokines and injury+cytokines (↑Cyt, ↑Inj+Cyt), and decreased release by cytokines and injury+cytokines (↓Cyt, ↓Inj+Cyt). These three patterns were used to designate the grouping categories in Table 1.

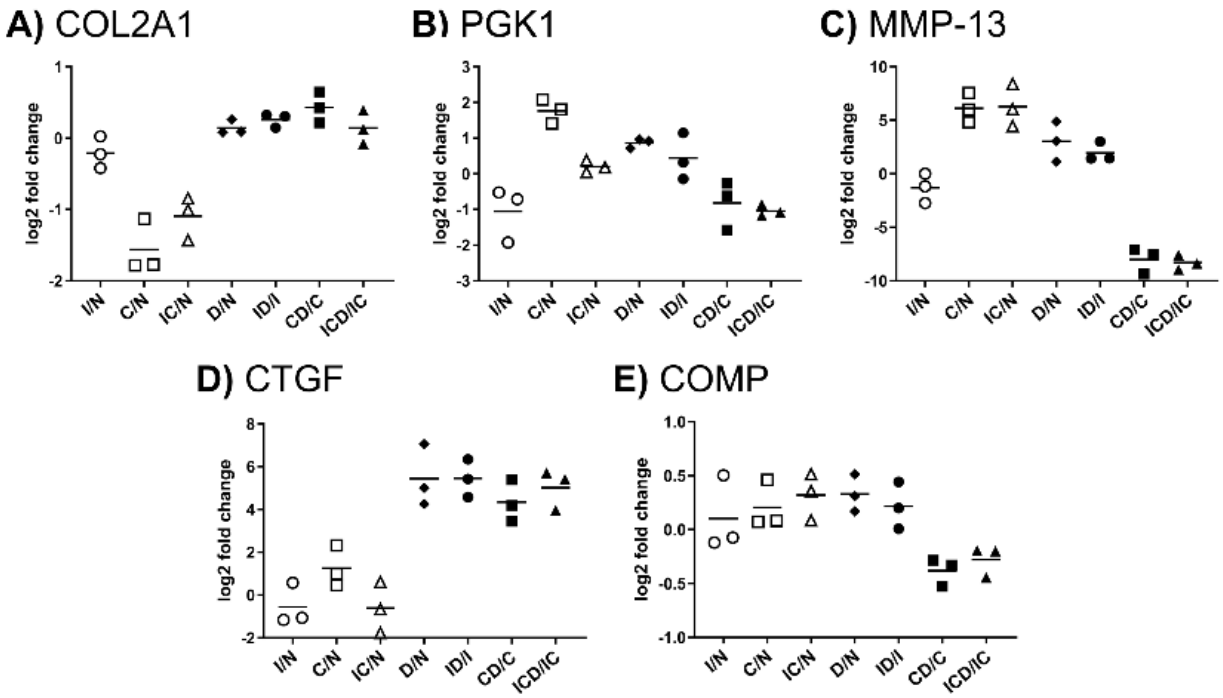

Figure 2.4. Representative proteins for each response profile. The simplified graphical representation for each protein shows the ratio for each treatment comparisons: injury (I), cytokines (C), and injury+cytokines (IC) versus control (N), and treatments with Dex versus their non-Dex controls: D *vs*. N, ID *vs*. I, CD *vs*. C, and ICD *vs*. IC. The mean fold change values from three replicates are indicated with horizontal lines. Representative proteins for the different profile categories (**Table 1**): **(A)** Group I, collagen type II (COL2A1); **(B)** Group II, phosphoglycerate kinase (PGK1); **(C)** Group III, collagenase-3 (MMP-13). Also shown are **(D)** connective tissue growth factor (CTGF), a representative of proteins with a consistent effect of Dex after addition to any treatment, and **(E)** cartilage oligomeric matrix protein (COMP), which undergoes no statistically significant change in release with any treatment.

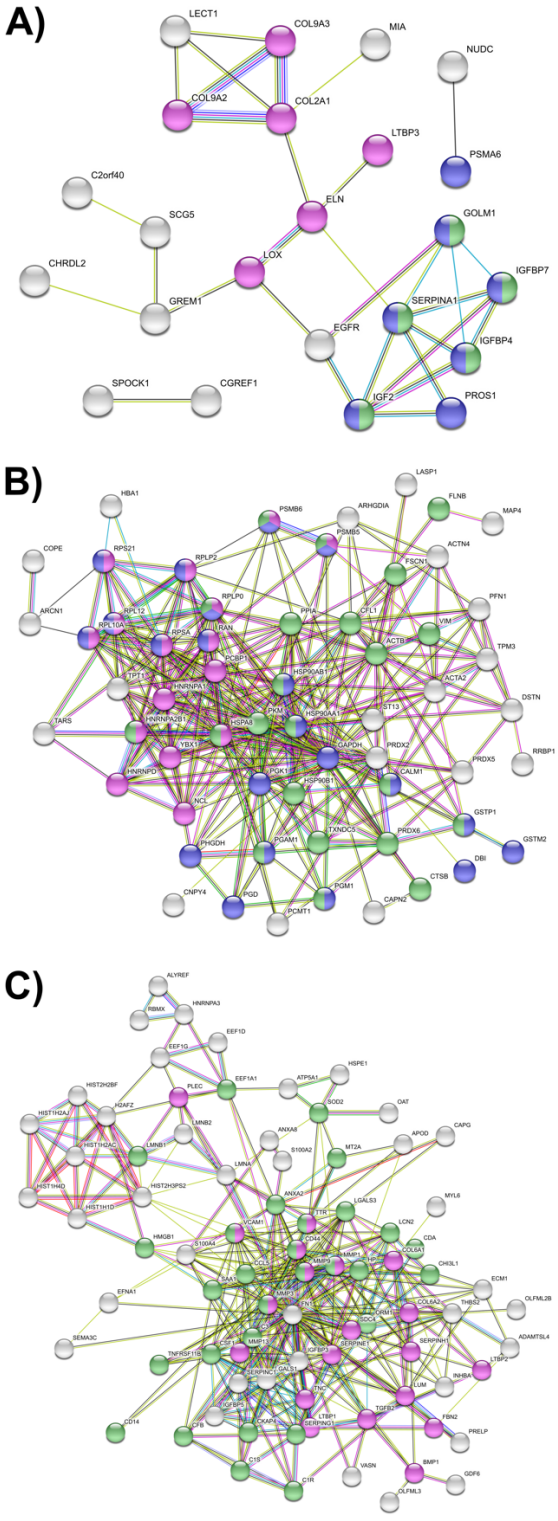

Figure 2.5. STRING network analysis plots. STRING network maps of proteins in each of the three groups of shared release profiles, colored based on KEGG pathway enrichment. Unconnected nodes were removed from network maps. **(A)** Group I: proteins with decreased release after C or IC treatment. Magenta: ECM and ECM-modifying proteins; blue: metabolism; green: IGF transport and uptake. **(B)** Group II: proteins with increased release after C treatment only. Magenta: RNA-metabolizing proteins; blue: metabolism; green: immune system. **(C)** Group III: proteins with increased release after C and IC treatment. Magenta: ECM organization; green: immune system.

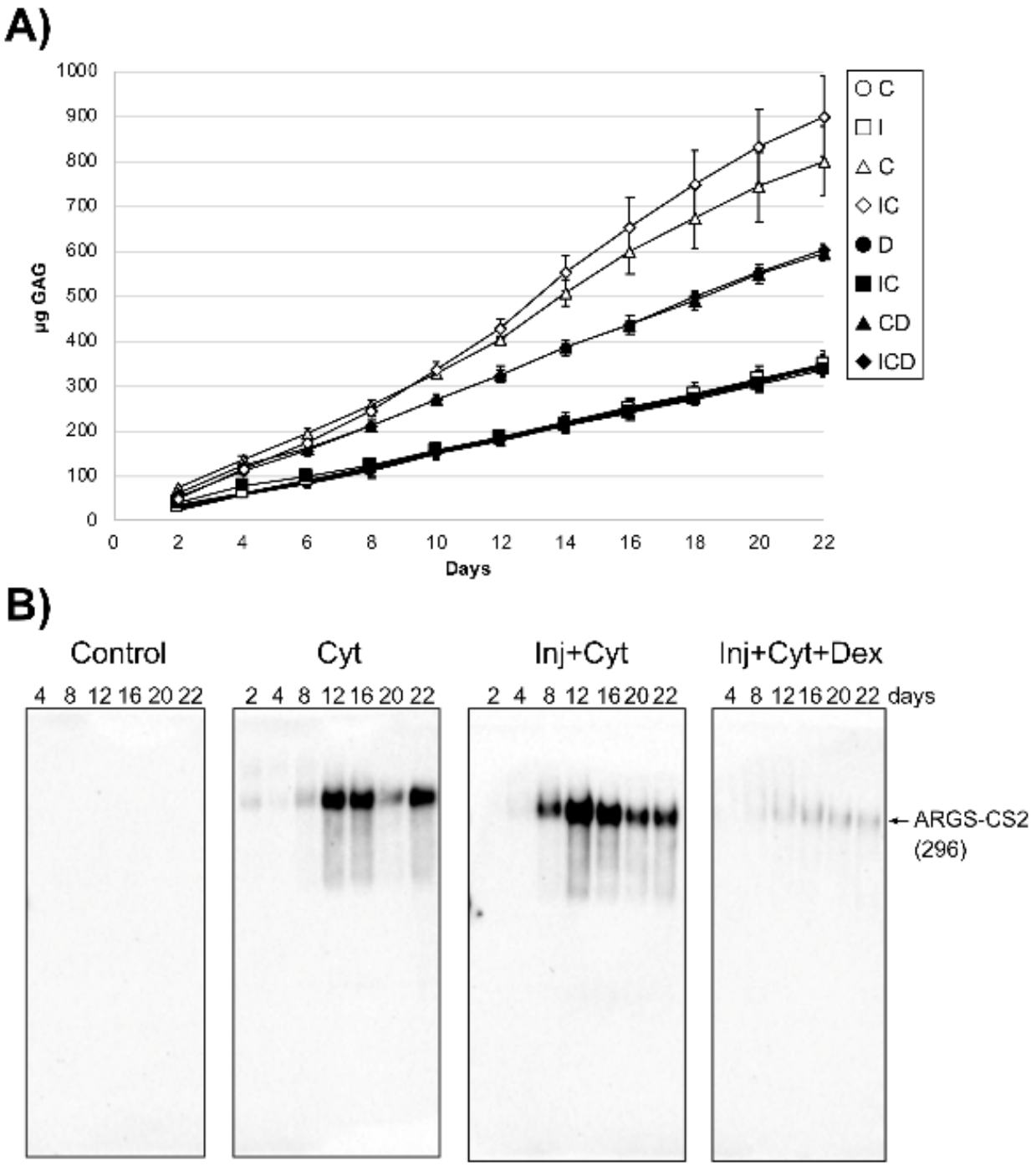

Figure 2.6. Time dependent release of aggrecan constituents into explant culture media. **(A)** Cartilage explants (n=3) were cultured from 2 up to 22 days. The amounts of sGAG (mean ± SD) released at each day of culture was measured by the DMMB assay for all treatment groups: control (N), injury alone (I), cytokine (C), injury+cytokines (IC), Dex (D), injury+Dex (ID), cytokines+Dex (CD), and injury+cytokines+Dex (ICD). The release of sGAG was elevated with cytokine treatment; the addition of Dex reduced this release. **(B)** Medium samples were deglycosylated and run (44 to 100µl medium/lane) on 3-8% Tris-acetate SDS-gels and applied for Western blot using ARGS-aggrecan N-terminal neoepitope antibodies. Bovine protein fragments (previously described [172]) and their molecular weight in kDa are shown at the right. CS2 = chondroitin sulfate region 2. Cyt = cytokine treatment, Inj = applied injury, Dex = Dex treatment.

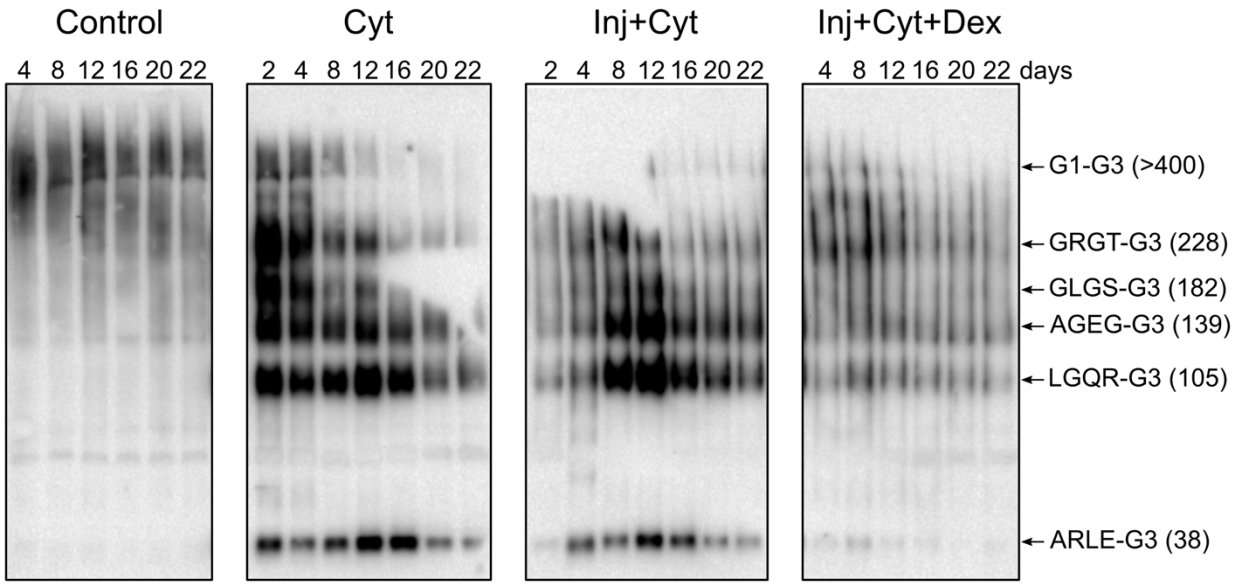

Figure 2.7. Aggrecan G3-fragment time dependent release into the explant culture medium. Treatment conditions: control, cytokines (Cyt), injury+cytokines (Inj+Cyt), and injury+cytokines+Dex (Inj+Cyt+Dex). Samples were deglycosylated and run (44 to 100 µl medium/lane) on 3-8% Tris-acetate SDS-gels and applied for Western blot using anti-G3-aggrecan antibody. Representative Western blots images from full-sized blotted gels are shown. Bovine protein fragments (previously described [143,172]) are shown at the right side with the molecular mass in kDa indicated. G3 = globular domain 3.

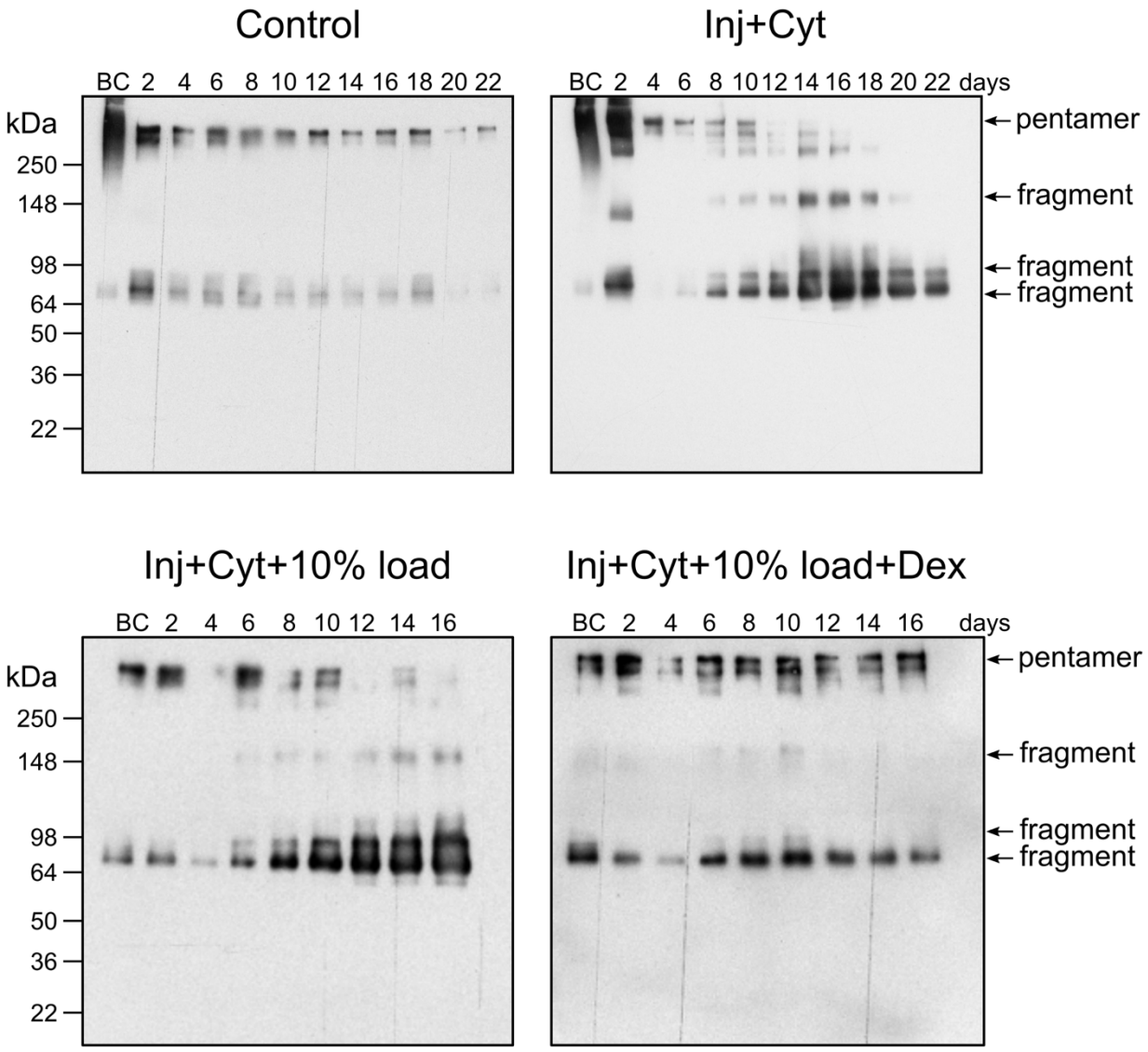

Figure 2.8. Time dependent release into medium of cartilage oligomeric matrix protein (COMP). Western blots were performed on culture medium collected from a separate experiment using cartilage cultured under the same conditions (control and applied injury + cytokines, Inj+Cyt), with the addition of 10% cyclic load. COMP whole pentamer proteolyzed fragments are indicated.

I (n = 32)	II (n = 64)		III (n = 92)		DEX (n = 6)
Inhibition by C and/or IC	*Increase by C alone*		*Increase by IC alone or C and IC*		*Dex effect in every condition*
ELN	**AGT**	*PCBP1*	**DKK3**	*CKAP4*	**AGT**
IGFBP4	*ACTA2*	*PCMT1*	**SAA1**	*COL6A1*	**CTGF**
IGFBP7	*ACTB*	*PFN1*	**TNFRSF6B**	*COL6A2*	**SERPINA1**
LOX	*ACTN4*	*PGAM1*	ANXA8	*COL6A2_2*	**SPOCK1**
SERPINA1	*ARCN1*	*PGD*	BMP1	*ECM1*	NUCB1
SPOCK1	*ARHGDIA*	*PGK1*	C1S	*EEF1A1*	RPL36A
SPON1	*BLVRB*	*PGM1*	CATHL1	*EEF1D*	
COL9A2	*CALM1*	*PHGDH*	CCL5	*EFNA1*	
ECRG4	*CAPN2*	*PKM2*	CDA	*FN1*	**Increased with Dex**
IGF2	*CFL1*	*PPIA*	CHI3L1	*H2AFZ*	Decreased with Dex
AEBP1	*CNPY4*	*PRDX2*	CSF1	*HIST1H1D*	*No change with Dex*
CDON	*COPE*	*PRDX5*	EEF1G	*HIST1H2AC*	
CGREF1	*CTSB*	*PRDX6*	FBN2	*HIST1H2AJ*	
CHRDL2	*DBI*	*PSMB5*	GDF6	*HIST1H4D*	
CLSTN1	*DSTN*	*PSMB6*	HAPLN3	*HIST2H2BF*	
CNMD	*EFEMP1*	*RAN*	HP	*HIST2H3PS2*	
COL2A1	*FLNB*	*RPL10A*	IGFBP5	*HMGB1*	
COL9A3	*FSCN1*	*RPL12*	INHBA	*HMGN3*	
CTHRC1	*GAPDH*	*RPLP0*	LGALS1	*HNRNPA3*	
EDIL3	*GSTM2*	*RPLP2*	LTBP1	*HSPE1*	
EGFR	*GSTP1*	*RPS21*	MMP1	*IGFBP3*	
EIF5B	*HBA1*	*RPSA*	MMP13	*LCN2*	
GOLM1	*HNRNPA1*	*RRBP1*	MMP3	*LGALS3*	
GREM1	*HNRNPA2B1*	*ST13*	MMP9	*LMNA*	
LTBP3	*HNRNPD*	*TARS*	OAT	*LMNB1*	
MIA	*HSP90AA1*	*TPM3*	OLFML2B	*LMNB2*	
NUDC	*HSP90AB1*	*TPT1*	PLEC	*LTBP2*	
PROS1	*HSP90B1*	*TUBA1D*	S100A2	*LUM*	
PSMA6	*HSPA8*	*TXNDC5*	SEMA3C	*M-SAA3.2*	
SCG5	*LASP1*	*Unknown***	SERPING1	*MT2*	
SULF2	*MAP4*	*VIM*	TGFB2	*MYL6*	
SUSD5	*NCL*	*YBX1*	THBS2	*OLFML3*	
			VASN	*ORM1*	
			VCAM1	*PRELP*	
			ADAMTSL4	*RBMX*	

** accession #G5E6G2

ALYREF	*S100A4*
ANXA2	*SAA3*
APOD	*SDC4*
ATP5A1	*SERPINC1*
C1R	*SERPINE1*
C3	*SERPINH1*
CAPG	*SOD2*
CCDC80	*TMA7*
CD14	*TNC*
CD44	*TNFRSF11B*
CFB	*TTR*

Table 2.1. 188 proteins grouped by response profile and proteins with consistent Dex effect. 188 selected proteins were categorized into subgroups (I-III) based on their shared release profiles under different treatment conditions. Those proteins with the same Dex effect in every treatment condition (D, CD, or ICD) are also listed. Proteins increased by Dex treatment are bolded, those decreased by Dex have no formatting, and proteins with no change with Dex are italicized.

Chapter 3. Proteomic Clustering Reveals the Kinetics of Disease Biomarkers in Bovine and Human Models of Post-Traumatic Osteoarthritis

Rebecca Mae Black[1], Yang Wang[1], André Struglics[2], Pilar Lorenzo[3], Susan Chubinskaya[4], Alan J. Grodzinsky[1,5,6]*, and Patrik Önnerfjord[3]*

[1]Departments of Biological Engineering, [5]Mechanical Engineering, [6]Electrical Engineering and Computer Science, Massachusetts Institute of Technology, Cambridge, MA, USA
[2]Orthopaedics, [3]Rheumatology and Molecular Skeletal Biology, Department of Clinical Sciences Lund, Faculty of Medicine, Lund University, Lund, Sweden
[4]Departments of Pediatrics, Orthopedic Surgery and Medicine (Section of Rheumatology), Rush University Medical Center, Chicago, IL, USA

[1]shared senior authorship

Published in Osteoarthritis and Cartilage Open 2021; 3(4):100191. The full text and supplemental material can be found at https://doi.org/10.1016/j.ocarto.2021.100191.

Abstract:

Objectives: In this study, we apply a clustering method to proteomic data sets from bovine and human models of post-traumatic osteoarthritis (PTOA) to distinguish clusters of proteins based on their kinetics of release from cartilage and examined these groups for PTOA biomarker candidates. We then quantified the effects of dexamethasone (Dex) on the kinetics of release of the cartilage media proteome.

Design: Mass spectrometry was performed on sample medium collected from two separate experiments using juvenile bovine and human cartilage explants (3 samples/treatment condition) during 20- or 21-day treatment with inflammatory cytokines (TNF-α, IL-6, sIL-6R) with or without a single compressive mechanical injury. All samples were incubated with or without 100 nM Dex. Clustering was performed on the correlation between normalized averaged release vectors for each protein.

Results: Our proteomic method identified the presence of distinct clusters of proteins based on the kinetics of their release over three weeks of culture. Clusters of proteins with peak release after one to two weeks had biomarker candidates with increased release compared to control. Dex rescued some of the changes in protein release kinetics the level of control, and in all conditions except control, there was late release of immune-related proteins.

Conclusions: We demonstrate a clustering method applied to proteomic data sets to identify and validate biomarkers of early PTOA progression and explore the relationships between the release of spatially related matrix components. Dex restored the kinetics of release to many matrix components, but not all factors that contribute to cartilage homeostasis.

3.1 Introduction

There are over five million annual U.S. cases of posttraumatic osteoarthritis (PTOA), the degeneration of cartilage and subchondral bone after a traumatic joint injury. However, not all traumatic joint injuries progress to PTOA: reported PTOA prevalence after anterior cruciate ligament (ACL) rupture is only 13-40%, with higher prevalence if combined with a meniscal injury [173]. While there are no approved disease-modifying drugs for OA or PTOA, promising targets such as the corticosteroid dexamethasone (Dex) have been suggested to rescue cartilage matrix breakdown and prevent chondrocyte death in models of PTOA [17,18,129,174], but use of these drugs remains controversial due to a lack of consensus on potential off-target effects. PTOA is an attractive target for the application of disease-modifying drugs, as the time of disease onset, the injury, is known. However, some patients will not progress to PTOA after injury; therefore, a prognostic biomarker to differentiate the most at-risk patients is desirable.

An ideal prognostic biomarker would identify patients at risk of PTOA before cartilage degeneration becomes irreversible. Previously identified biomarker candidates include matrix molecules indicative of cartilage catabolism – i.e. aggrecan, cartilage oligomeric matrix protein (COMP), collagen II (and associated degradation products such as crosslinked C-telopeptide collagen II fragments (CTX-II)); proinflammatory cytokines, e.g. tumor necrosis factor-alpha (TNF-α), interleukins (IL) -1, -6, -8, and -10; and proteases and protease inhibitors, e.g. matrix metalloproteinase (MMP) -3 and -13 and tissue inhibitor of metalloproteinase 1 (TIMP-1) [154,175]. Though there are many potential biomarker candidates identified in the literature, their prognostic use to predict the patients most at risk for PTOA still remains unclear [175]. In one study of synovial fluid aspirates after ACL injury, aggrecan, COMP, MMP-3, and TIMP-1 were

elevated at early time points, but failed to predict radiographic knee OA 16 years after ACL injury [176]. This suggests that it may be necessary to discover a more targeted combination of specific disease progression-associated biomarkers that considers the timing of the appearance of biomarkers in synovial fluid. Proteomics is an excellent tool for biomarker identification, as it can be used to screen samples from clinical or *in vitro* PTOA models for hundreds of proteins that could be biomarker candidates. The timing of biomarker release must be considered as well, as the cellular response to injury and PTOA progression is time-dependent with distinct catabolic and anabolic phases [151].

In *ex vivo* human and animal models of PTOA, Dex has been shown to have protective effects against disease progression, but literature reports conflict regarding its safety to cartilage and chondrocyte health [129]. In an IL-1 challenge of human cartilage explants, the low dose of 100 nM Dex rescued glycosaminoglycan (GAG) loss and maintained chondrocyte viability [18]. This finding was supported in two further studies utilizing IL-6 and TNF-α-challenged human explant models of PTOA that reported Dex attenuated GAG loss and MMP-1 release [16,17]. However, some studies using high doses and long durations of Dex treatment reported negative effects on cartilage, from chondrocyte cell death to cartilage degeneration in explant and whole-animal models [35,41,66]. Our recent proteomic study using a juvenile bovine explant model of PTOA reported that Dex attenuated catabolic effects of mechanical injury and IL-6/TNF-α-challenge, but did not rescue suppressive effects on certain anabolic pathways [174]. Differences between ages, species, and dosing in the above models complicate interpretation of the safety of Dex use, necessitating investigation into the effects of Dex on matrix breakdown in human explant models and how those results compare to commonly used animal models of PTOA.

In the present study, we demonstrate a method of clustering proteomic data using an existing proteomic data set from a bovine cartilage explant PTOA model, and validate this method by comparison to a human knee explant model of PTOA. Our aims are (1) to distinguish distinct clusters of proteins having different profiles of release from cartilage, (2) to determine biomarker candidates based on their timing and relative amount released to explant medium (as a surrogate for synovial fluid), and (3) to quantify the effects of Dex on the kinetics of release of the cartilage medium proteome.

3.2 Materials and Methods

3.2.1 Explant harvest and culture

Proteomic data were obtained from two separate experiments: a juvenile bovine explant study [174] to establish the analytical technique, and a human data set [17] to validate the model. Cartilage disks (3 mm diameter x 1 mm height, including the intact superficial zone) were harvested from the femoropatellar grooves of three 1-2-week-old bovines (Research '87, Boylston, MA) as described [18] (**Figure 3.1A**). Human explants were harvested from the tibial plateau of a 74-year-old male donor (Collins Grade 1, near-normal tissue [177]) obtained postmortem through the Gift of Hope Organ and Tissue Donor Network (Itasca, IL) (**Figure 3.1B)**. All procedures were approved by Rush University Medical IRB and the MIT COUHES committee. After harvesting, explant disks were pre-equilibrated for two days. Four bovine explants were cultured per well, with one replicate per treatment condition for each animal; human explants were cultured with one per well, and three total replicates per treatment condition (**Figure 3.1**).

3.2.2 Explant treatments

After pre-equilibration, samples were treated for 20 or 21 days (**Figure 3.1A-B)**: no treatment (N), continuous culture with inflammatory cytokines (10 ng/ml recombinant human TNF-α, 20 ng/ml recombinant human IL-6 and 100 ng/ml soluble IL-6 receptor (sIL-6R) (R&D Systems) for bovine, 100 ng/mL TNF-α, 50 ng/mL IL-6, 250 ng/mL sIL-6R for human; treatment C), cytokines with a single mechanical impact injury at day 0 (for bovine, unconfined compression to 50% final strain at 100%/s strain rate; for human, 60% final strain at 300%/s strain rate; both followed by immediate release at the same rate [130,131]; treatment IC), and the two disease models receiving 100 nM Dex (treatments CD and ICD, respectively). Culture medium was collected every three or four days and stored at -20°C until analysis.

3.2.3 Mass spectrometry preparation and identification

Culture medium (50 µL) was prepared for mass spectrometry (MS) analysis as described [130,174]. Discovery MS was performed on medium samples using a quadrupole Orbitrap benchtop mass spectrometer (Q-Exactive, Thermo Scientific). Identification was performed using the UniProt bovine (UP000009136, 2017-10) and human (UP000005640) sequence databases with Proteome Discoverer 2.2 (Thermo Scientific). The protein false discovery rate (FDR) was 0.01. Label-free protein abundance quantification was obtained by summing peak area intensities from all of the unique peptides for each protein.

3.2.4 Bioinformatics analysis

For both the bovine and human data sets, proteins were filtered out if they were exogenously added or not identified and quantified in at least 70% of samples, and missing values were imputed using the *k*-nearest neighbor method, with a *k* of 6 for the bovine data and 4 for the human data [178]. Protein abundance data were $\log_2$-transformed and principle component analysis (PCA) was performed on treatments N, C, and IC using the "prcomp" function [174]. Pairwise comparisons between treatments were performed on the summed peptide abundance over all timepoints. Statistical analysis was performed using the R package limma [132] and MATLAB (MathWorks). The amount of each protein released at each timepoint was normalized to the total amount released, then averaged across three biological replicates. Release vectors were clustered based on correlation using Euclidian distance (**Figure 3.1C**). Cluster enrichment for proteins with increased or decreased release from control was determined by finding the number of proteins with a significant fold change from control in each cluster, selecting that number from the total population, and generating 10,000 bootstrapped distributions to determine the likelihood of having so many proteins with increased or decreased release [138]. Enrichment analysis was performed as previously described [174].

3.3 Results

3.3.1 Protein identification and differential analysis

Raw MS data are available via Proteome Xchange with identifiers PXD020756 and PXD024359. After filtering as described above, the data sets were reduced to 405 proteins for bovine samples and 416 proteins for human, PCA clustering on $\log_2$-transformed control, C, and IC data for both bovine and human samples revealed a strong separation by time for bovine samples (**Figure 3.2A**),

with a less prominent trend plotting principal components 1 and 3 for human samples (**Figure 3.2B**).

3.3.2 Bovine kinetic clustering

To explore the time-dependent effects on protein release from bovine cartilage, we clustered the proteins based on the vectors of their averaged, normalized release at each timepoint (**Figure 3.1C**). We included for discussion the clusters with fifteen or more members, as below that threshold few conclusions on enrichment of biological processes could be made (**Figures 3.3** and **3.4**). For the control condition, four major clusters emerged: a cluster with day 4 peak release that decreased steadily over time (**Figure 3.3Ai**), clusters with peak release on day 8 (**Figure 3.3Aii**) and day 12 (**Figure 3.3Aiii**), and a cluster with a slight, steady increase in amount released (**Figure 3.3Aiv**). Cluster **3.3Aii** was enriched for intracellular metabolic proteins.

Clusters for treatments C and IC are depicted in **Figure 3.3B** and **3.3C**. Clusters **3.3Bi**, **3.3Bii**, **3.3Biii**, **3.3Cii**, and **3.3Cv** were enriched for proteins with increased total release versus control, while **3.3Bv**, **3.3Civ**, and **3.3Cvi** had decreased release versus control. Many of the proteins in **3.3Ai** were found in clusters with increased release later in culture (**3.3Bii**, **3.3Biii**, **3.3Cii**), suggesting that these proteins are affected by disease processes that cause increased matrix breakdown and hence transport permeability. Clusters **3.3Biv** and **3.3Ciii** contain proteins without a significant change in total amount released including complement components C1R, C1S, B, and I, as well as transforming growth factor beta-2 for treatment C. Some ECM components with peak release on day 12 or an increase starting on day 12 (**3.3Bv** and **3.3Civ**) had decreased release versus control, including collagen II.

3.3.3 Dex effects on bovine release kinetics

The Dex-treated conditions (**Figures 3.3D**, **3.3E**) had large clusters of proteins that experienced peak release on day 4 (**3.3Di**, **3.3Ei**). These clusters contained many proteins that followed the diffusive pattern of release in control (**3.3Ai**), but experienced different release kinetics with C or IC treatment. Notable proteins that were not restored back to their diffusive behavior include collagens I and II and extracellular matrix protein 1 (ECM1), with steadily increasing release starting day 12 (**3.3Diii**, **3.3Eiii**). CD treatment yielded a cluster of proteins with increased total release from control peaking on day 8 (**3.3Aii**). A cluster enriched for similar proteins released after ICD treatment had increased release each day after day 12 (**3.3Eiii**), though the total amount released for these proteins was not significantly different than control. Many immune-related proteins, including complement factors C1R, C1S, C1Q, I, and pentraxin related protein PTX3, had late release (**3.3Diii-iv**, **3.3Eiv**). The total amount released for some proteins having CD treatment (**3.3Div**) was less than in control, but for some proteins with ICD treatment (**3.3Eiv**) was greater than in control.

3.3.4 Validation with human data set

After observing that this clustering method could distinguish different profiles of release kinetics in our bovine proteomic data set, we applied the same methods to the human medium proteome to determine whether this method would reveal proteins having shared release kinetics, and whether those human clusters would be similar to bovine. Four distinct protein clusters were found in the control condition (**Figure 3.4A**), the largest with peak release on day 3 (**3.4Ai**), a cluster with peak

release on day 12 (**3.4Aii**), one with increasing release starting on day 6 (**3.4Aiii**), and the last with relatively constant release across all timepoints (**3.4Aiv**). Cluster **3.4Ai** (with early peak release) was similar to bovine cluster **3.3Ai**, containing ECM components and signaling factors. The human day 12 peak cluster (**3.4Aii**) shared similarities to the bovine day 8 peak cluster (**3.3Aii**), enriched for many of the same intracellular proteins. For both C and IC treatment conditions (**3.4B** and **3.4C**, respectively,) large clusters were present with peak release at day 3, enriched for matrix proteins exhibiting decreased release versus control (e.g., collagens VI, IX, and XI). The cytokine-treated samples had two clusters with intracellular proteins peaking on day 12 (**3.4Bii-iii**) not present with the addition of mechanical injury. The increased release of proteases and matrix proteins, including aggrecan, metalloproteinases, and collagen I, was apparent in a cluster with a peak at day 12-18 (**3.4Biv**), and in two clusters that had an earlier release for injury+cytokines (**3.4Cii-iii**). Both models of disease had late release of cathepsins and immune proteins peaking at day 18 (**3.4Bv-vi** and **3.4Civ**), but with no change in total release of these proteins versus control.

3.3.5 Dex effects on human release kinetics

Similar to results with bovine explants, many of the proteins in cluster **3.4Ai** experienced a change in release kinetics with C or IC treatment that was attenuated with addition of Dex (**3.4Di, 3.4Ei**), with the notable exceptions of several proteases, some collagens, and immune factors (MMPs -2, -3, -10, collagens III, IX, XII, serum amyloid A, beta-2-microglobulin, complement factors 3, C1S, C1R). Both Dex treatment regimens caused a group of proteins including MMP-2 and -3 to experience peak release on day 12 or day 8 (**3.4Dii**, **3.4Eii**), that had increased release versus control. These proteins had decreased total release compared to their non-Dex treated counterparts. The Dex-treated conditions also had clusters with peak release on day 18 with many immune

proteins, proteases, and protease inhibitors with increased release versus control (**3.4Div**, **3.4Eiii-v**). With treatment CD, some proteins had relatively steady release across the entire culture (**3.4Dv-vi**).

3.3.6 Release kinetics of selected spatially and functionally related proteins

Heinegård [179] reviewed macromolecular constituents of the cartilage extracellular matrix; to investigate when spatially and functionally related matrix components were released from cartilage explants, we examined the kinetics of release of selected proteoglycans, collagens, and matrix-binding proteins that are well-characterized. Selected were the large proteoglycan aggrecan (ACAN), and the small leucine-rich repeat (SLRR) collagen-binding proteoglycans biglycan (BGN), decorin (DCN), and fibromodulin (FMOD). Collagens selected were collagen II (COL2A1), collagen VI (COL6A1), and collagen IX (COL9A1). Additional matrix-binding proteins were the collagen-binding proteins COMP and matrilin 3 (MATN3), and the integrin-binding chondroadherin (CHAD). Proteins were selected if they were present in both bovine and human systems to enable comparison: **Figure 3.5** (bovine) and **Figure 3.6** (human).

Overall, the selected proteoglycans released from bovine cartilage with cytokine or injury+cytokine treatment behaved similarly to control (**Figure 3.5A-C**). Aggrecan had a peak in the amount released on day 12 in the diseased treatments, with a moderate amount released on days 4 and 8. Particularly in the injury+cytokine treated samples (**Figure 3.5C**), the SLRR proteoglycans had a large amount released at the earliest timepoint but a steadily increasing rate of release later in culture after the peak in aggrecan release, which was also reflected in the behavior of collagens II, VI, and IX (**Figure 3.5E-F**). In untreated bovine controls, the collagens

except collagen IX followed a diffusion-like pattern of release (**Figure 3.5D**). The additional matrix binding proteins (**Figure 3.5H-J**) behaved similarly to control with cytokines and/or mechanical injury, except with relatively more matrilin-3 released at later timepoints than in control (~25% of total release occurring at each of days 12 and 16).

In untreated human control explants (**Figure 3.6A, D, H**), nearly all proteins had their peak release at the first timepoint (day 3). This behavior changed noticeably with inflammatory cytokines and mechanical injury: collagen VI, IX, and CHAD still experienced peak release at day 3, but other proteins had a peak release at days 12-18. With cytokine-only treatment, aggrecan release peaked on day 12, similarly to the peaks of COMP and matrilin-3 on day 12. These peaks were followed by a day 15 peak in collagen II release and later increases in decorin, biglycan, and fibromodulin release (**Figure 3.6B, E, I**); this trend was less noticeable with mechanical injury (**Figure 3.6C, F, J**).

Overall, the addition of Dex did not have a major impact on the release of most of these selected proteins in the bovine model (**Figures 3.5** and **3.6**). In the human model, Dex changed the behavior of nearly all selected proteins to have peak release at the earliest timepoint, with some proteins (e.g. CHAD) experiencing a small increase at day 18.

3.4 Discussion

Our clustering method allowed us to analyze existing bovine and human proteomic data sets for information on matrix breakdown kinetics and potential biomarker candidates, which could easily be adapted to new data sets. The data from the explant model of human PTOA closely match the

kinetics of matrix breakdown for *in vivo* knee injury, as measured by COMP, osteopontin, osteonectin, complement factor, and collagenase-generated collagen II fragment release into the synovial fluid [180–184]. Thus, our results from the human model closely follow the same breakdown events that occur in patients, though the timing is likely not 1:1 as the presence of other joint tissues could affect the rate of catabolic processes.

In general, the human and bovine results had the same patterns of release. Both sets of control data showed a large cluster of proteins with peak release at the earliest timepoint. Proteins with this profile are assumed to have no direct biological or biochemical initiators of loss from explant culture, most likely following passive diffusion-like transport out of the cartilage. This diffusive profile may be associated in part with the newly-cut radial edges of the cartilage plugs upon harvest. Interestingly, this profile may also model initial diffusive loss *in vivo* when traumatic knee injury results in cracks in the cartilage surface, as can commonly occur [173,185]. In addition, both human and bovine untreated conditions also had a group of intracellular proteins of low abundance that had peak release about one week into the culture, assumed to be indicative of early cell death [174].

The bovine and human C and IC conditions had large clusters of proteins peaking least one week into culture. The human clusters often had sudden, sharp increases in the amount of protein released, while the bovine proteins had more gradual increase over time. The proteins in these clusters are the most likely candidates for biomarkers of PTOA progression due to the increased amount released compared to control. Notably, the addition of a single mechanical impact injury

caused matrix breakdown to begin several days sooner than cytokines alone. This may be associated with injury-induced microdamage to the matrix, enabling enhanced transport of cytokines into cartilage and release of matrix breakdown products, or an increase in intracellular catabolic processes with mechanical stimulus. Treatment with cytokines alone may also model OA progression influenced by inflammation due to the shared pathways that will be affected by exposure to inflammation, though it is difficult to apply our analysis of the kinetics of release of biomarkers to this disease model, as the timing of disease initiation is not as distinct as with PTOA.

This method of biomarker identification is validated by the overlap of our results with previously posited ECM-related biomarker candidates such as aggrecan, MMP-3, collagen II, vascular cell adhesion protein-1, lumican, and COMP [186–189]. Other biomarker candidates identified by our method are cytokines that may be part of the early breakdown signaling process, such as IL-8, secreted phosphoprotein-1, PTX3, and C-C motif chemokine ligands 5 and 20 [190–194]. Our study suggested the importance of biomarkers related to cell death as well as matrix breakdown, such as cathepsins L1, D, and S, which may be indicators of cellular response to PTOA progression and are under consideration as potential non-invasive biomarkers for early OA [195,196]. A novel set of candidate markers of PTOA progression identified with this method as well as previous proteomic analysis of the bovine data set [174] were lamin and histone proteins present in the culture medium (LMNA, LMB2, HIST1H4A, HIST1H1D, H2AFV, H3FA, HIST2H2BF). The presence of these nuclear proteins in culture medium could be indicative of cell death in the early stages of cartilage damage, and they have been identified in previous proteomic studies of synovial fluid in OA models [197–199].

Just as critical as the biomarker identity itself is the timing of its release into synovial fluid. Based on our human data, increased levels of matrix degradation products and signaling proteins that have been previously identified as biomarker candidates peaked in their release 9-15 days after the initial injury. While some biomarkers have been identified in synovial fluid months to years after injury [176], it is difficult to maintain an *ex vivo* model this long, limiting our window of investigation to relatively early timepoints. However, there is reason to investigate this window of time for identifying patients with an elevated risk for PTOA development, as early intervention with a drug such as Dex might prevent irreversible damage to the cartilage that could occur.

Some matrix components such as collagen II in the bovine C and IC conditions experienced a decrease in their total amount released compared to control. As previously reported [174], some ECM components experience a decreased release under inflammatory and mechanical stress due to a decrease in synthesis. However, the kinetics of the release of collagen II did change (**Figure 3.3Bv**, **3.3Cvi**, **3.6E-F**), demonstrating that collagen II release was still affected by protease activity and disease progression. Particularly in the bovine model, where collagen II synthesis is high, the release of collagen II into the matrix will be dependent on its synthesis as well as its proteolytic cleavage and matrix permeability. Within the selected matrix proteins, some proteins that decorate the surface of larger ECM macromolecular complexes (e.g., COMP, collagen IX, and matrilin-3) experienced their peak release before collagen II (**Figure 3.5&3.6E, F, I, J**) [60]. The sequential loss of specific matrix components supports the hypothesis that highly abundant and space-filling matrix proteins such as aggrecan must first be degraded and released to some extent before proteases can then reach the cleavage sites of other proteins such as collagen II, decorin, biglycan, and fibromodulin [200].

The addition of a low dose of Dex rescued the increased release of many matrix breakdown products, though not entirely to control levels, in both the human and bovine model. This is in agreement with previous studies showing that Dex reduced the activity of matrix proteases and attenuating collagen and GAG loss in models of OA/PTOA [16,18,129,130,174]. Further evidence that Dex rescues ECM homeostasis to control is demonstrated by many proteins with their kinetics of release affected by cytokines and/or injury returning to their control behavior (**Fig. 3.3Di**, **3.3Ei**, **3.4Di**, **3.4Ei**), though some MMPs and collagens still had release later than they did without treatment.

The most significant off-target effect of Dex we observed was the increased release of inflammatory mediators late into culture in the human model, where both CD and ICD conditions had clusters enriched for inflammatory proteins with a day 18 peak release. Dex has been shown to have anti-inflammatory effects on the joint space in animal models of PTOA [23], but the specific pathways through which it exerts this effect are currently not well-understood [129], and likely dependent on many tissues including the joint capsule synovium. This deviation from the signaling and release of inflammatory proteins in healthy, untreated cartilage justifies more studies on appropriate doses and timing of Dex and the interaction of Dex with multiple joint tissue types [98]. If Dex is to be used for its anti-catabolic effects to protect against PTOA progression and avoid potential off-target effects on immune signaling or other pathways, targeted strategies of drug delivery specifically to cartilage at the lowest possible dose will be necessary [117,119,149].

3.4.1 Study limitations

Mass spectrometry as a technique has specific limitations. We used a high threshold of confidence to compensate for any single-peptide identifications or missing values, with a false discovery rate of 0.01 and proteins required to have quantification values in at least 70% of samples. Some putative OA biomarkers are specific cleavage fragments of matrix components, such as CTX-II [188] and COMP neoepitopes [130,182]; with our broad discovery approach, these peptides would not be distinguished from the rest of the peptides used to calculate protein abundance due to trypsin cleavage. Thus, this method for biomarker identification is best validated with other biochemical or targeted proteomic analyses [174]. The bovine experiment used three biological replicates, a low number for statistical confidence but balanced by the repeatable nature of these juvenile bovine experiments, and our human data set used only one donor with three internal technical replicates. Donor-to-donor variability can be extremely high, and our ongoing studies with more donor joints will be used to further validate our application of the clustering method used here. The difference in cytokine concentrations and culture conditions between the models was due to the difference in young juvenile chondrocytes versus aged and potentially more sensitive adult human cells. These differences in age, developmental state and phenotype will contribute to differences between our models, such as differences in baseline synthesis rates of collagen II between less metabolically active adult human cartilage and the young bovine system, which may be more similar to human children or adolescents [201]. Hypoxic conditions in the *in vivo* joint environment may affect some of the pathways discussed. Ongoing studies including bone and synovial tissue will elucidate the effect of crosstalk from these tissues on cartilage response and the media proteome and further refine this model of PTOA progression [98].

3.5 Conclusions

Our analysis identified the presence of distinct clusters of proteins based on the kinetics of their release over three weeks of culture. In our model of early PTOA progression, our data suggest that many biomarkers for cartilage matrix breakdown are released at their peak nine to fifteen days after initial injury. Utilizing this method allows for broad identification of biomarker candidates for early monitoring of PTOA risk in patients after a traumatic joint injury. We found that a period between 9-15 days post-injury had the highest relative release of previously identified and novel biomarker candidates in our model. Our study also provided insight into the sequential loss of matrix constituents, where some proteins such as collagen II are shielded from breakdown and release into the media until other matrix components are degraded. Dex showed promise as an anti-catabolic disease-modifying treatment, restoring most ECM and ECM-modifying proteins to their control behavior and amount released. However, in all treatment conditions except control, there was a late peak in the release of complement factors, suggesting an immune response in cartilage that is not attenuated with Dex treatment. This highlights the need to better understand the effect of Dex on other pathways involved in cartilage homeostasis beyond matrix breakdown, and the potential need to target these pathways with additional combinatorial therapeutics [202]. The clustering results had the same broad trends between human and bovine models, but the release kinetics for specific proteins often differed; a bovine model may not be appropriate to search for OA biomarkers without validation against human data.

Acknowledgements

Supported by grants and NIH-NCATS UG3/UH3 TR002186 and NIH-NIBIB R01 EB026344 (AJG), A*STAR (Singapore) Fellowship and Poitras Pre-doctoral Fellowship (YW), the Rush Klaus Kuettner Endowed Chair (SC), the Swedish Research Council (2014−3303), the Swedish Rheumatism Association (AS and PÖ), the Krapperup Foundation (PÖ), the Alfred Österlund Foundation (AS, PÖ), the Greta & Johan Kock and Crafoord Foundations (AS, PÖ). The authors acknowledge Gift of Hope Organ & Tissue Donor Network (Itasca, IL) and donors' families.

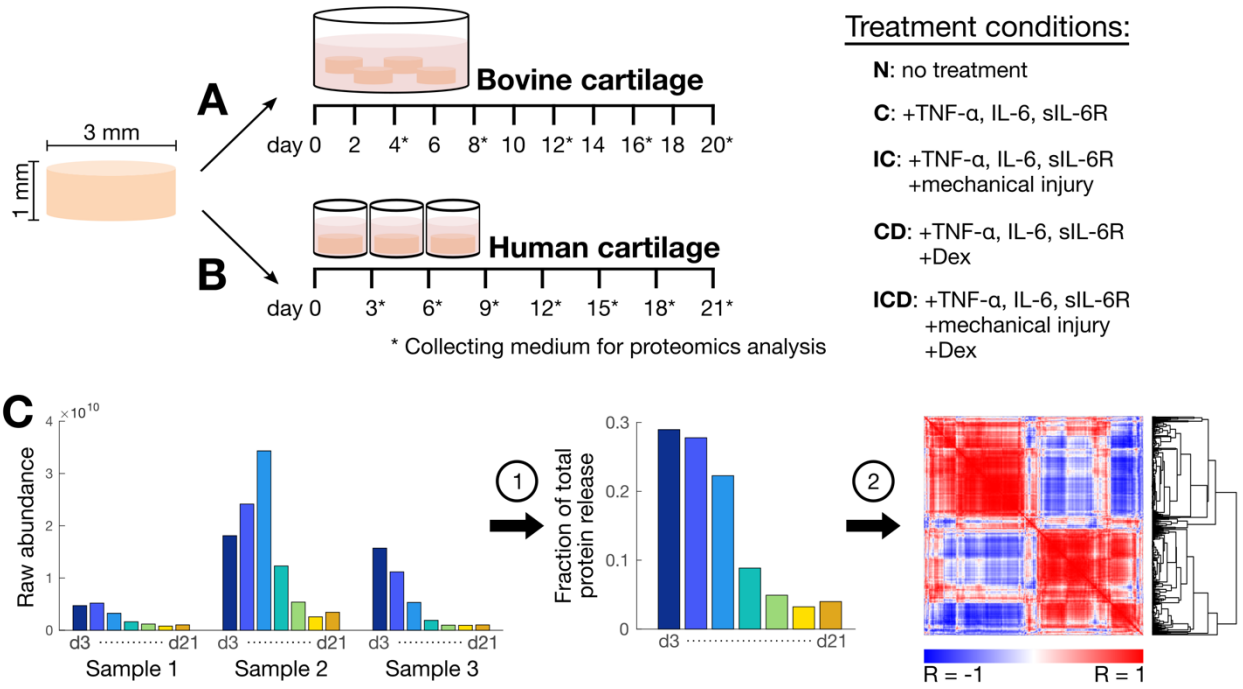

Figure 3.1. Experimental overview and clustering method. Bovine **(A)** and human **(B)** cartilage explants (3 mm diameter x 1 mm height) were cultured for 20 or 21 days with media collected every four or three days, respectively, for mass spectrometry analysis. The explants were untreated (N), treated with inflammatory cytokines (C, 10 ng/ml TNF-α + 20 ng/ml IL-6 + 100 ng/ml sIL-6R for bovine, 100 ng/mL TNF-α + 50 ng/mL IL-6 + 250 ng/mL sIL-6R for human), treated with cytokines plus a single impact mechanical injury (IC, 50% final strain at 100%/s strain rate for bovine, 60% final strain at 300%/s strain rate for human,) or received treatments C and IC with 100 nM Dex (CD and ICD, respectively). **(C)** To cluster the proteins based on time release profile, the raw abundance data of each protein (represented by collagen II, COL2A1) was normalized to the total amount released within that replicate and averaged across all three replicates (1), then the resulting vectors for each protein were clustered based on correlation using Euclidian distance (2), which can be visualized in an n-by-n heatmap, where n is the number of proteins, and each comparison is colored based on correlation. R: correlation coefficient.

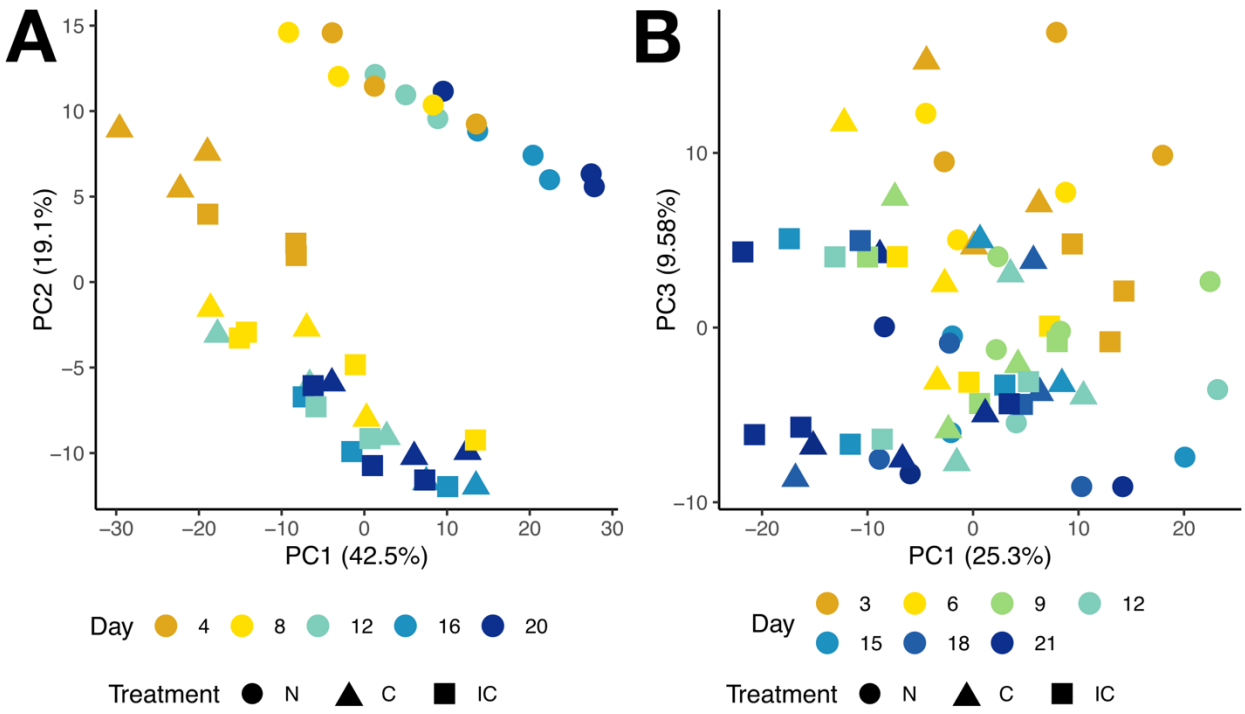

Figure 3.2. Principal component analysis of proteomic data. (A) PCA clustering was performed on bovine control (N), cytokine-treated (C), and injury + cytokine-treated (IC) samples. C and IC samples separated from control samples, and there was a noticeable separation of early timepoints from later ones, particularly for treatments C and IC. **(B)** PCA on human N, C, and IC samples revealed a similar trend apparent when plotting the first and third principal components. Percentages on axes represent percent variance explained by that principal component.

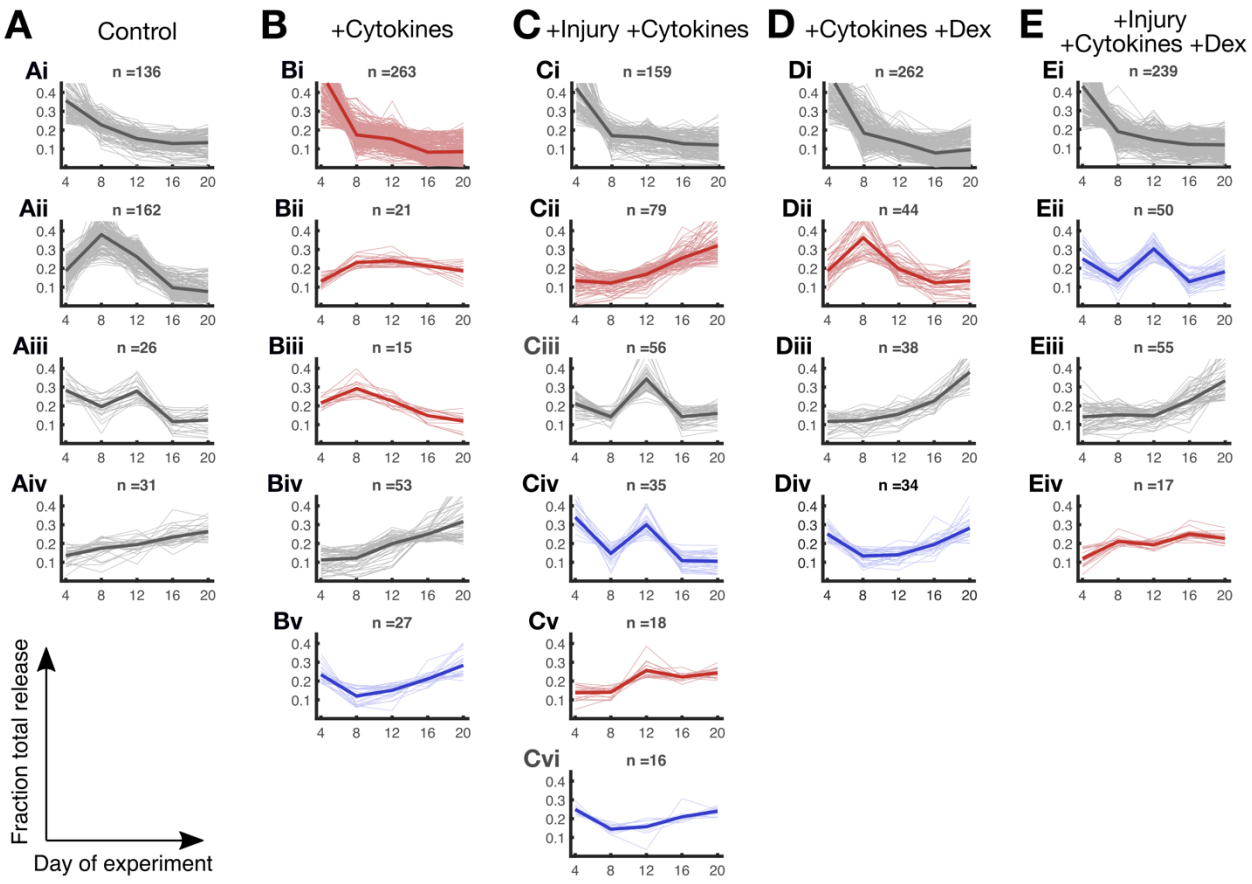

Figure 3.3. Clusters of bovine protein time release profiles. After clustering based on correlation, clusters of proteins with distinct time release profiles emerged for all treatment conditions: control **(A)**, cytokine-treated **(B)**, injury + cytokines **(C)**, cytokines + Dex **(D)**, injury + cytokines + Dex **(E)**. Cluster enrichment for proteins with increased (red) or decreased (blue) release from control was determined by finding the number of proteins with a significant fold change from control in each cluster and bootstrapping 10,000 random distributions based on the total protein population. Lighter lines represent each individual averaged vector, dark lines represent the average of all proteins in that cluster. Clusters are arranged in descending order based on timing of approximate peak release of proteins in that cluster and/or when a steadily increasing trend begins. X-axis: days of the experiment. Y-axis: fraction of total protein release collected each day. n: number of proteins in each cluster.

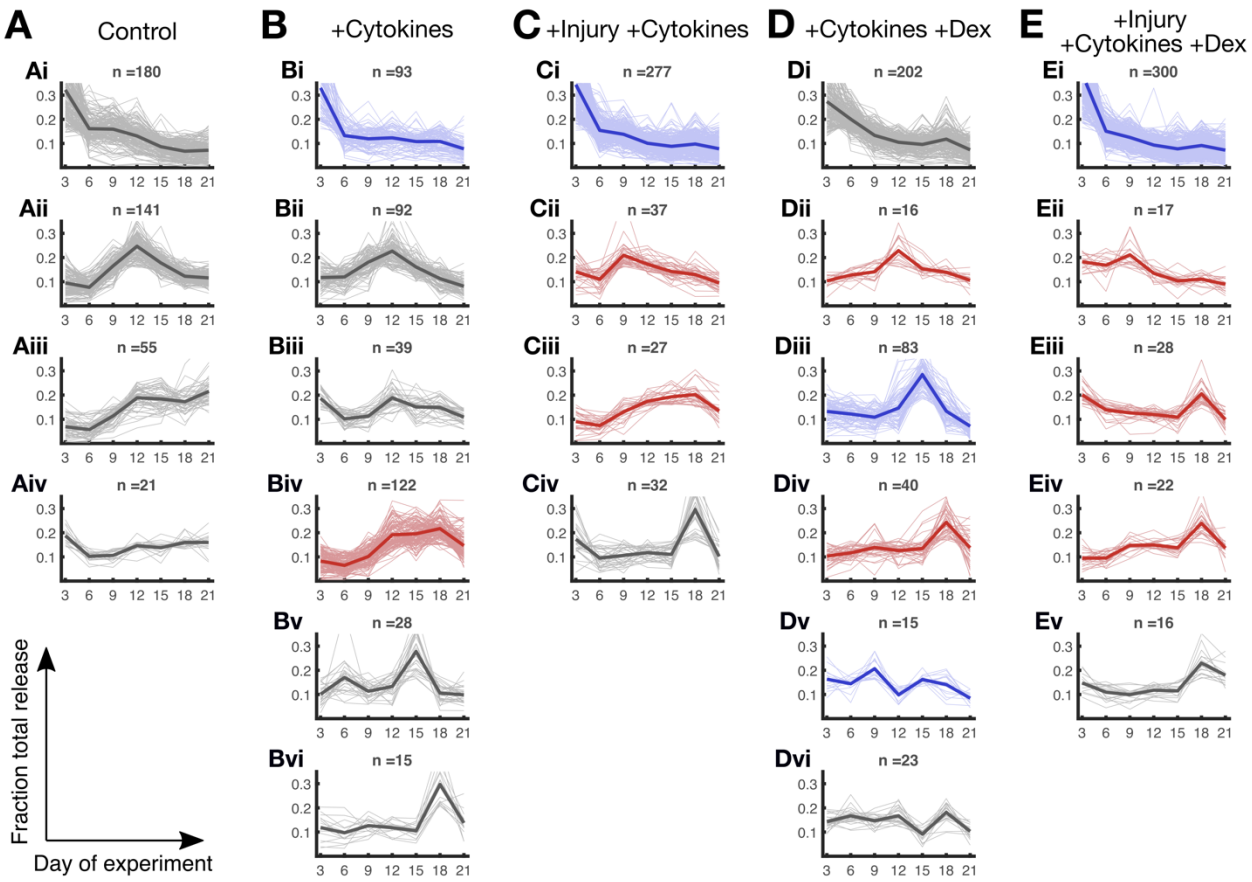

Figure 3.4. Clusters of human protein time release profiles. Time profile clustering of the human data: control **(A)**, cytokine-treated **(B)**, injury + cytokines **(C)**, cytokines + Dex **(D)**, injury + cytokines + Dex **(E)**. Red: cluster with significant number of proteins with increased release from control. Blue: cluster with significant number of proteins with decreased release from control. Lighter lines represent each individual averaged vector, dark lines represent the average of all proteins in that cluster. Clusters are arranged in descending order based on timing of approximate peak release of proteins in that cluster and/or when a steadily increasing trend begins. X-axis: days of the experiment. Y-axis: fraction of total protein release collected each day. n: number of proteins in each cluster.

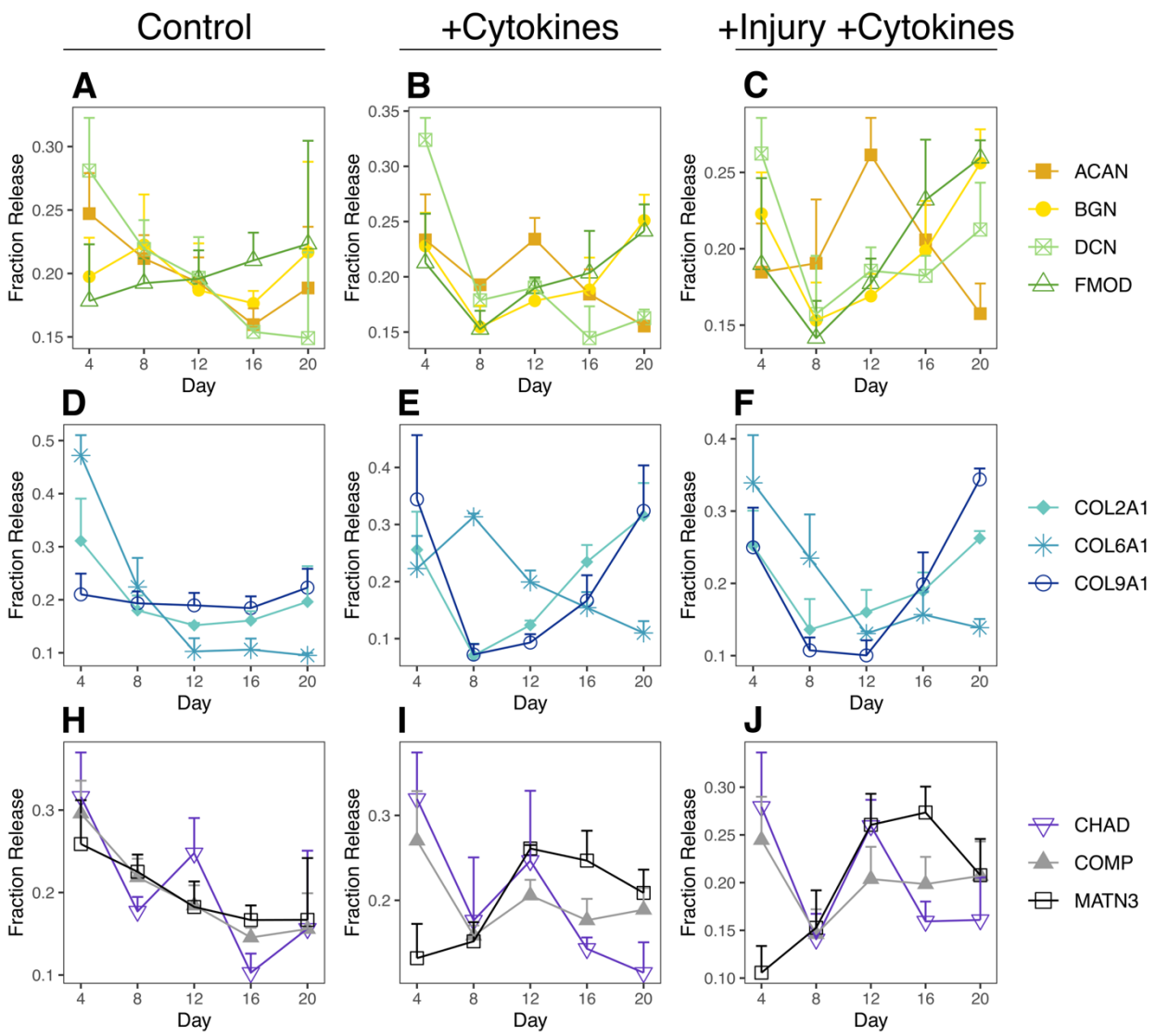

Figure 3.5. Kinetics of selected proteoglycans, collagens, and matrix-binding proteins from bovine model. Averaged normalized protein release vectors for aggrecan (ACAN), biglycan (BGN), decorin (DCN), fibromodulin (FMOD), collagens II, VI, and IX (COL2A1, COL6A1, COL9A1), chondroadherin (CHAD), COMP, and matrilin-3 (MATN3). **A-C:** proteoglycans. **D-F:** collagens. **H-J:** matrix-binding proteins. Columns represent untreated control (**A, D, H**), cytokine (**B, E, I**), and injury+cytokine treatments (**C, F, J**). Error bars: standard deviation across three replicates.

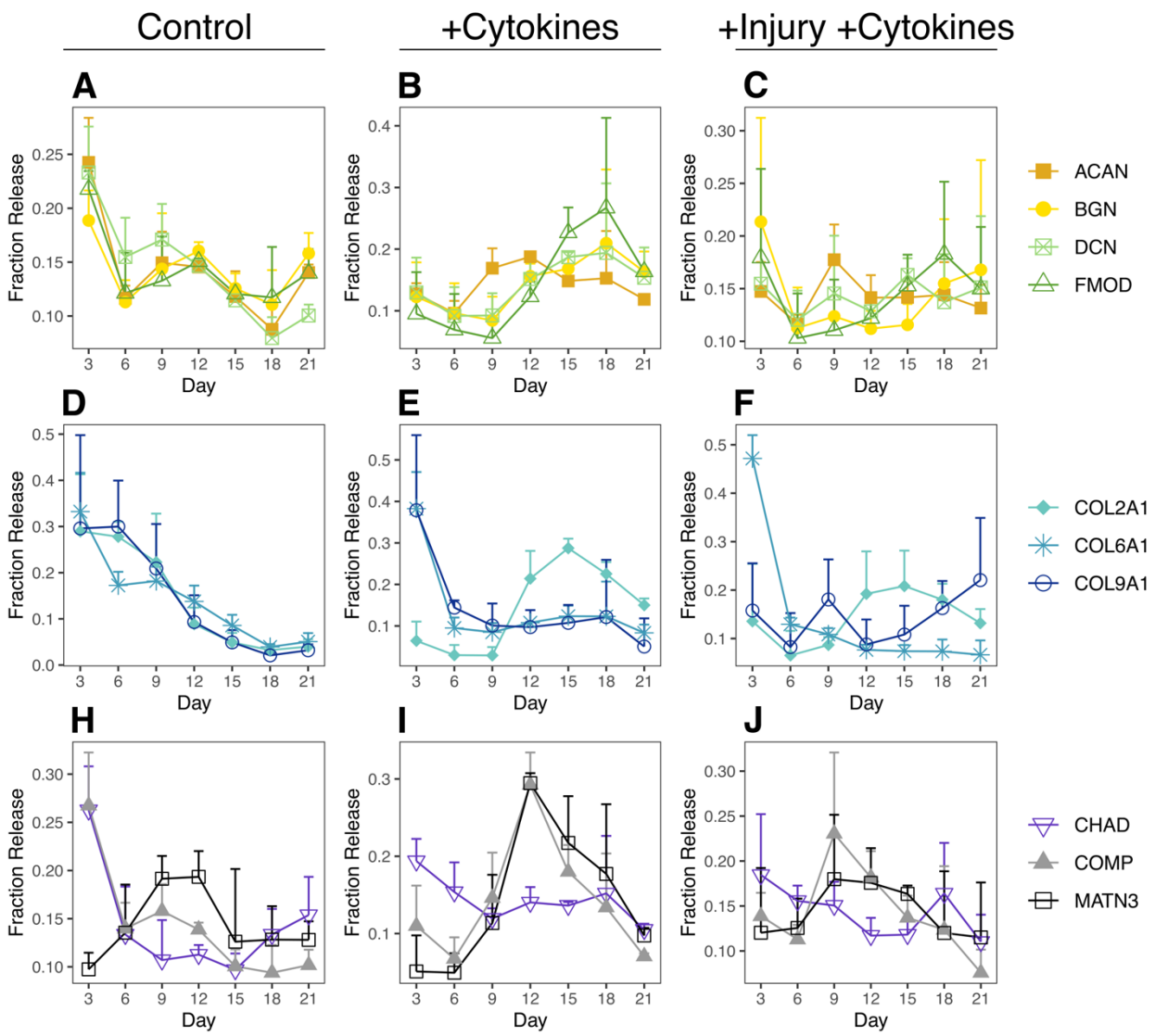

Figure 3.6. Kinetics of selected proteoglycans, collagens, and matrix-binding proteins from human model. Averaged normalized protein release vectors for aggrecan (ACAN), biglycan (BGN), decorin (DCN), fibromodulin (FMOD), collagens II, VI, and IX (COL2A1, COL6A1, COL9A1), chondroadherin (CHAD), COMP, and matrilin-3 (MATN3). **A-C:** proteoglycans. **D-F:** collagens. **H-J:** matrix-binding proteins. Columns represent untreated control (**A, D, H**), cytokine (**B, E, I**), and injury+cytokine treatments (**C, F, J**). Error bars: standard deviation across three replicates.

Chapter 4. Tissue Catabolism and Donor-Specific Dexamethasone Response in a Human Osteochondral Model of Post-Traumatic Osteoarthritis

Rebecca Mae Black[1], Lisa L. Flaman[1], Karin Lindblom[2], Susan Chubinskaya[3], Alan J. Grodzinsky[1,4,5], and Patrik Önnerfjord[2]

[1]Departments of Biological Engineering, [4]Mechanical Engineering, [5]Electrical Engineering and Computer Science, Massachusetts Institute of Technology, Cambridge, MA, USA
[2]Rheumatology and Molecular Skeletal Biology, Department of Clinical Sciences Lund, Faculty of Medicine, Lund University, Lund, Sweden
[3]Departments of Pediatrics, Orthopedic Surgery and Medicine (Section of Rheumatology), Rush University Medical Center, Chicago, IL, USA

This work is in revision for publication in Arthritis Research and Therapy.

Abstract

Background:

Post-traumatic osteoarthritis (PTOA) does not currently have clinical prognostic biomarkers to find patients most at risk of disease after injury, or to find disease-modifying drugs, though promising candidates such as dexamethasone (Dex) exist. Many challenges in studying and treating this disease stem from multi-tissue interactions that complicate understanding of drug effects. We present an *ex vivo* human osteochondral model of PTOA to investigate disease effects on catabolism and cellular homeostasis in a multi-tissue system and discover biomarkers for disease progression and drug efficacy.

Methods:

Human osteochondral explants were harvested from normal (grade 0-1) ankle talocrural joints of seven human donors. After pre-equilibration, osteochondral explants were treated with a single-impact mechanical injury and TNF-α, IL-6, and sIL-6R ± 100 nM Dex for 21 days. Chondrocyte viability, tissue DNA content, and glycosaminoglycan (sGAG) loss to the media were assayed and compared to untreated controls using a linear mixed effects model. Mass spectrometry analysis identified proteins in both cartilage tissue and culture medium**,** and statistical significance was determined with the R package limma and empirical Bayes statistics. Partial least squares regression analyses of sGAG loss and Dex rescue effect on sGAG loss against proteomic data were performed.

Results:

Dex maintained chondrocyte viability and rescued increased sGAG loss caused by injury and cytokine treatment, but with donor-specific differences in the sGAG rescue effect. Injury and cytokine treatment caused an increase in the release of ECM components, proteases, pro-inflammatory factors, and intracellular proteins, while tissue lost intracellular metabolic proteins, effects that were mitigated with the addition of Dex. Biomarkers of bone metabolism had mixed effects, and collagen II synthesis was suppressed with both disease and Dex treatment. Semitryptic peptides associated with increased sGAG loss were identified. Pro-inflammatory humoral proteins and apolipoproteins were associated with lower donor-specific Dex responses.

Conclusions:

Catabolic effects on cartilage tissue caused by injury and cytokine treatment were rescued with the addition of Dex in this osteochondral PTOA model, while bone metabolism was dysregulated. This study presents potential peptide biomarkers of early PTOA progression and Dex efficacy that can help identify and treat patients at risk of PTOA.

4.1 Introduction

Though millions of patients worldwide suffer from osteoarthritis (OA), no disease-modifying OA drug (DMOAD) has been approved due to many challenges in the drug development pipeline, and promising candidates often fail at the level of clinical trials [203–205]. OA affects multiple tissues in the joint including the cartilage, meniscus, bone, and the synovial joint capsule. Many *in vitro* models of OA that use a single tissue such as cartilage do not capture the complex interactions between these tissues. *In vivo* animal models of OA can aid in this regard, but do not always translate to the same efficacy in humans. Outcome measures of drug efficacy also often focus on late-stage pain or structural changes, while early tissue breakdown events can progress years before macroscopic changes are observed. Molecular biomarkers of disease progression can offer insight into early disease processes that could help in drug development as therapeutic endpoints as well as potential prognostic measurements of patients for the earliest stages of OA, when intervention may prevent joint damage.

Many *in vitro* models of OA using human cartilage and isolated chondrocytes offer insights into disease progression, but do not capture the complexity of a full joint that has vasculature, bone, and synovial cross-talk, involving complex signaling networks that are affected by OA progression [206]. The subchondral and cortical bone undergo changes and resorption during OA, and osteoblasts and osteoclasts from sclerotic bone have been shown to inhibit chondrocyte anabolism and promote the synthesis of matrix proteases. Therefore, it is desirable to use a multi-tissue model to better understand disease progression and drug effects on healthy as well as diseased joint tissues.

Post-traumatic OA (PTOA) is an important disease target since the time of the disease onset (the injury) is known. In a previous model of PTOA using human knee cartilage explants, mass spectrometry analysis of culture media identified the time-dependent release of proteases and catabolic signaling processes within days after mechanical injury and inflammatory cytokine exposure, hypothesized to be potential biomarkers of disease progression [89]. The observed sequential order of extracellular matrix (ECM) breakdown allowed for increased understanding of how proteases access specific ECM components and, additionally, the timing of immune and anabolic responses affected by both disease and corticosteroid treatment. However, this *in vitro* model did not incorporate tissue crosstalk that could affect signaling processes and only focused on changes in the media proteome. A full understanding of PTOA progression also requires attention to changes within the cartilage tissue as well.

Recent studies using discovery proteomics have also worked towards proposing and validating prognostic biomarkers of PTOA progression, which could serve to identify patients at risk of disease and to provide clinical endpoints for drug candidates. Proteins with increased synthesis or release from cartilage into the joint space are possible biomarker candidates, but another set of targets are protein fragments produced by enzymatic activity not present in healthy cartilage. A neoepitope of cartilage oligomeric protein (COMP) produced by proteolytic activity was discovered in the synovial fluid of patients and later validated in a human knee cartilage explant model of PTOA, and there is potential to identify fragments of other proteins that are generated under disease stress [130,182].

In the search for DMOADs for patients at risk of PTOA development, corticosteroids have been identified as promising therapeutics. One of the most well-studied is dexamethasone (Dex), the most potent of the corticosteroid family [129]. In human and animal cartilage tissue models of PTOA, Dex exerted strong anti-catabolic effects on matrix breakdown and protease production, making it a promising candidate for the prevention of early catabolic events in PTOA [16,18,89,174]. However, there is high variability in patient disease progression, and also in the response to Dex at the cellular level [39,207]. It is of interest to identify which patients might be the most or least responsive to Dex in order to personalize treatment and reduce exposure to potential off-target side effects. Corticosteroids affect many signaling pathways beyond protease synthesis, and in some models using isolated chondrocytes, higher doses of Dex have been shown to negatively affect chondrocyte viability [64,66]. In models using cartilage explants, negative effects on cartilage viability are not commonly observed; however, Dex can exacerbate dysregulation of immune signaling late into disease treatment [18,89]. Long-term systemic corticosteroid treatment has also been shown to increase incidence of osteoporosis, leading to concerns over effects on bone homeostasis [208]. Distinguishing which patients may respond positively to Dex could enable targeted treatment for a balance of anti-inflammatory and anti-catabolic effects, without exposing patients that will not benefit from treatment to off-target effects.

In the present study, we use a human ankle osteochondral model of PTOA, starting with initially normal donor joints, to study early disease progression and to better understand catabolic and anabolic responses in this multi-tissue context. Ankle tissues are relevant since up to 90% of the incidence of ankle OA is post-traumatic [209]. Using discovery proteomics, we search for

biomarkers of both protein release and proteolytic events; disease-related effects are revealed by the media proteome as well as the intra-cartilage tissue proteome. This system allows investigation of donor-specific responses to drugs like Dex in the context of multiple joint tissues, and to identify potential ways of stratifying patients that do or do not respond to such treatment. We hypothesize that, in this model of PTOA that incorporates cartilage-bone crosstalk, 1) the cartilage and bone tissues will undergo catabolic degradation, 2) anabolic and homeostatic cellular processes will be dysregulated, and 3) donors will respond differently to disease and drug treatment due to donor-specific differences in cartilage and bone biology (**Fig. 4.1A**).

4.2 Materials and Methods

4.2.1 Explant harvest and treatment

Human osteochondral explants (3.5 mm diameter, full-thickness cartilage and ~4 mm bone) were harvested from ankle talocrural joints of seven human donors (62F, 66M, 66M, 44F, 23M, 39M, 70M, Collins grade 0-1) obtained postmortem through the Gift of Hope Organ and Tissue Donor Network (Itasca, IL). Explants were pre-equilibrated for two days in high glucose phenol red-free Dulbecco's Modified Eagle Medium (DMEM) (Thermo Fisher) before switching to low-glucose phenol red-free DMEM, supplemented as described [174]. After pre-equilibration, osteochondral explants were treated for 21 days ± a single-impact mechanical injury (60% final strain at 300%/s strain rate; both followed by immediate release at the same rate [130,131]) and inflammatory cytokines (25 ng/mL tumor necrosis factor alpha (TNF-α) + 50 ng/mL interleukin-6 (IL-6) + 250 ng/mL soluble IL-6 receptor (sIL-6R); treatment IC), as well as with 100 nM Dex alone (D) or treatment IC plus 100 nM Dex (ICD) (**Fig. 4.1B)**. All donors provided both left and right ankles,

and explants from one ankle were used for proteomic analysis while the other ankle was used for sGAG and DNA biochemical analysis. Viability analysis was performed on samples randomized from both ankles. Culture medium was collected and stored at -20°C until analysis.

4.2.2 Biochemical and viability analysis

Cartilage tissue was removed from the underlying bone and digested in 1 mg/mL proteinase K (Sigma). sGAG content in the medium and digested cartilage tissue was determined using the dimethylmethylene blue (DMMB) assay [139], and tissue DNA content was quantified with the Quanti-iT PicoGreen dsDNA kit (Thermo) according to manufacturer instructions. Significance for biochemical measurements was determined fitting the data to a linear mixed effects model with donor as a random effect followed by a least squares means test, using the R package lmerTest. To determine chondrocyte viability within the cartilage, 100-200 μm vertical slices were cut from intact cartilage and stained with fluorescein diacetate and propidium iodide (Sigma) as previously described [18].

4.2.3 Mass spectrometry preparation and identification

Culture medium (50 μL) was prepared for mass spectrometry (MS) analysis as described [130,174]. Cartilage tissue samples were removed from the underlying bone and prepared for MS analysis as described [210]. Discovery MS was performed using a quadrupole Orbitrap benchtop mass spectrometer (Q-Exactive HFX, Thermo Scientific) with prior separation of peptides using a liquid chromatography system (EASY-nLC 1000, Thermo Scientific) on an analytical column (PepMap RSLC C18, 75μm x 25cm, Thermo Scientific) coupled on-line using a nano-electrospray ion source with a column temperature at +45°C (EASY-Spray, Thermo Scientific) using a flow

rate of 300nL/min. Protein identification was performed in Proteome Discoverer 2.5 (Thermo Scientific) using two search engines in parallel: a tryptic search against the UniProt human (UP000005640 from 2021-01) sequence database combined with an MSPep spectral search against the NIST_human_Orbitrap_HCD_20160923 library (mass tolerance: 10 and 20ppm in MS1, MS2 respectively. Other Sequest search settings were modifications: carbamidomethylation (fixed: C), oxidation (variable: M, P) missed cleavages (max 2), mass tolerance (MS1-10ppm, MS2-0.02Da). Label-free protein abundance quantification was obtained by averaging peak area intensities from the top three unique peptides for each protein. To determine individual peptide abundances, we performed a semi-tryptic database search to enable identification of non-tryptic cleavages within the dataset. This was performed using the same combined searches as above but in series. The protein false discovery rate (FDR) was 0.01 for both searches.

4.2.4 Bioinformatics analyses

For both the peptide and protein MS data sets, proteins were filtered out if they were exogenous or not identified and quantified in at least 70% of samples, and missing values were imputed using the *k*-nearest neighbor method [89,178]. Cartilage tissue data was normalized to the DNA content per wet weight of cartilage tissue to adjust for different cell densities between donors. The media data had significant batch effects due to two collections of donors, so data used for principle component and regression analyses were batch corrected using the R limma package function "removeBatchEffect" [132]. Protein and peptide abundance data were $\log_2$-transformed and scaled, and principle component analysis (PCA) was performed using the "prcomp" function [174]. Pairwise comparisons between treatments were performed on the individual peptide and protein abundances. Statistical analysis on proteomic and peptide data was performed using limma

and MATLAB (MathWorks). Protein and peptide abundances were regressed using partial least squares regression against total sGAG loss or the percent of sGAG loss that was rescued by Dex treatment, which yielded a dot product of the first two loading vectors for each protein or peptide. The proteins and peptides were ranked by their dot product and analyzed using Gene Set Enrichment Analysis (GSEA) c5 gene sets with the Human UniProt IDs chip and 1,000 repeats for enrichment score distributions [128,211]. Enrichment analysis for biological processes was performed using the PANTHER database and STRING analysis as previously described [174,212].

4.3 Results

4.3.1 Cartilage viability and sGAG loss during disease and drug treatment

Osteochondral plugs from seven pairs of Collins grade 0-1 human donor ankles were successfully cultured for three weeks. Without any treatment, the cartilage tissue lost around 20% sGAG content and maintained chondrocyte viability, consistent with other studies using isolated cartilage (**Fig. 4.1C, Fig. 4.2**). Low-dose treatment of only Dex had no effect on cell viability or sGAG loss, while treatment with injury and cytokines (IC) caused widespread cell death in the cartilage and increased sGAG loss significantly. The addition of Dex to IC treatment (ICD) ameliorated sGAG loss, though not back to control levels, and reduced the amount of chondrocyte death. There were donor-specific differences in how much sGAG loss each individual donor experienced, as well as the degree to which Dex rescued sGAG loss, if at all (**Fig. 4.3**).

4.3.2 Mass spectrometry identification of proteins in media and cartilage tissue and disease and Dex effects on media and cartilage proteomes

MS analysis identified 18,913 peptides with 2,041 identified and quantified proteins in the media, and 8,732 peptides corresponding to 1,389 proteins in the cartilage tissue. The raw data are available via ProteomeXchange with identifier PXD032213 [146]. After filtering as described in the methods, the media contained 8,718 peptides corresponding to 1,451 proteins, and the cartilage tissue 7,082 peptides and 1,141 proteins. The biological processes with the greatest representation in proteins identified in the media were cellular process, metabolic process, and biological regulation, with the same processes represented in the tissue proteome as well. PCA revealed that injury and cytokine treatment had the strongest contribution to sample variability in the media, while the donor effect was more significant for tissue samples (**Fig. 4.4**). Dex alone reduced the release of some collagens and proteases into the media, with mixed effect on protease inhibitors (**Table 4.1**). Dex had little effect on the tissue proteome normalized to DNA content (**Table 4.2**), with a notable increase in tissue levels of matrix metalloproteinase 3 (MMP3) and superoxide dismutase 2 (SOD2), and a decrease in tissue levels of procollagen-lysine, 2-oxoglutarate 5-dioxygenase 1 and 2 (PLOD1 and 2), and collagen XI.

IC treatment caused an increase in the release of ECM components, proteases, pro-inflammatory factors, and intracellular proteins to the media, with mixed effect on protease inhibitors. The major effect on the tissue proteome was a loss of intracellular metabolic proteins, and an increase in MMP2, MMP3, SOD2, and collagen II. Adding Dex to IC-treated osteochondral plugs reduced the media release of ECM proteins including many collagens and proteases, and mostly increased the release of protease inhibitors compared to IC alone. Many pro-inflammatory factors had increased levels with ICD treatment compared to IC, while in the tissue there was no effect on protein abundances.

4.3.3 Disease and Dex effects on cartilage tissue and bone homeostasis

To investigate proteins identified in both the tissue and media proteomes and their behavior in each compartment under disease stress, we compared the proteins with a significant effect of IC treatment to their corresponding changes in the media with IC treatment (**Fig. 4.5A**). Some proteins had a decrease in both media and tissue, including PLOD1, collagen IX, and collagen XI. The majority had a decrease in the tissue and a corresponding increase in the media, which had many intracellular metabolic and homeostatic proteins such as ribosomal proteins, alcohol dehydrogenase, and protein disulfide-isomerase A6. Proteins with increased levels in both tissue and the media included MMPs -1, -2, and -3, serpin family E member 1 and member 2 (SERPINE1 and -2), and SOD2.

Media levels of osteomodulin (OMD), osteopontin (SPP1), osteonectin (SPARC), sclerostin (SOST), and alkaline phosphatase (ALPL) were decreased with IC treatment (**Fig. 4.5B**). With ICD treatment, media levels of SPARC and ALPL were increased compared to IC treatment, but SPP1 was further decreased. Dex alone only caused the increase of OMD abundance in the media. Osteoprotegerin (TNFRSF11B) did not experience a change with Dex or IC treatment alone, and was slightly decreased by Dex addition to IC treatment compared to IC only.

4.3.4 Analysis of matrix breakdown at the peptide level

Aggrecan (ACAN, **Fig. 4.6A**) had peptides identified in the G1, G2, and G3 globular domains that were mostly increased with IC treatment compared to control in the media. The tryptic peptides identified in the media for collagen II (COL2A1, **Fig. 4.6B**) were decreased with IC treatment in

the N- and C- terminal regions but increased in the center of the protein. In the tissue, all tryptic peptides identified in the G3 domain of aggrecan had decreased release compared to control under injury and disease stress (**Fig. 4.6C**), and the effect on collagen II was only significant in the C-terminal region (**Fig. 4.6D**). Semitryptic peptides found only in the IC-treated condition were found from proteins including fibronectin-1 (FN1), COMP, biglycan (BGN), and collagen VI in the tissue, and collagen II, MMP3, MMP13, fibrillin-1 (FBN1), and FN1 in the media.

Dex had mixed effects on semitryptic peptides, those generated by endogenous proteases and not through trypsin digestion during MS preparation. Many proteins with several identified semitryptic peptides had opposite effects, such as aggrecan (**Fig. 4.6E**), where semitryptic peptides found in the G1 domain had increased release into the media with Dex treatment, but semitryptic peptides from the G2 and G3 domains were decreased compared to control. Dex broadly caused a decrease in media levels of peptides from collagen II (**Fig. 4.6F**), including in the N- and C-terminal regions, with only three having increased abundances compared to control. Collagen I (COL1A1) peptides in both the N- and C-terminal propeptide regions were decreased in the media with both Dex and IC treatment (**Fig. 4.7**).

To investigate which semitryptic peptides may be biomarkers of disease progression, the abundances of each semitryptic peptide were averaged across three biological replicates within each treatment condition and donor, and then regressed against the total percent sGAG loss, an analogue for disease severity, for that treatment condition and donor. From the top 50 peptides with the greatest association with increased sGAG loss, the most represented proteins were MMP1,

ACAN, lumican (LUM), COMP, and MMP3, with other ECM components fibromodulin (FMOD), and FBN1 notably among the top 50 as well (**Fig. 4.8**).

4.3.5 Donor-specific effects on sGAG loss and media proteome

To investigate what protein biomarkers in the media correlated with Dex response, we calculated the percent of the increased sGAG loss caused by IC treatment compared to control that was rescued by Dex for each donor, and regressed the batch-corrected media proteomic data against this Dex rescue percent. When regressing all samples, apolipoproteins, proteins involved in the complement response, and pro-inflammatory factors were all associated with a lower response to Dex, i.e. less of a rescue of increased sGAG loss with IC treatment (**Fig. 4.9A**). To look for potentially predictive markers of a lack of a Dex response, we regressed only the control samples against the Dex percent rescue effect (**Fig. 4.9B**). As with the regression against all media samples, higher levels of proteins associated with humoral immune responses was associated with a lack of a Dex response, as well as proteasomes 20S and 26S.

4.4 Discussion

In this *ex vivo* model of human ankle PTOA, we sought to answer how initial stages of cartilage catabolism occur in the presence of both cartilage and underlying bone. We also investigated how anabolic and metabolic processes would be dysregulated, and what donor-specific responses to both disease and drug treatment would occur. This system used healthy primary osteochondral plugs to study PTOA, rather than total joint replacement discards, as is often the default for *in vitro* osteochondral studies [213]. The effects of injury and cytokine exposure were significant factors driving variance within the proteomic data from both the media and tissue (**Fig. 4.4A & C**). IC

treatment increased the release of ECM components, proteases, pro-inflammatory factors, and intracellular proteins to the media, with mixed effect on protease inhibitors. This agrees with previous models using isolated human knee cartilage [89,174]. The addition of Dex to injury and cytokine-treated osteochondral explants reduced the release of many ECM proteins including aggrecan, collagen VII, lumican, and fibrillin-2, as well as proteases including MMPs 1, 3, 9, and 10, consistent with previous conclusions on the anti-catabolic actions of Dex in models of PTOA [18,89,129,174]. Many intracellular proteins identified in both the tissue and media proteomes had decreased levels in tissue and corresponding increases in the media under injury and cytokine stress (**Fig. 4.5A**), and under IC stress, there was a significant amount of chondrocyte death compared to control (**Fig. 4.2**). As previously hypothesized, the presence of these proteins in the media could be markers of early necrotic cell death [89,174].

This model allowed for the analysis of specific mechanisms of matrix breakdown by observing the behavior of individual regions of proteins such as aggrecan. Under disease stress, the G2 and G3 globular domains saw significant levels of cleavage and release into the media, while there was less of an effect on the G1 domain as determined by the behavior of peptides identified in those regions (**Fig. 4.6A**). The aggrecan found in the tissue was depleted for peptides from the G3 region under IC stress, while the abundances of peptides from the G1 and G2 domains were relatively unchanged. This supports previous findings that aggrecan is degraded primarily from the G3 domain in the N-terminal direction towards the other interglobular regions [130,172,214].

Changes in anabolic protein synthesis important to cartilage recovery from disease processes can also be observed by analyzing effects on specific peptides. Peptides found in the N- and C- terminal

domains of collagen II had decreased abundance in the media with injury and cytokine treatment (**Fig. 4.6B**), and the C-terminal domain peptide identified in the tissue had significantly lower levels with IC treatment (**Fig. 4.6D**). The N- and C- terminal domains of collagen II are cleaved during maturation and incorporation into the matrix, and lower levels of these domains in the media and tissue suggest decreases in the synthesis of new collagen II and suppression of anabolic repair [215]. Dex also suppressed the synthesis of new collagen II as indicated by lower levels of the N- and C-terminal peptides in the media compared to control (**Fig. 4.6F**). These findings are consistent with the anti-catabolic effects of Dex in suppressing protease activity under injury and cytokine stress, thereby decreasing matrix breakdown; however, reports on the effects of Dex on matrix homeostasis in healthy cartilage and chondrocytes are mixed [129]. Additionally, Dex affected the activity of proteases and protease inhibitors in healthy tissue, as indicated by increasing the release of specific semitryptic peptides from aggrecan and decreasing the release of others (**Fig. 4.6E**).

This multi-tissue model combining bone and cartilage incorporates the effects of crosstalk, as bone also undergoes changes due to disease and Dex treatment. OMD, SPP1, SPARC, SOST, and ALPL are common biomarkers of bone health and disease responses. Secreted levels of all these biomarkers were decreased in the media with IC treatment compared to controls. Some of the selected biomarkers are protective under osteoarthritic stress: OMD stimulates osteogenesis, and SOST was protective of cartilage viability in a mouse model of OA/PTOA [216–218]. However, SOST inhibits bone formation, implicating complex regulation of bone and cartilage viability during disease pathogenesis. The synthesis of collagen I, an indicator of osteoblast metabolism, was decreased under disease stress based on levels of its propeptides in the media (**Fig. 4.7B**),

though changes in collagen I synthesis in the cartilage could also have contributed to this effect [219]. The results presented here contradict some previous reports on the presence of these biomarkers under OA stress. SPP1, ALPL, and SPARC have all been shown to be increased in models of OA or associated with OA severity in patient serum, but were decreased with IC treatment in this model [186,220,221]. This could be due to the lack of synovial and other joint tissues, and the crosstalk between all these tissues in the joint, as well as the contribution of the synthesis of these biomarkers from the synovium [186].

In addition, the present model focuses on early stages of PTOA progression, and effects on the production of these biomarkers or on the bone itself could be delayed compared to early changes observed in the cartilage, as osteopontin levels were not elevated compared to control with injury and cytokine treatment [186,222]. Corticosteroids are expected to affect bone biology, as at certain doses and durations of exposure they can cause osteoporosis and are generally considered detrimental to bone health [208,223]. However, in this study Dex had mixed effects on these biomarkers of bone health, rescuing decreased levels of ALPL and SPARC when added to IC-treated osteochondral explants, but further decreasing the levels of SPP1. Dex alone only caused a change in secreted OMD, increasing the amount of this osteogenic biomarker compared to control. However, Dex alone also decreased the synthesis of collagen I overall (**Fig. 4.7A**). The relatively short duration (3 weeks) and low dose of Dex used in our study (100 nM) may mitigate against strong catabolic effects on the bone, as negative effects on bone health may be more prevalent with longer exposure and later stages of PTOA progression.

As semitryptic peptides are generated by endogenous protease activity and not by trypsin treatment during MS preparation, these peptides can serve as potential biomarkers for the identification of PTOA progression. Other protease-generated neoepitope fragments such as the COMP neoepitope Ser^{77} are already being investigated as disease biomarkers [182]. Proteases including MMPs are synthesized and released at the earliest stages of PTOA progression in *in vitro* models, so the production of semitryptic peptides as proteases begin to act on matrix proteins is a promising target to find prognostic PTOA biomarkers. This study identified semitryptic peptides that were only present with IC treatment from matrix proteins including COMP, FN1, and BGN, as well as many that were highly associated with sGAG loss. This regression against sGAG loss identified semitryptic peptides from aggrecan, COMP, FBN1, FMOD, LUM, MMP1, and MMP3 (**Fig. 4.8**), as those most predictive of disease severity. These are promising candidates for PTOA biomarkers that should be investigated further in clinical samples to determine their potential prognostic use.

Biomarkers are desirable to determine which patients are most at risk of developing PTOA immediately after an injury, as well as to determine which might respond best to a therapeutic such as Dex, particularly because of potential off-target effects [5,224]. This study demonstrated differences in donor responses to Dex (**Fig. 4.3**) that allowed for investigation of proteins that best predicted which donors were responders and non-responders. Proteomic data were regressed against the amount of sGAG lost under disease stress that was rescued by Dex treatment in order to determine which proteins best predicted anti-catabolic activity. Over all samples, high levels of apolipoproteins and proinflammatory immune factors were associated with a lack of a Dex response. Apolipoproteins A, B, C, and H were all inversely associated with a Dex rescue effect on sGAG loss, while the anti-inflammatory apolipoprotein E was associated with a Dex rescue

effect [225–227]. However, apolipoproteins A and B have also been shown to have anti-inflammatory activity, inhibiting T cell activation and the innate immune response [228]. Dex does have anti-inflammatory effects, but a highly elevated initial inflammatory state could prevent its anti-catabolic activity. When regressing only the untreated control condition, most analogous to healthy patients or very early stages of the disease, a lack of a Dex rescue response was associated again with humoral immune processes, as well as proteasomes 20S and 26S. Proteasomes play a role in T cell activation and immune responses, and circulating proteasomes have been associated with immunological activity and cellular damage [229,230]. This finding further supports that elevated immunological activity before disease induction is associated with a lack of Dex response, which may help to distinguish patients that may best respond to Dex. The baseline inflammatory state of a joint and presence of proteins such as apolipoproteins is likely tied to sex, diet, BMI, lifestyle, genetic disposition, and many other factors that cannot be explored with such a small number of donors, and all of this information was not available for these anonymized samples [231]. Further investigation of clinical samples from many Dex-treated patients is necessary to follow up on the possibility that apolipoproteins and proteasomes are predictors of a stronger Dex response, and what relationship those protein biomarkers have to other characteristics such as sex or weight that could be used in tandem to predict drug responses.

4.4.1 Study limitations

PTOA of the talocrural joint is a relevant model system to study as the incidence of ankle PTOA is expected to rise as our population ages; however, ankles are not the only joints that can undergo PTOA progression [209]. Because of differences between joint physiology, these results must be validated in samples from knee and hip cartilage to confirm their translatability to those models,

as the drug and disease responses may be different in this same time span in a different joint. For example, it has been shown that protein turnover rate for COMP and G1 aggrecan was higher in the ankle compared to the knee [232]. The use of primary human samples allowed for a more translatable *in vitro* model system but introduced several limitations. Depending on the area of the ankle that the osteochondral plugs were harvested from, the cartilage thickness could vary by up to a millimeter. Normalizing to cartilage weight and DNA content addressed differences in both the amount of tissue and number of cells within the tissue, but differences in drug transport could still affect the biological response of the tissue. Osteochondral plugs from different areas of the ankles were randomized between treatment conditions to further address the location-specific variation. The donor osteochondral plugs had differences in bone density, vascularity, and cellularity, and while the bone could be cut to approximately the same length, it did not always cut perfectly. Nevertheless, this work builds off previous studies that used more repeatable juvenile bovine cartilage explants which could be cut to the same thickness. Our present results confirm several of those previous findings of disease and Dex effects [174], specific to the timing and dosing of Dex treatment, as well as continuous exposure to inflammation. The current approach to intra-articular injection of corticosteroids involves a much higher initial dose that is maintained for a much shorter time due to rapid clearance from the joint. However, novel methods of drug delivery are currently under investigation to replicate low-dose Dex delivery over a longer durations targeted to cartilage [117,119,149]. The addition of synovial tissue to this system would broaden applicability to knee and other joints, but would introduce uncontrolled and inconsistent levels of inflammatory cytokines compared to controlled addition of exogenous cytokines [98]. Our proteomic analysis used MS identification based on trypsin digestion of media and tissue proteins, which removes the ability to identify some endogenously produced peptides. Using other

digestions enzymes would allow for more identifications, but every enzyme will have limitations. We utilized a high threshold of confidence for identification and strict filtering for inclusion to compensate for any single-peptide identifications or quantifications. The tissue proteome only includes proteins that could be solubilized and extracted from the tissue, leaving cross-linked matrix proteins behind. Proteins identified in the media by MS could have been released from both cartilage and bone, so it is difficult to explicitly say what tissue changes in media levels of proteins originate from.

4.5 Conclusions

This osteochondral human *ex vivo* model of PTOA allowed for the analysis of disease progression and Dex effects in a multi-tissue context allowing crosstalk between cartilage and bone starting with healthy tissue. The combination of a single mechanical injury, TNF-α, and IL-6 treatment caused catabolic changes and a suppression of cartilage anabolism, in line with other studies using isolated cartilage. This model of early PTOA caused some changes to bone metabolism as well, which did not extend to full bone breakdown but suppressed normal homeostatic processes. The addition of Dex to this PTOA model confirmed the anti-catabolic effects seen in previous studies using isolated cartilage, and peptidomic analyses revealed a suppression of collagen II synthesis and dysregulation of endogenous protease activity, even with healthy cartilage. Elevated levels of humoral proteins and apolipoproteins were associated with a lack of a Dex response, a promising set of predictive biomarkers for patient Dex response that could allow for targeted, personalized drug treatment that can be combined with pro-anabolic drugs to offset potential off-target effects [18]. The potent anti-catabolic effects of Dex must be balanced with its potential off-target effects, so its use as a DMOAD is likely most appropriate with a targeted delivery system to cartilage and

much lower doses than what is currently used clinically. With Dex as a promising DMOAD candidate for early PTOA intervention, prognostic biomarkers are critical to determine patients most at risk of developing PTOA as well as those most likely to respond to Dex. Semitryptic peptide biomarkers associated with PTOA progression from several ECM proteins and proteases presented in this study should be validated against longitudinal clinical samples and used in tandem with other biomarker candidates, as with patient heterogeneity there is likely not only one single sufficient biomarker.

4.6 Declarations

Ethics approval

All procedures were approved by Rush University Medical IRB and the MIT COUHES committee.

Availability of data and materials

The mass spectrometry proteomics data have been deposited to the ProteomeXchange Consortium (http://proteomecentral.proteomexchange.org) via the PRIDE partner repository [146] with the dataset identifier PXD032213.

Acknowledgements

Supported by grants NIH-NCATS UG3/UH3 TR002186 (AJG), the 2022 Siebel Scholars award (RMB), the Rush Klaus Kuettner Endowed Chair (SC), the Swedish Rheumatism Association (PÖ), the Alfred Österlund Foundation (PÖ), the Greta & Johan Kock and Crafoord Foundations (PÖ), the Olle Engkvist Foundation (PÖ). Instrument funding (MS) from the IAB Lundberg Foundation (PÖ). The authors acknowledge Gift of Hope Organ & Tissue Donor Network (Itasca, IL) and donors' families.

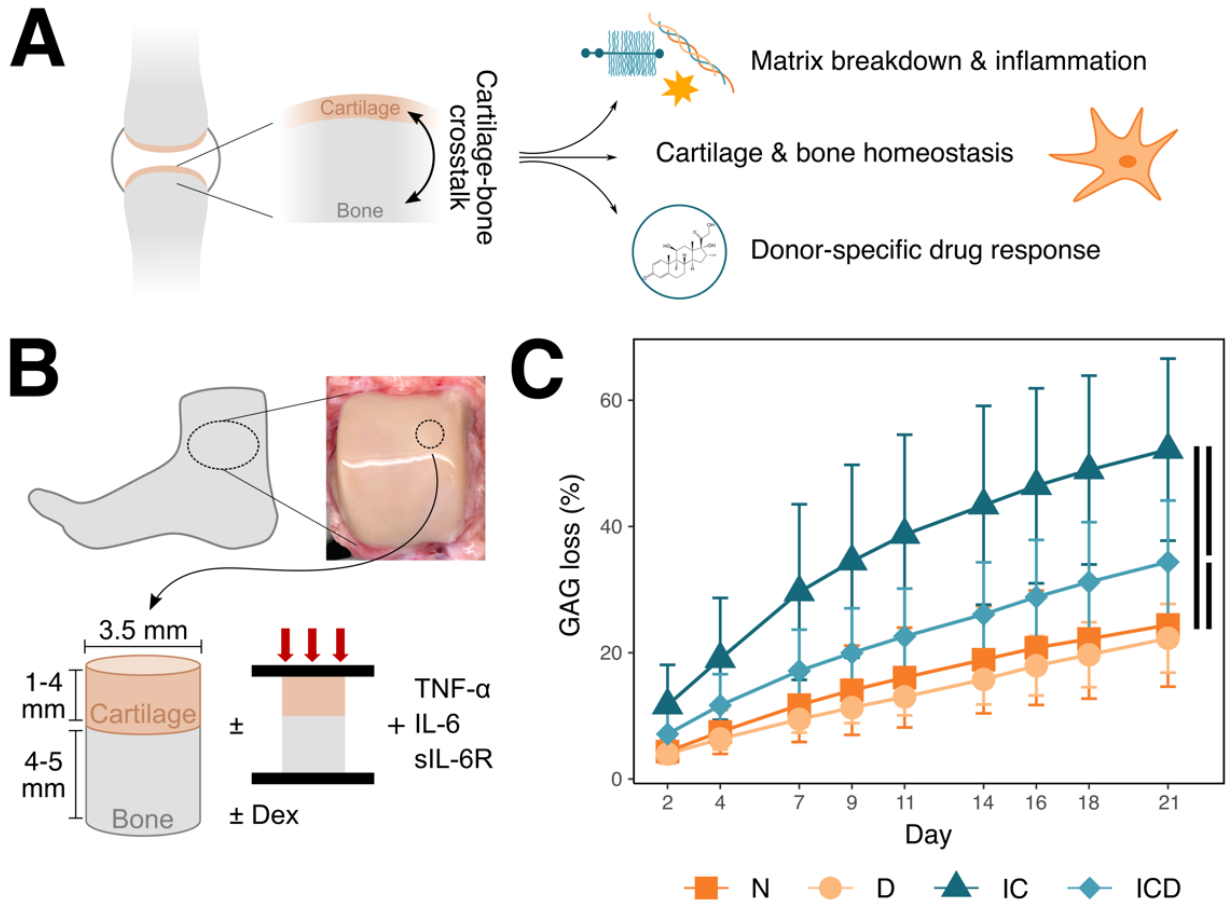

Figure 4.1. Graphical abstract, methods overview, and summed sGAG loss across all donors. A. This model of PTOA incorporates crosstalk between cartilage and bone, which is involved in the progression of catabolism under disease stress, dysregulation of homeostatic processes, and donor-specific responses to drug treatment. **B.** Grade 0-1 osteochondral plugs containing full-thickness cartilage and 4-5 mm of the underlying bone were harvested from the talus joints of seven adult human donors. After two days of equilibration, plugs were left untreated, treated with 100 nM Dex, subjected to a single impact mechanical injury and cultured with 25 ng/mL TNF-α, 50 ng/mL IL-6, and 250 ng/mL sIL-6R, or treated with injury, cytokines, and Dex for three weeks. **C.** sGAG loss over three weeks across all seven donors. N: no treatment; D: Dex alone treatment, IC: injury and cytokine treatment; ICD: injury, cytokines, and Dex. Error bars represent standard deviation. Bar: $p < 0.05$, day 21 total % sGAG loss.

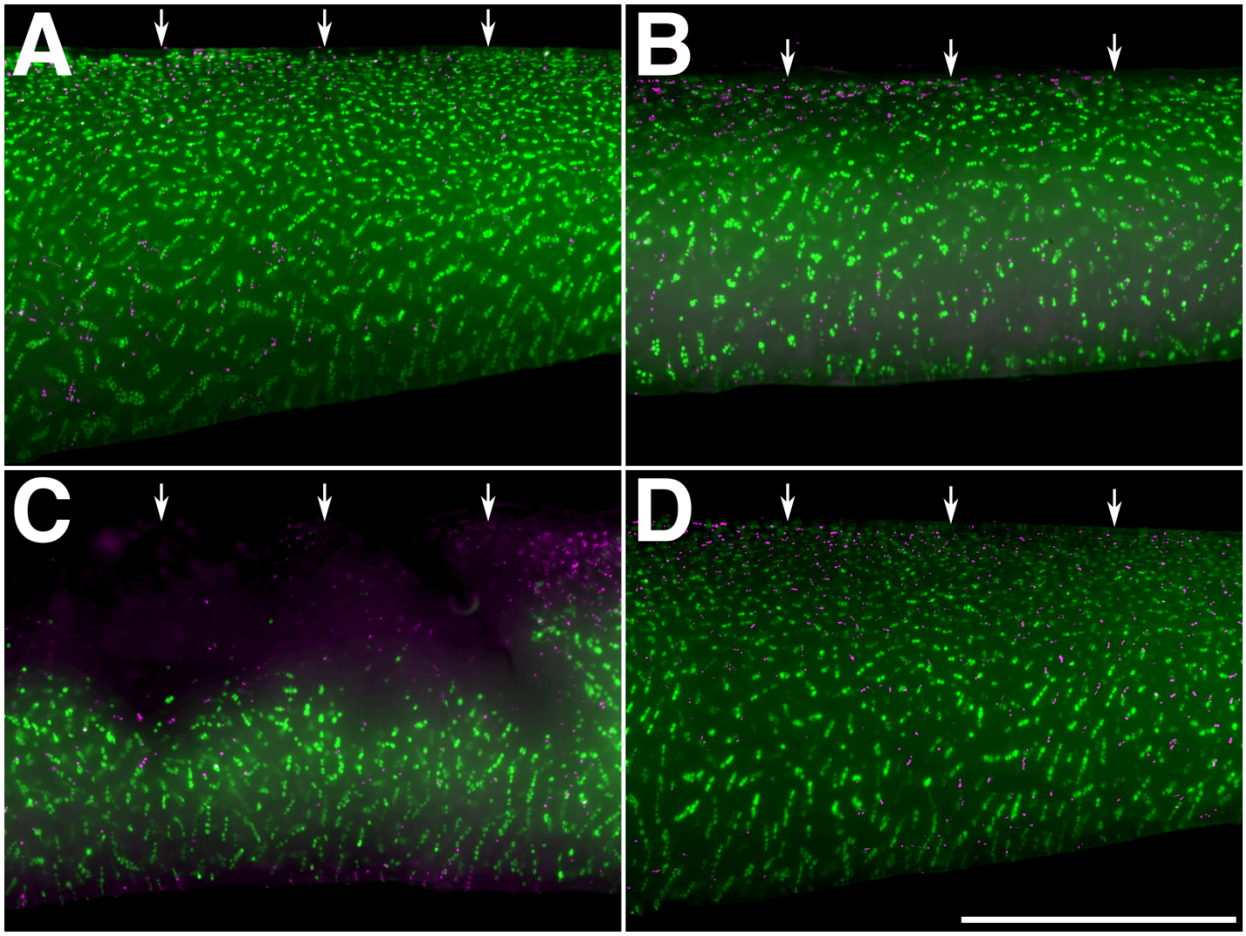

Figure 4.2. Fluorescent imaging assessment of cartilage viability from osteochondral plugs. Vertical cartilage tissue sections (~100 μm thick) were stained with fluorescein diacetate (green) and propidium iodide (magenta) after three weeks with no treatment (**A**), Dex alone (**B**), injury and cytokine treatment (**C**), and injury, cytokines, and Dex (**D**). Scale bar: 1 mm. Arrows: superficial cartilage surface.

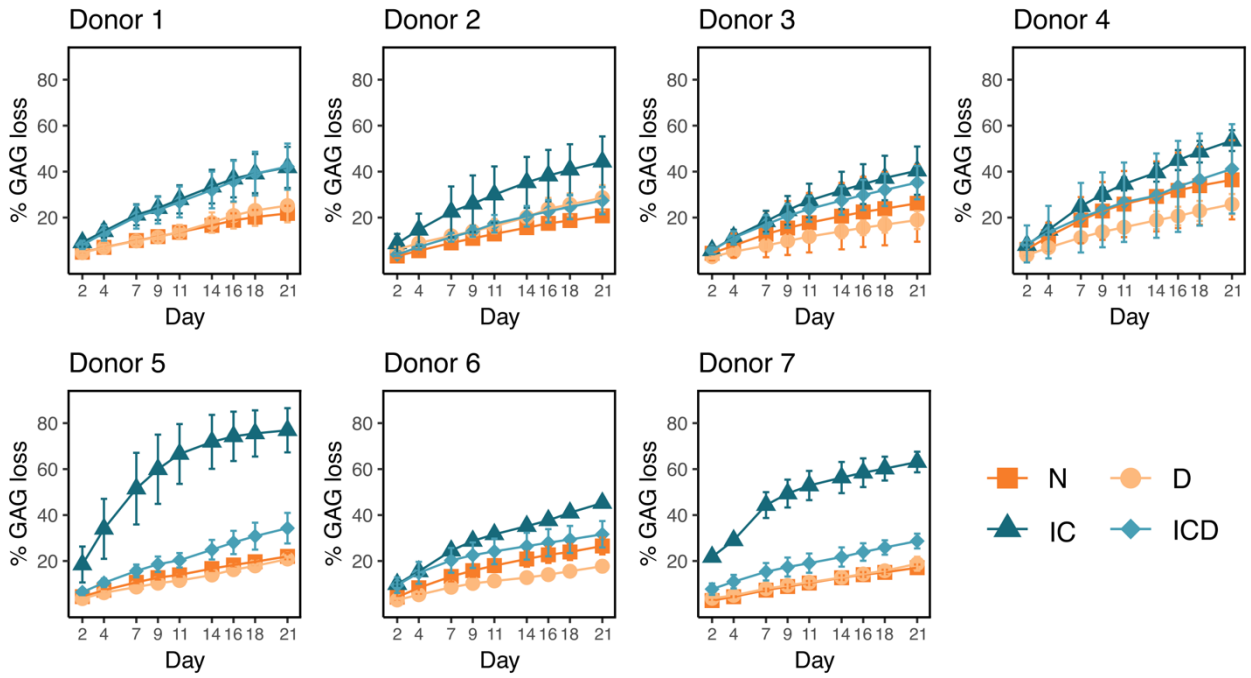

Figure 4.3. sGAG loss within individual donors. sGAG loss over three weeks across for each donor. N: no treatment; D: Dex alone treatment, IC: injury and cytokine treatment; ICD: injury, cytokines, and Dex. Error bars represent standard deviation.

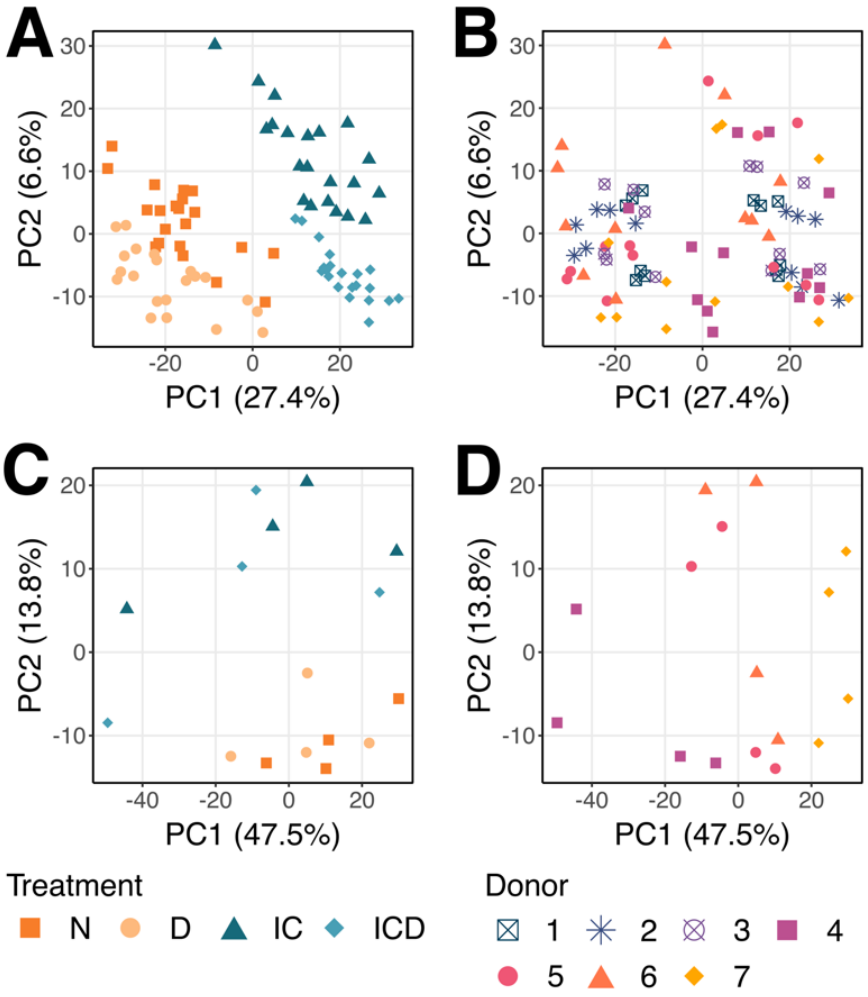

Figure 4.4. Principal component analysis of media and tissue proteomes. PCA was performed on filtered and imputed proteomic data for batch-corrected media samples (**A**, **B**) and DNA-normalized tissue samples (**C**, **D**). N: no treatment; D: Dex alone treatment, IC: injury and cytokine treatment; ICD: injury, cytokines, and Dex. Percentages on axes represent percent variance explained by that principal component.

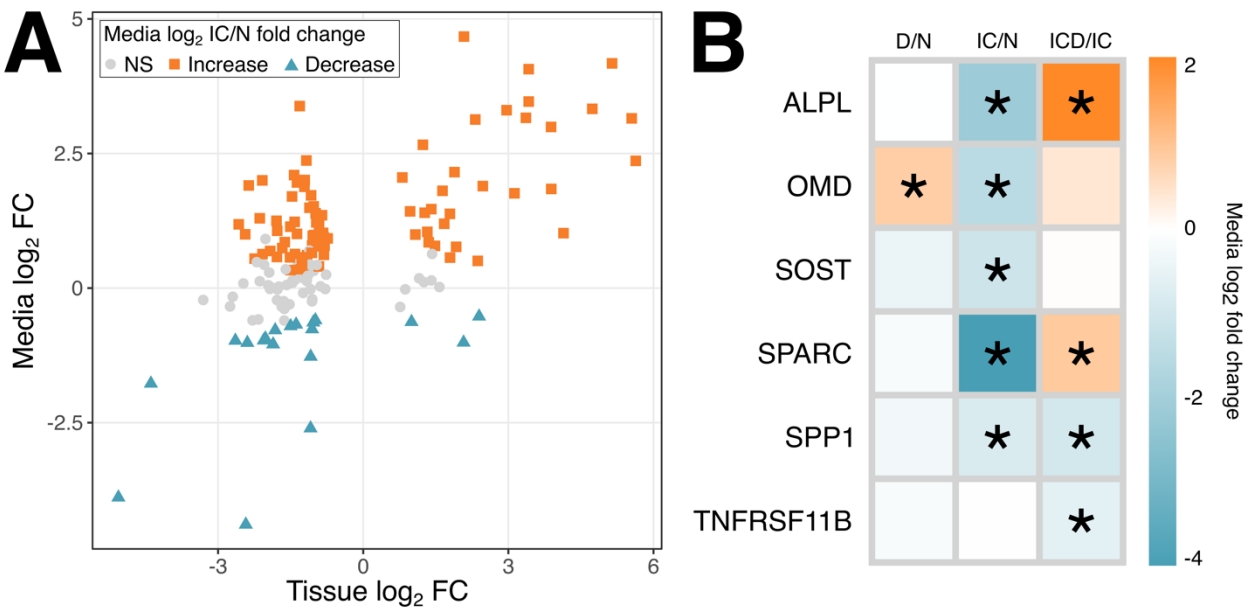

Figure 4.5. Effects of disease on cartilage tissue and biomarkers of bone homeostasis. A. Log_2 fold change (FC) of proteins with a significant effect with injury and cytokine (IC) treatment versus control (N) in cartilage tissue plotted against their media log_2 FC of IC/N. Colors represent significance and direction of effect in media. **B.** Log_2 fold change of media levels for selected biomarkers of bone health. N: no treatment; D: Dex alone treatment, IC: injury and cytokine treatment; ICD: injury, cytokines, and Dex. ALPL: alkaline phosphatase; OMD: osteomodulin; SPARC: osteonectin; SPPI: osteopontin; SOST: sclerostin; TNFRSF11B: osteoprotegerin. *: $p < 0.05$.

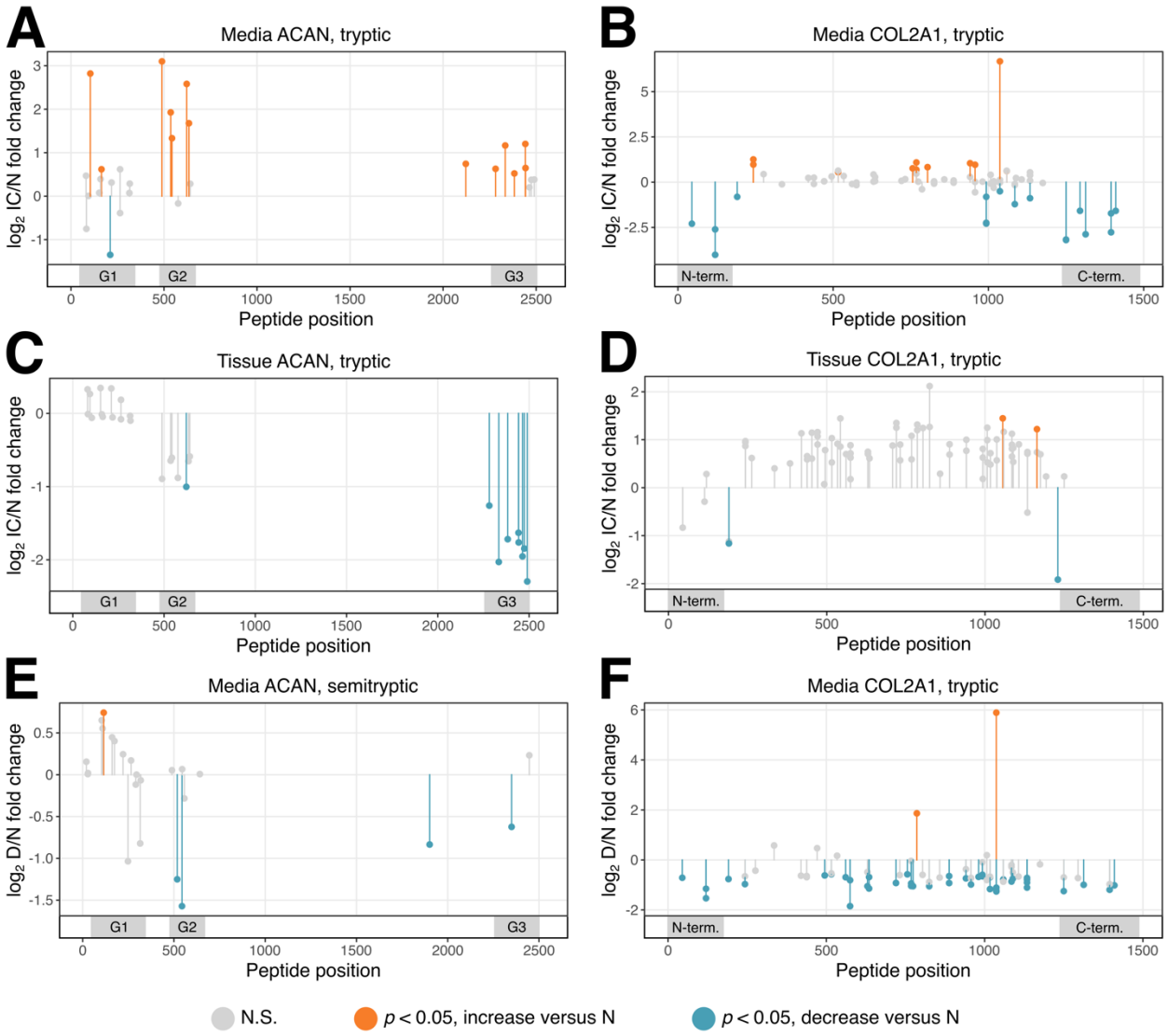

Figure 4.6. Effects of disease and Dex on individual tryptic and semitryptic peptides from aggrecan and collagen II. Log_2 fold change of injury and cytokine treatment versus control (**A-D**) or Dex versus control (**E-F**) abundances of peptides identified in aggrecan (ACAN; **A**, **C**, **E**) and collagen II (COL2A1l; **B**, **D**, **E**). Peptides identified in media (**A**, **B**, **E**, **F**) or tissue (**C**, **D**). x-axis: residue position of first amino acid for each peptide. Orange: significant ($p < 0.05$) increase compared to control. Blue: significant ($p < 0.05$) decrease compared to control. Grey: no significant change compared to control (N.S.) Positions of globular domains for aggrecan (G1, G2, G3) and collagen II N- and C-terminal regions (N-term. and C-term., respectively) are highlighted.

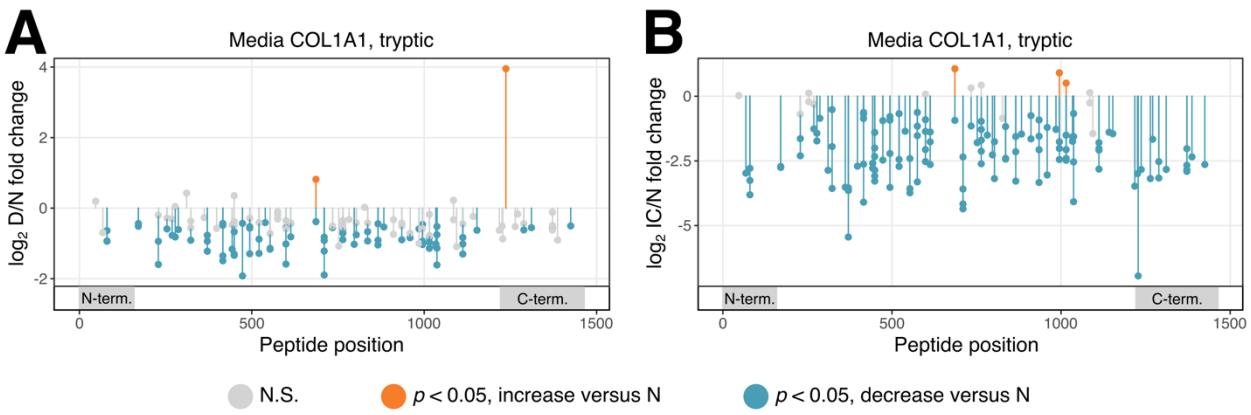

Figure 4.7. Changes in media abundances of collagen I tryptic peptides with Dex and disease treatment. Log_2 fold change of Dex treatment versus control (**A**) or injury and cytokine treatment versus control (**B**). x-axis: residue position of first amino acid for each peptide. Orange: significant ($p < 0.05$) increase compared to control. Blue: significant ($p < 0.05$) decrease compared to control. Grey: no significant change compared to control (N.S.) Positions of N- and C-terminal regions (N-term. and C-term., respectively) are highlighted.

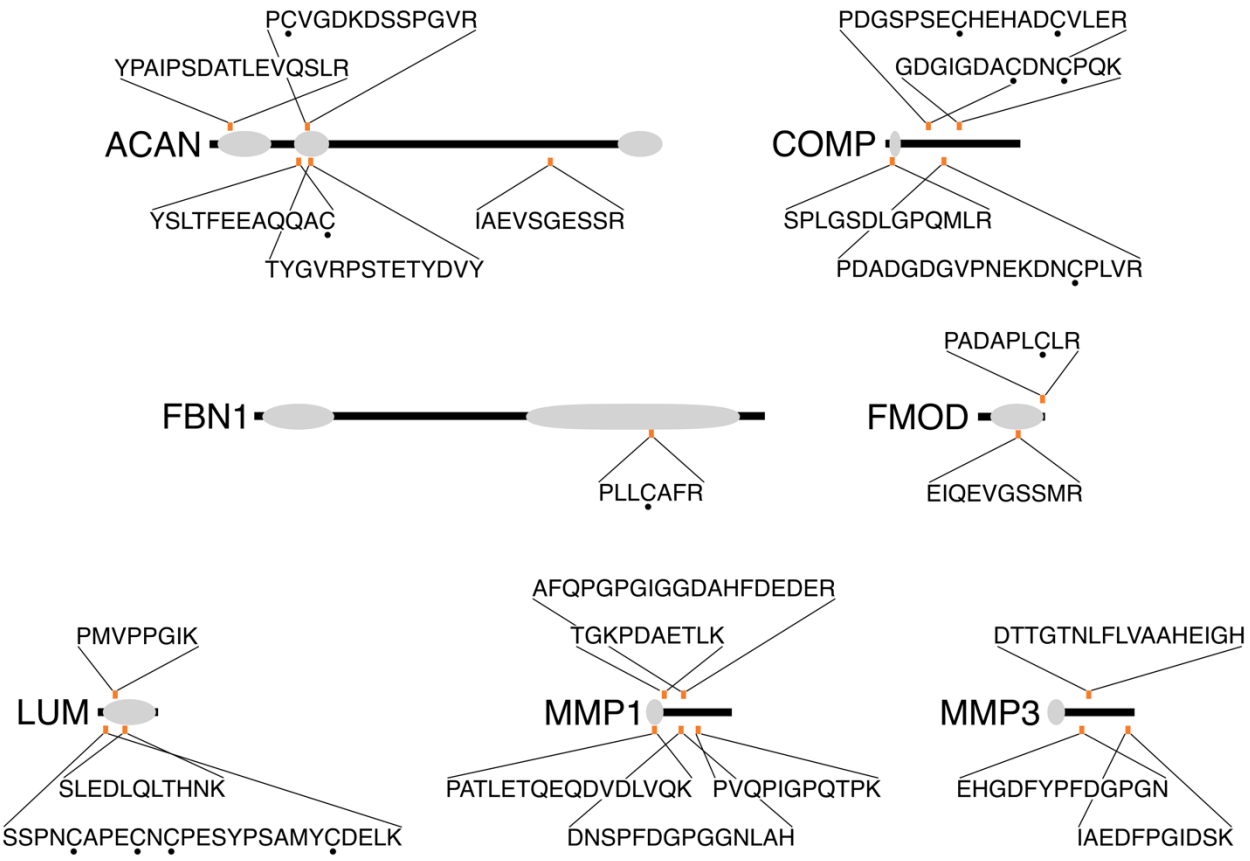

Figure 4.8. Semitryptic peptides associated with increased sGAG loss. Semitryptic peptide abundance data across all media samples were regressed against sGAG loss for each donor and treatment condition. Selected peptides from among the top 50 highest associated peptides are Grey areas represent notable domains for each protein; ACAN: globular domains; COMP: N-terminal domain, FBN1: N- and C-terminal domains; FMOD: leucine-rich repeats; LUM: leucine-rich repeats; MMP1: propeptide; MMP3: propeptide. • : Carbamidomethylation of cysteine residue.

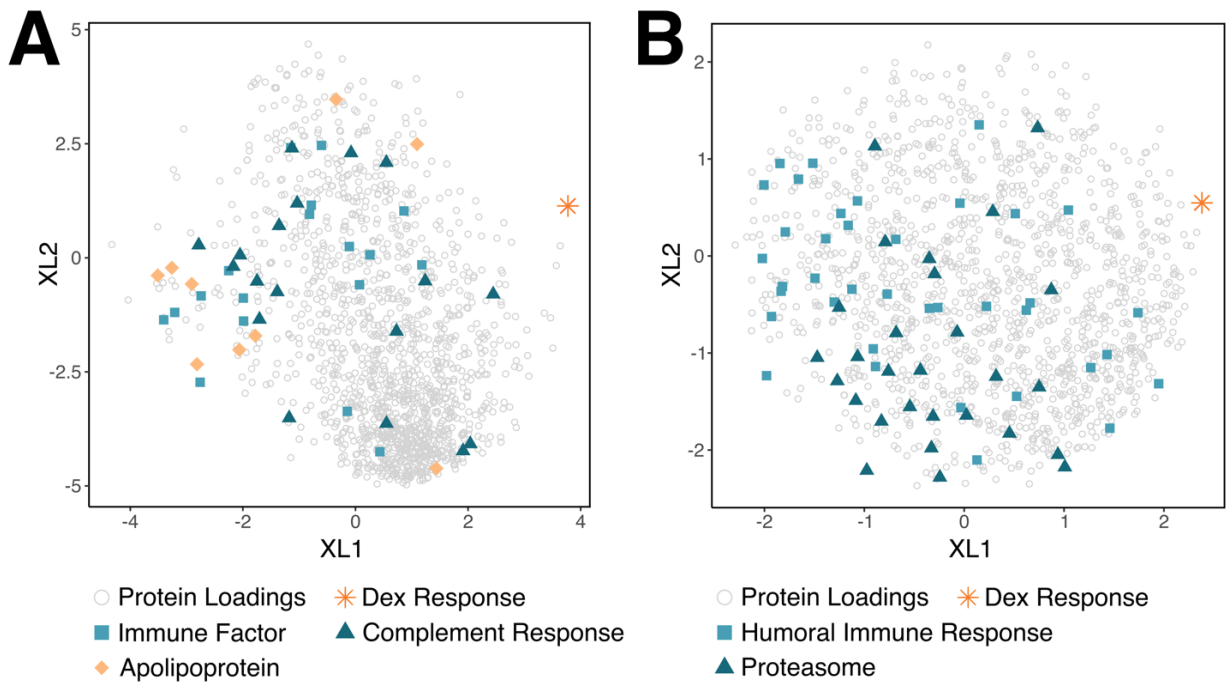

Figure 4.9. Partial least squares regression of Dex rescue effect on sGAG loss. A. Protein loadings after PLSR of all batch-corrected media proteomic data against the percent of increased sGAG loss caused by IC treatment that was rescued by Dex for each donor. Enriched biological processes were determined with Gene Set Enrichment Analysis. XL: predictor loading values. **B.** PLSR of only untreated control media against the percent Dex rescue of increased sGAG loss with IC treatment.

D/N				
	Biological Process	FDR	Molecular Function	FDR
Increased	Cellular response to vitamin k	0.0282	Fibronectin binding	0.00012
	Negative regulation of smooth muscle cell-matrix adhesion	0.0282	Proteoglycan binding	2.03E-06
	UDP-glucuronate biosynthetic process	0.0418	Collagen binding	1.08E-06
	Positive regulation of substrate-dependent cell migration, cell attachment to substrate	0.0418	Laminin binding	0.04
	Negative regulation of plasminogen activation	0.005	Lipoprotein particle binding	0.04
Decreased	Positive regulation of cell proliferation by vegf-activated pdgf receptor signaling pathway	0.0029	Procollagen-lysine 5-dioxygenase activity	0.0066
	Esophagus smooth muscle contraction	0.0383	Phosphodiesterase i activity	0.0213
	Hydroxylysine biosynthetic process	0.0383	Platelet-derived growth factor binding	0.00028
	Glomerular capillary formation	0.0093	Extracellular matrix structural constituent conferring tensile strength	2.89E-10
	Peptidyl-lysine hydroxylation	0.0153	Low-density lipoprotein particle binding	0.0159

IC/N				
	Biological Process	FDR	Molecular Function	FDR
Increased	Actin filament fragmentation	0.0023	Peroxiredoxin activity	0.00033
	Helper t cell extravasation	0.0151	Thioredoxin peroxidase activity	0.0108
	Cellular hyperosmotic salinity response	0.0151	Copper chaperone activity	0.0108
	Positive regulation of establishment of protein localization to telomere	2.99E-06	Extracellular matrix constituent conferring elasticity	0.0027
	CRD-mediated mRNA stabilization	0.0037	Threonine-type endopeptidase activity	1.35E-06
Decreased	Collagen fibril organization	4.85E-05	Extracellular matrix structural constituent conferring tensile strength	1.31E-07
	Chondroitin sulfate proteoglycan biosynthetic process	0.0053	Heparan sulfate proteoglycan binding	0.0126
	Chondroitin sulfate biosynthetic process	0.0275	Insulin-like growth factor binding	0.00021
	Protein hydroxylation	0.0301	Extracellular matrix structural constituent	3.48E-09
	Chondroitin sulfate proteoglycan metabolic process	0.0025	Proteoglycan binding	0.0131

ICD/N				
	Biological Process	FDR	Molecular Function	FDR
Increased	Actin filament fragmentation	0.0031	Peroxiredoxin activity	0.00041
	Fumarate metabolic process	0.0188	Threonine-type endopeptidase activity	5.16E-12
	Helper t cell extravasation	0.0188	Thioredoxin peroxidase activity	0.0143

	Protein unfolding	0.0188	Copper chaperone activity	0.0143
	Cellular hyperosmotic salinity response	0.0188	Extracellular matrix constituent conferring elasticity	0.004
Decreased	Hydroxylysine biosynthetic process	0.0346	Procollagen-lysine 5-dioxygenase activity	0.0021
	Peptidyl-lysine hydroxylation	0.0112	Insulin-like growth factor ii binding	0.0145
	pdgf receptor-beta signaling pathway	0.0112	Extracellular matrix structural constituent conferring tensile strength	3.20E-08
	Type b pancreatic cell proliferation	0.0137	Insulin-like growth factor i binding	0.0242
	Basement membrane assembly	0.0137	Platelet-derived growth factor binding	0.0291

ICD/IC				
	Biological Process	FDR	Molecular Function	FDR
Increased	Negative regulation of plasminogen activation	0.0011	Threonine-type endopeptidase activity	1.11E-07
	Viral translational termination-reinitiation	0.0126	Peptide disulfide oxidoreductase activity	0.0031
	Proteasomal ubiquitin-independent protein catabolic process	4.16E-08	S100 protein binding	0.0041
	Modulation of age-related behavioral decline	0.0033	Fibroblast growth factor binding	0.0136
	Negative regulation of dendritic cell apoptotic process	0.0224	Low-density lipoprotein particle receptor binding	0.0153
Decreased	Hydroxylysine biosynthetic process	0.0235	Heparan sulfate proteoglycan binding	0.0021
	Gonadotrophin-releasing hormone neuronal migration to the hypothalamus	0.0345	CXCR chemokine receptor binding	0.0478
	Positive regulation of cell proliferation by vegf-activated platelet derived growth factor receptor signaling pathway	0.0345	Fibronectin binding	0.0088
	Formaldehyde catabolic process	0.0345	Extracellular matrix structural constituent conferring tensile strength	0.0096
	Facioacoustic ganglion development	0.0345	Laminin binding	0.0105

Table 4.1. Biological process and molecular function enrichment for media proteins significantly affected by Dex or injury treatment. Proteins with a significant effect (either increased or decreased, $p < 0.05$) of Dex versus control (D/N), mechanical injury and cytokine treatment versus control (IC/N), or injury, cytokines, and Dex versus injury and cytokines (ICD/IC) were analyzed with STRING protein association network analysis, and the five biological processes and molecular functions with the strongest enrichment ($\log_{10}$(number of observed proteins/number of expected proteins)) were selected. FDR: false discovery rate.

IC/N				
	Biological Process	FDR	Molecular Function	FDR
Increased	Negative regulation of plasminogen activation	0.0409	Protease binding	0.0064
	Negative regulation of metallopeptidase activity	0.049	Endopeptidase inhibitor activity	0.0182
	Extracellular matrix disassembly	4.33E-06	Enzyme inhibitor activity	0.0483
	Collagen catabolic process	0.0033	Signaling receptor binding	7.85E-05
	Regulation of cellular senescence	0.0495	Binding	0.0182
Decreased	Hydroxylysine biosynthetic process	0.0491	Procollagen-lysine 5-dioxygenase activity	0.0042
	Isocitrate metabolic process	0.0092	Procollagen-proline dioxygenase activity	0.0164
	Valine metabolic process	0.0092	Peptide disulfide oxidoreductase activity	0.0042
	Peptidyl-lysine hydroxylation	0.016	Racemase and epimerase activity, acting on carbohydrates and derivatives	0.0404
	Positive regulation of rna polymerase ii transcription preinitiation complex assembly	0.0252	L-ascorbic acid binding	0.0011

ICD/N				
	Biological Process	FDR	Molecular Function	FDR
Decreased	Telomerase holoenzyme complex assembly	0.0074	Procollagen-lysine 5-dioxygenase activity	0.0075
	Isocitrate metabolic process	0.00088	Proteasome-activating atpase activity	0.0075
	Positive regulation of rna polymerase ii transcription preinitiation complex assembly	0.00022	Isocitrate dehydrogenase activity	0.0168
	Valine metabolic process	0.0153	Procollagen-proline dioxygenase activity	0.0313
	Positive regulation of establishment of protein localization to telomere	0.0032	Peptide disulfide oxidoreductase activity	0.001

Table 4.2. Biological process and molecular function enrichment for tissue proteins significantly affected by Dex or injury treatment. Proteins with a significant effect (either increased or decreased, $p < 0.05$) of mechanical injury and cytokine treatment versus control (IC/N), or injury, cytokines, and Dex versus injury and cytokines (ICD/IC) were analyzed with STRING protein association network analysis, and the five biological processes and molecular functions with the strongest enrichment ($\log_{10}$(number of observed proteins/number of expected proteins)) were selected. FDR: false discovery rate.

Chapter 5. Conclusions and Future Directions

The research in this thesis used systems-level proteomics analyses of cartilage monoculture and osteochondral co-culture of human and bovine explants in *ex vivo* models of post-traumatic osteoarthritis (PTOA) to better understand the effects of disease progression on catabolism and anabolism and identify disease biomarkers. These models were further used to study the effects of Dex on suppressing catabolic changes without entirely restoring anabolic processes to control levels, with minimal effects on healthy untreated controls.

Cartilage monoculture from juvenile bovine joints in a PTOA model using a mechanical injury and inflammatory cytokine treatment allowed analysis of the differential release of proteins from diseased and healthy tissues over three weeks. In this model, mechanical injury had little effect on the media proteome over the entire duration of treatment. Proteomic analysis of culture media revealed increases in extracellular matrix components and inflammatory mediators that were mostly attenuated with the addition of Dex, demonstrating its protective effect against matrix breakdown. The anti-catabolic effect of Dex was further confirmed with biochemical analyses of aggrecan and COMP fragmentation, with the addition of Dex preventing the generation of specific protease-generated breakdown products. Several proteins with increased release were suggested as novel biomarker candidates for early disease identification.

The disease response on the release of some anabolic factors was mixed, with some having increased levels and others decreased in the media, and Dex did not rescue most of these disease effects. Dex did, however, increase the release of some proteins across all conditions, even in healthy cartilage, providing insights into its minimal but non-negligible off-target effects.

This bovine PTOA model was expanded to use adult human *ex vivo* cartilage from a healthy knee joint, and differential and hierarchical clustering analyses of culture media proteomes were

performed to assess both the differential release of proteins as well as the timing of their release in diseased and Dex-treated contexts. This model of early PTOA progression showed the peak release of many biomarker candidates nine to fifteen days after the induction of disease, relevant to when a patient may visit a clinician post-injury. Many biomarker candidates identified in the previous bovine model were confirmed in the human data, confirming the utility of animal model systems in some contexts. These data on the timing of the release of extracellular matrix components also provided insight into the sequential release of different matrix proteins, with collagen-binding proteins and some proteoglycans proteolytically cleaved and released before larger proteins such as collagen II can be accessed by proteases.

In this model of early human PTOA, Dex continued to show anti-catabolic effects, reducing the release of many proteases and matrix components indicative of cartilage breakdown. Dex treatment also restored most of the kinetics of release of the proteome to control levels. However, notably several proteases, protease inhibitors, and immune regulators such as complement proteins did not return to their control kinetics with Dex treatment, with some proteases still experiencing increased release within a week of disease induction and many immune factors released approximately two and a half weeks intro treatment. This suggests that the anti-inflammatory effects of Dex do not entirely maintain that signaling at control levels, but still cause some dysregulation of immune signaling with extended treatment with Dex.

As PTOA progression is regulated by several joint tissues and not cartilage alone, the human PTOA model was expanded to include osteochondral plugs consisting of full-thickness cartilage and the underlying subchondral and trabecular bone from macroscopically healthy human cadaver ankles. Catabolic effects on cartilage including chondrocyte death, increased release of extracellular matrix components, and protease release were consistent with findings of cartilage

monoculture PTOA models. The suppression of anabolism was further explored by analyzing not only the media proteome, but also changes within the tissue and disease effects on individual peptides. Collagen II and collagen I synthesis were decreased with both inflammatory cytokine and Dex treatment as indicated by changes in their N- and C-terminal propeptide regions, and bone homeostatic processes were suppressed with injury and cytokine treatment. Proteomic data were regressed against biochemical analysis of sGAG loss, an analogue for disease severity, to determine semitryptic peptides associated the most with disease progression. Many peptides from matrix components such as cartilage oligomeric matrix protein, lumican, and aggrecan were identified as being highly associated with sGAG loss, suggesting they may have utility as prognostic disease biomarkers during early breakdown events.

Adding Dex to healthy as well as cytokine-treated osteochondral plugs suppressed endogenous protease activity as indicated by the reduction of protease-generated aggrecan semitryptic peptides. Broadly, Dex decreased matrix breakdown and sGAG loss, but individually the seven donors had different magnitudes of Dex rescue of sGAG loss. The Dex rescue effect was regressed against media proteomic data for each donor to find proteins most predictive of a Dex effect, and elevated levels of immune and humoral proteins were associated with a lack of a Dex response. Regression against control samples alone revealed proteasomes and humoral immune proteins as those most associated with a low Dex response, providing a promising set of biomarkers to stratify patients that might benefit the most from Dex treatment.

Future directions of this work involve expanding these model systems to cover more joint tissues such as the synovial joint capsule and to study the effects of treatment-relevant doses of Dex, such as adding a bolus dose of Dex several days after the induction of injury or using targeted delivery methods to deliver a low dose for an extended duration without adding new Dex every

media change. The results on potential prognostic disease biomarker candidates at both the protein and peptide level must be validated against longitudinal clinical samples, which will allow for early disease identification and more targeted clinical outcome measures to assess drugs like Dex. Overall, these results broadly suggest that Dex has potent anti-catabolic effects and minimal effects on cartilage homeostasis early in treatment, with only extended doses causing some changes in immune signaling and regulation of matrix organization, painting it as a safe and effective method of preventing PTOA progression with early, targeted intervention.

References

1. Creamer P. Intra-articular corticosteroid treatment in osteoarthritis. Current Opinion in Rheumatology; 1999. p. 11(5):417-421.

2. Hollander JL, Brown EM, Jessar RA, Brown CY. Hydrocortisone and cortisone injected into arthritic joints: comparative effects of and use of hydrocortisone as a local antiarthritic agent. JAMA. 1951;147:1629–35.

3. Benedek TG. History of the development of corticosteroid therapy. Clin Exp Rheumatol. 2011;29.

4. Jüni P, Hari R, Rutjes AWS, Fischer R, Silletta MG, Reichenbach S, et al. Intra-articular corticosteroid for knee osteoarthritis. Cochrane Database Syst Rev. 2015;2015.

5. Saklatvala J. Glucocorticoids: Do we know how they work? Arthritis Res. 2002;4:146–50.

6. Conaghan PG, Hunter DJ, Cohen SB, Kraus VB, Berenbaum F, Lieberman JR, et al. Effects of a single intra-articular injection of a microsphere formulation of triamcinolone acetonide on knee osteoarthritis pain. J Bone Jt Surg. 2018;100:666–77.

7. Samuels J, Pillinger MH, Jevsevar D, Felson D, Simon LS. Critical appraisal of intra-articular glucocorticoid injections for symptomatic osteoarthritis of the knee. Osteoarthr Cartil. 2021;29:8–16.

8. Arroll B, Goodyear-Smith F. Corticosteroid injections for osteoarthritis of the knee: meta-analysis. Br Med J. 2004;328:869–70.

9. Hepper CT, Halvorson JJ, Duncan ST, Gregory AJM, Dunn WR, Spindler KP. The efficacy and duration of intra-articular corticosteroid injection for knee osteoarthritis: A systematic review of level I studies. J Am Acad Orthop Surg. 2009;17:638–46.

10. McAlindon TE, LaValley MP, Harvey WF, Price LL, Driban JB, Zhang M, et al. Effect of intra-articular triamcinolone vs saline on knee cartilage volume and pain in patients with knee osteoarthritis a randomized clinical trial. JAMA - J Am Med Assoc. 2017;317:1967–75.

11. Mankin HJ, Zarins A, Jaffe WL. The effect of systemic corticosteroids on rabbit articular cartilage. Arthritis Rheum. 1972;15:593–9.

12. Gibson T, Burry HC, Poswillo D, Glass J. Effect of intra-articular corticosteroid injections on primate cartilage. Ann Rheum Dis. 1977;74–9.

13. Wernecke C, Braun HJ, Dragoo JL. The effect of intra-articular corticosteroids on articular cartilage: A systematic review. Orthop J Sport Med. 2015;3:1–7.

14. Duke University. Dexamethasone and pain following total knee arthroplasty [Internet]. https://clinicaltrials.gov/show/nct02271698. 2014.

15. Kim TK. Efficacy and safety of single, low-dose dexamethasone in patients after total knee arthroplasty [Internet]. https://clinicaltrials.gov/ct2/show/NCT01612702; 2012.

16. Lu YCS, Evans CH, Grodzinsky AJ. Effects of short-term glucocorticoid treatment on changes in cartilage matrix degradation and chondrocyte gene expression induced by mechanical injury and inflammatory cytokines. Arthritis Res Ther. 2011;13:R142.

17. Wang Y, Lorenzo P, Chubinskaya S, Grodzinsky AJ, Önnerfjord P. Dexamethasone treatment alters the response of human cartilage explants to inflammatory cytokines and mechanical injury as revealed by discovery proteomics (Abstract). Osteoarthr Cartil. Elsevier; 2017;25:S381–2.

18. Li Y, Wang Y, Chubinskaya S, Schoeberl B, Florine E, Kopesky P, et al. Effects of insulin-like growth factor-1 and dexamethasone on cytokine-challenged cartilage: Relevance to post-traumatic osteoarthritis. Osteoarthr Cartil. 2015;23:266–74.

19. Manson SC, Brown RE, Cerulli A, Vidaurre CF. The cumulative burden of oral corticosteroid side effects and the economic implications of steroid use. Respir Med. Elsevier Ltd; 2009;103:975–94.

20. Bordag N, Klie S, Jürchott K, Vierheller J, Schiewe H, Albrecht V, et al. Glucocorticoid (dexamethasone)-induced metabolome changes in healthy males suggest prediction of response and side effects. Sci Rep. Nature Publishing Group; 2015;5:1–12.

21. Rauchhaus U, Schwaiger FW, Panzner S. Separating therapeutic efficacy from glucocorticoid side-effects in rodent arthritis using novel, liposomal delivery of dexamethasone phosphate: Long-term suppression of arthritis facilitates interval treatment. Arthritis Res Ther. 2009;11:1–9.

22. Islander U, Jochems C, Stubelius A, Andersson A, Lagerquist MK, Ohlsson C, et al. Combined treatment with dexamethasone and raloxifene totally abrogates osteoporosis and joint destruction in experimental postmenopausal arthritis. Arthritis Res Ther. BioMed Central Ltd; 2011;13:R96.

23. Ashraf S, Mapp PI, Walsh DA. Contributions of angiogenesis to inflammation, joint damage, and pain in a rat model of osteoarthritis. Arthritis Rheum. 2011;63:2700–10.

24. Bai H, Yuan R, Zhang Z, Liu L, Wang X, Song X, et al. Intra-articular injection of baicalein inhibits cartilage catabolism and NLRP3 inflammasome signaling in a posttraumatic OA model. Oxid Med Cell Longev. 2021;2021.

25. Wang T, Yang J, Chen X, Zhao K, Wang J, Zhang Y, et al. Systems study on the antirheumatic mechanism of Tibetan medicated-bath therapy using Wuwei-Ganlu-Yaoyu-Keli. Biomed Res Int. 2017;2017:1–10.

26. Celvin B, Zaman F, Aulin C, Sävendahl L. Humanin prevents undesired apoptosis of chondrocytes without interfering with the anti-inflammatory effect of dexamethasone in collagen-induced arthritis. Clin Exp Rheumatol. 2020;38:129–35.

27. Huebner KD, Shrive NG, Frank CB. Dexamethasone inhibits inflammation and cartilage damage in a new model of post-traumatic osteoarthritis. J Orthop Res. 2014;32:566–72.

28. Heard BJ, Barton KI, Chung M, Achari Y, Shrive NG, Frank CB, et al. Single intra-articular dexamethasone injection immediately post-surgery in a rabbit model mitigates early inflammatory responses and post-traumatic osteoarthritis-like alterations. J Orthop Res. 2015;33:1826–34.

29. Malfait AM, Tortorella M, Thompson J, Hills R, Meyer DM, Jaffee BD, et al. Intra-articular injection of tumor necrosis factor-α in the rat: an acute and reversible in vivo model of cartilage proteoglycan degradation. Osteoarthr Cartil. Elsevier Ltd; 2009;17:627–35.

30. Huhtakangas JA, Huovinen J, Laaksonen S, Voipio HM, Vuolteenaho O, Finnilä MAJ, et al. A single intra-articular dose of vitamin D analog calcipotriol alleviates synovitis without adverse effects in rats. PLoS One. 2021;16.

31. Chen L, Ni Z, Huang J, Zhang R, Zhang J, Zhang B, et al. Long term usage of dexamethasone accelerating accelerates the initiation of osteoarthritis via enhancing chondrocyte apoptosis and the extracellular matrix calcification and apoptosis of chondrocytes. Int J Biol Sci. 2021;17:4140–53.

32. Jaffré B, Watrin A, Loeuille D, Gillet P, Netter P, Laugier P, et al. Effects of antiinflammatory drugs on arthritic cartilage: A high-frequency quantitative ultrasound study in rats. Arthritis Rheum. 2003;48:1594–601.

33. Dearden LC, Mosier HD, Brundage M, Thai C, Jansons R. The effects of different steroids on costal and epiphyseal cartilage of fetal and adult rats. Cell Tissue Res. 1986;246:401–12.

34. Mushtaq T, Ahmed SF. The impact of corticosteroids on growth and bone health. Arch Dis Child. 2002;87:93–6.

35. Glade MJ, Krook L, Schryver HF, Hintz HF. Morphologic and biochemical changes in cartilage of foals treated with dexamethasone. Cornell Vet. 1983;73:170–92.

36. Li Q, Chen H, Li Z, Zhang F, Chen L. Glucocorticoid caused lactic acid accumulation and damage in human chondrocytes via ROS-mediated inhibition of Monocarboxylate Transporter 4. Bone. 2022;155.

37. Podbielski A, Raiss R. Dose related effects of dexamethasone treatment on the ultrastructure of articular cartilage in rats. Agents Actions. 1986;17:322–4.

38. Annefeld M, Erne B. The mode of action of a glycosaminoglycan-peptide-complex (Rumalon®) on articular cartilage of the rat in vivo. Clin Rheumatol. 1987;6:340–9.

39. Chan MWY, Gomez-Aristizábal A, Mahomed N, Gandhi R, Viswanathan S. A tool for evaluating novel osteoarthritis therapies using multivariate analyses of human cartilage-synovium explant co-culture. Osteoarthr Cartil. 2022;30:147–59.

40. Arabiyat AS, Chen H, Erndt-Marino J, Burkhard K, Scola L, Fleck A, et al. Hyperosmolar ionic solutions modulate inflammatory phenotype and sGAG loss in a cartilage explant model. Cartilage. 2021;13:713S-721S.

41. Busschers E, Holt JP, Richardson DW. Effects of glucocorticoids and interleukin-1β on expression and activity of aggrecanases in equine chondrocytes. Am J Vet Med. 2010;71:176–85.

42. D'Lima DD, Hashimoto S, Chen PC, Colwell CW, Lotz MK. Human chondrocyte apoptosis in response to mechanical injury. Osteoarthr Cartil. 2001;9:712–9.

43. Saito S, Katoh M, Masumoto M, Matsumoto S, Masuho Y. Dexamethasone inhibits collagen degadation induced by the combination of interleukin-1 and plasminogen in cartilage explant culture. Biol Pharm Bull. 1999;22:727–30.

44. Genemaras AA, Ennis H, Bradshaw B, Kaplan L, Huang CYC. Effects of Anti-Inflammatory Agents on Expression of Early Responsive Inflammatory and Catabolic Genes in Ex Vivo Porcine Model of Acute Knee Cartilage Injury. Cartilage. 2018;9:293–303.

45. Garvican ER, Vaughan-thomas A, Redmond C, Gabriel N, Clegg PD. MMP-mediated collagen breakdown induced by activated protein C in equine cartilage is reduced by corticosteroids. 2010;370–8.

46. Bian L, Stoker a. M, Marberry KM, Ateshian G a., Cook JL, Hung CT. Effects of dexamethasone on the functional properties of cartilage explants during long-term culture. Am J Sports Med. 2010;38:78.

47. Siengdee P, Radeerom T, Kuanoon S, Euppayo T, Pradit W, Chomdej S, et al. Effects of corticosteroids and their combinations with hyaluronanon on the biochemical properties of porcine cartilage explants. BMC Vet Res. BMC Veterinary Research; 2015;11:1–11.

48. Datuin JP, Ng KP, Hayes TB, Bern HA. Effects of glucocorticoids on cartilage growth and response to IGF-I in the tilapia (Oreochromis mossambicus). Gen Comp Endocrinol. 2001;121:289–94.

49. Pemmari A, Leppänen T, Hämäläinen M, Moilanen T, Vuolteenaho K, Moilanen E. Widespread regulation of gene expression by glucocorticoids in chondrocytes from patients with osteoarthritis as determined by RNA-Seq. Arthritis Res Ther. 2020;22:1–13.

50. Stöve J, Schöniger R, Huch K, Brenner R, Günther KP, Puhl W, et al. Effects of dexamethasone on proteoglycan content and gene expression of IL-1β-stimulated osteoarthrotic chondrocytes in vitro. Acta Orthop Scand. 2002;73:562–7.

51. Villiger PM, Terkeltaub R, Lotz M. Monocyte chemoattractant protein-1 (MCP-1) expression in human articular cartilage. Induction by peptide regulatory factors and differential effects of dexamethasone and retinoic acid. J Clin Invest. 1992;90:488–96.

52. Tu Y, Xue H, Francis W, Davies AP, Pallister I, Kanamarlapudi V, et al. Lactoferrin inhibits dexamethasone-induced chondrocyte impairment from osteoarthritic cartilage through up-regulation of extracellular signal-regulated kinase 1/2 and suppression of FASL, FAS, and Caspase 3. Biochem Biophys Res Commun. Elsevier Inc.; 2013;441:249–55.

53. Shalom-Barak T, Quach J, Lotz M. Interleukin-17-induced gene expression in articular chondrocytes is associated with activation of mitogen-activated protein kinases and NF-κB. 1998;273:27467–73.

54. Palmer G, Guerne PA, Mezin F, Maret M, Guicheux J, Goldring MB, et al. Production of interleukin-1 receptor antagonist by human articular chondrocytes. Arthritis Res. 2002;4:226–31.

55. Wang Y, Wan S, Drago J, White FM, Grodzinsky AJ. Phosphoproteomics analysis of signaling changes in human chondrocytes following treatment with Il-1, IGF-1 and dexamethasone. Osteoarthr Cartil. Elsevier; 2017;25:S165–6.

56. Tuure L, Hämäläinen M, Nummenmaa E, Moilanen T, Moilanen E. Downregulation of microsomal prostaglandin E synthase-1 (mPGES-1) expression in chondrocytes is regulated by MAP kinase phosphatase-1 (MKP-1). Int Immunopharmacol. 2019;71:139–43.

57. Sadowski T, Steinmeyer J. Effects of non-steroidal antiinflammatory drugs and dexamethasone on the activity and expression of matrix metalloproteinase-1, matrix metalloproteinase-3 and tissue inhibitor of metalloproteinases-1 by bovine articular chondrocytes. Osteoarthr Cartil. 2001;9:407–15.

58. Richardson DW, Dodge GR. Dose-dependent effects of corticosteroids on the expression of matrix-related genes in normal and cytokine-treated articular chondrocytes. Inflamm Res. 2003;52:39–49.

59. Roach BL, Kelmendi-Doko A, Balutis EC, Marra KG, Ateshian GA, Hung CT. Dexamethasone release from within engineered cartilage as a chondroprotective strategy against interleukin-1α. Tissue Eng Part A. 2016;22:621–32.

60. Geng Y, McQuillan D, Roughley PJ. SLRP interaction can protect collagen fibrils from cleavage by collagenases. Matrix Biol. 2006;25:484–91.

61. McCoy JM, Wicks JR, Audoly LP. The role of prostaglandin E2 receptors in the pathogenesis of rheumatoid arthritis. J Clin Invest. 2002;110:651–8.

62. Sheibanie AF, Khayrullina T, Safadi FF, Ganea D. Prostaglandin E2 exacerbates collagen-induced arthritis in mice through the inflammatory interleukin-23/interleukin-17 axis. Arthritis Rheum. 2007;56:2608–19.

63. Chan MM-Y, Moore AR. Resolution of Inflammation in Murine Autoimmune Arthritis Is Disrupted by Cyclooxygenase-2 Inhibition and Restored by Prostaglandin E 2 -Mediated Lipoxin A 4 Production . J Immunol. 2010;184:6418–26.

64. Zaman F, Chrysis D, Huntjens K, Chagin A, Takigawa M, Fadeel B, et al. Dexamethasone differentially regulates Bcl-2 family proteins in human proliferative chondrocytes: Role of pro-apoptotic Bid. Toxicol Lett. 2014;224:196–200.

65. Liu N, Wang W, Zhao Z, Zhang T, Song Y. Autophagy in human articular chondrocytes is cytoprotective following glucocorticoid stimulation. Mol Med Rep. 2014;9:2166–72.

66. Shen C, Cai GQ, Peng JP, Chen XD. Autophagy protects chondrocytes from glucocorticoids-induced apoptosis via ROS/Akt/FOXO3 signaling. Osteoarthr Cartil. 2015;23:2279–87.

67. Huang Y, Cai G quan, Peng JP, Shen C. Glucocorticoids induce apoptosis and matrix metalloproteinase-13 expression in chondrocytes through the NOX4/ROS/p38 MAPK pathway. J Steroid Biochem Mol Biol. 2018;181:52–62.

68. Dragoo JL, Danial CM, Braun HJ, Pouliot MA, Kim HJ. The chondrotoxicity of single-dose corticosteroids. Knee Surgery, Sport Traumatol Arthrosc. 2012;20:1809–14.

69. Stueber T, Karsten J, Stoetzer C, Leffler A. Differential cytotoxic properties of drugs used for intra-articular injection on human chondrocytes: An experimental in-vitro study. Eur J Anaesthesiol. 2014;31:640–5.

70. Song YW, Zhang T, Wang WB. Gluococorticoid could influence extracellular matrix synthesis through Sox9 via p38 MAPK pathway. Rheumatol Int. 2012;32:3669–73.

71. Mushtaq T, Farquharson C, Seawright E, Ahmed SF. Glucocorticoid effects on chondrogenesis, differentiation and apoptosis in the murine ATDC5 chondrocyte cell line. J Endocrinol. 2002;175:705–13.

72. Maor G, Silbermann M. Supraphysiological concentrations of dexamethasone induce elevation of calcium uptake and depression of [3H]-Thymidine incorporation into DNA in cartilage in vitro. Calcif Tissue Int. 1986;39:284–90.

73. Hainque B, Dominice J, Jaffray P, Ronot X, Adolphe M. Effects of dexamethasone on the growth of cultured rabbit articular chondrocytes:relation with the nuclear glucocorticoid-receptor complex. Ann Rheum Dis. 1987;46:146–52.

74. Miyazaki Y, Tsukazaki T, Hirota Y, Yonekura A, Osaki M, Shindo H, et al. Dexamethasone inhibition of TGFβ-induced cell growth and type II collagen mRNA expression through ERK-integrated AP-1 activity in cultured rat articular chondrocytes. Osteoarthr Cartil. 2000;8:378–85.

75. Guilak F, Alexopoulos LG, Upton ML, Youn I, Choi JB, Cao L, et al. The pericellular matrix as a transducer of biomechanical and biochemical signals in articular cartilage. Ann N Y Acad Sci. 2006;1068:498–512.

76. Xue E, Zhang Y, Song B, Xiao J, Shi Z. Effect of autophagy induced by dexamethasone on senescence in chondrocytes. Mol Med Rep. 2016;14:3037–44.

77. James CG, Ulici V, Tuckermann J, Michael TM, Beier F. Expression profiling of Dexamethasone-treated primary chondrocytes identifies targets of glucocorticoid signalling in endochondral bone development. BMC Genomics. 2007;8:1–27.

78. Hinek A, Kawiak J, Czarnowska E, Barcew B. The effect of agarose and dexamethasone on the nature and production of extracellular matrix components by elastic cartilage chondrocytes. Acta Biol Hung. 1984;25:245–58.

79. Sekiya I, Koopman P, Tsuji K, Mertin S, Harley V, Yamada Y, et al. Dexamethasone enhances SOX9 expression in chondrocytes. J Endocrinol. 2001;169:573–9.

80. Jo A, Denduluri S, Zhang B, Wang Z, Yin L, Yan Z, et al. The versatile functions of Sox9 in development, stem cells, and human diseases. Genes Dis. Elsevier Ltd; 2014;1:149–61.

81. Fahey M, Mitton E, Muth E, Rosenthal AK. Dexamethasone promotes CPPD crystal formatino by articular chondrocytes. Analysis. 2009;36:163–9.

82. Buschmann MD, Gluzband YA, Grodzinsky AJ, Hunziker EB. Mechanical compression modulates matrix biosynthesis in chondrocyte/agarose culture. J Cell Sci. 1995;108 (Pt 4:1497–508.

83. Lepetsos P, Papavassiliou AG. ROS/oxidative stress signaling in osteoarthritis. Biochim Biophys Acta - Mol Basis Dis. Elsevier B.V.; 2016;1862:576–91.

84. Cheng NT, Meng H, Ma LF, Zhang L, Yu HM, Wang ZZ, et al. Role of autophagy in the progression of osteoarthritis: The autophagy inhibitor, 3-methyladenine, aggravates the severity of experimental osteoarthritis. Int J Mol Med. 2017;39:1224–32.

85. Feliu JE, Hue L, Hers HG. Hormonal control of pyruvate kinase activity and of gluconeogenesis in isolated hepatocytes. Proc Natl Acad Sci U S A. 1976;73:2762–6.

86. Hernvann A, Jaffray P, Hilliquin P, Cazalet C, Menkes CJ, Ekindjian OG. Interleukin-1β-mediated glucose uptake by chondrocytes. Inhibition by cortisol. Osteoarthr Cartil. 1996;4:139–42.

87. Ma R, Zhang W, Tang K, Zhang H, Zhang Y, Li D, et al. Switch of glycolysis to gluconeogenesis by dexamethasone for treatment of hepatocarcinoma. Nat Commun. Nature Publishing Group; 2013;4:1–12.

88. Roy S, Sannigrahi S, Ghosh B, Pusp P, Roy T. Combination therapy of dexamethasone with epigallocatechin enhances tibiotarsal bone articulation and modulates oxidative status correlates with cartilage cytokines expression in the early phase of experimental arthritis. Eur J Pharmacol. 2013;698:444–54.

89. Black RM, Wang Y, Struglics A, Lorenzo P, Chubinskaya S, Grodzinsky AJ, et al. Proteomic clustering reveals the kinetics of disease biomarkers in bovine and human models of post-traumatic osteoarthritis. Osteoarthr Cartil Open. 2021;3:100191.

90. Poulsen RC, Watts AC, Murphy RJ, Snelling SJ, Carr AJ, Hulley PA. Glucocorticoids induce senescence in primary human tenocytes by inhibition of sirtuin 1 and activation of the p53/p21 pathway: In vivo and in vitro evidence. Ann Rheum Dis. 2014;73:1405–13.

91. Behrens F, Shepard N, Mitchell N. Metabolic recovery of articular cartilage after intra articular injections of glucocorticoid. J Bone Jt Surg - Ser A. 1976;58:1157–60.

92. Pelletier JP. The influence of tissue cross-talking on OA progression: Role of nonsteroidal antiinflammatory drugs. Osteoarthr Cartil. 1999;7:374–6.

93. Koch AE, Kunkel SL, Harlow LA, Johnson B, Evanoff HL, Haines GK, et al. Enhanced production of monocyte chemoattractant protein-1 in rheumatoid arthritis. J Clin Invest. 1992;90:772–9.

94. Bartneck M, Peters FM, Warzecha KT, Bienert M, van Bloois L, Trautwein C, et al. Liposomal encapsulation of dexamethasone modulates cytotoxicity, inflammatory cytokine response, and migratory properties of primary human macrophages. Nanomedicine Nanotechnology, Biol Med. 2014;10:1209–20.

95. Gelderman KA, Hultqvist M, Pizzolla A, Zhao M, Nandakumar KS, Mattsson R, et al. Macrophages suppress T cell responses and arthritis development in mice by producing reactive oxygen species. J Clin Invest. 2007;117:3020–8.

96. Kraaij MD, van der Kooij SW, Reinders MEJ, Koekkoek K, Rabelink TJ, van Kooten C, et al. Dexamethasone increases ROS production and T cell suppressive capacity by anti-inflammatory macrophages. Mol Immunol. Elsevier Ltd; 2011;49:549–57.

97. Dwivedi G, Flaman L, Geischecke E, Rosen V, Chubinskaya S, Trippel SB, et al. Dexamethasone rescues chondrocyte viability and matrix degradation induced by injurious compression and exposure to inflammatory cytokines in a novel human cartilage-bone-synovium co-culture microphysiological system (Abstract). Trans 65th Orthopedic Research Society conference. Austin, TX; 2019.

98. Dwivedi G, Flaman L, Frank E, Geishecker E, Rosen V, Chubinskaya S, et al. Human cartilage-bone-synovium microphysiological system to study PTOA pathogenesis and treatment on earth and in space. Osteoarthr Cartil. 2019;27:S167.

99. Crofford LJ, Wilder RL, Ristimaki AP, Sano H, Remmers EF, Epps HR, et al. Cyclooxygenase-1 and cyclooxygenase-2 expression in rheumatoid synovial tissues - effects of interleukin-1β, phorbol ester, and corticosteroids. J Clin Invest. 1994;93:1095–101.

100. Sundy J. COX-2 inhibitors in rheumatoid arthritis. Curr Rheumatol Rep. 2001;3:86–91.

101. Laine L, White WB, Rostom A, Hochberg M. COX-2 selective inhibitors in the treatment of osteoarthritis. Semin Arthritis Rheum. 2008;38:165–87.

102. Buckley L, Greenwald M, Hochberg M, Lane N, Lindsey S, Paget S, et al. Recommendations for the prevention and treatment of glucocorticoid-induced osteoporosis: 2001 Update: American College of Rheumatology Ad Hoc Committee on glucocorticoid-induced osteoporosis. Arthritis Rheum. 2001;44:1496–503.

103. Oelzner P, Fleissner-Richter S, Bräuer R, Hein G, Wolf G, Neumann T. Combination therapy with dexamethasone and osteoprotegerin protects against arthritis-induced bone alterations in antigen-induced arthritis of the rat. Inflamm Res. 2010;59:731–41.

104. Hoes JN, Bultink IEM, Lems WF. Management of osteoporosis in rheumatoid arthritis patients. Expert Opin Pharmacother. 2015;16:559–71.

105. Liu Y, Cui Y, Chen Y, Gao X, Su Y, Cui L. Effects of dexamethasone, celecoxib, and methotrexate on the histology and metabolism of bone tissue in healthy Sprague Dawley rats. Clin Interv Aging. 2015;10:1245–53.

106. Quan L, Zhang Y, Dusad A, Ren K, Purdue PE, Goldring SR, et al. The evaluation of the therapeutic efficacy and side effects of a macromolecular dexamethasone prodrug in the collagen-induced arthritis mouse model. Pharm Res. 2016;33:186–93.

107. Tomaszewska E, Dobrowolski P, Puzio I. Morphological changes of the cartilage and bone in newborn piglets evoked by experimentally induced glucocorticoid excess during pregnancy. J Anim Physiol Anim Nutr (Berl). 2013;97:785–96.

108. Lieberthal J, Sambamurthy N, Scanzello CR. Inflammation in joint injury and post-traumatic osteoarthritis. Osteoarthritis and Cartilage. 2015. p. 1825–34.

109. Swärd P, Wang Y, Hansson M, Lohmander LS, Grodzinsky AJ, Struglics A. Coculture of bovine cartilage with synovium and fibrous joint capsule increases aggrecanase and matrix metalloproteinase activity. Arthritis Res Ther. 2017;19:1–12.

110. Kandarpa K, Schneider V, Ganapathy K. Human health during space travel: An overview. Neurol India. 2019;67:S176–81.

111. Smith K, Mercuri J. Microgravity and radiation effects on astronaut intervertebral disc health. Aerosp Med Hum Perform. 2021;92:342–52.

112. Injury Rate of Shuttle Astronauts. Longitud Study Astronaut Heal Newsl. NASA; 1999;8.

113. Ramachandran V, Dalal S, Scheuring RA, Jones JA. Musculoskeletal injuries in astronauts: Review of pre-flight, in-flight, post-flight, and extravehicular activity injuries. Curr Pathobiol Rep. 2018;6:149–58.

114. Scheuring RA, Mathers CH, Jones JA, Wear ML. Musculoskeletal injuries and minor trauma in space: Incidence and injury mechanisms in U.S. astronauts. Aviat Sp Environ Med. 2009;80:117–24.

115. Kerstman EL, Scheuring RA, Barnes MG, DeKorse TB, Saile LG. Space adaptation back pain: A retrospective study. Aviat Sp Environ Med. 2012;83:2–7.

116. Scheuring RA, Jones JA, Novak JD, Polk JD, Gillis DB, Schmid J, et al. The Apollo Medical Operations Project: Recommendations to improve crew health and performance for future exploration missions and lunar surface operations. Acta Astronaut. 2008;63:980–7.

117. Bajpayee AG, Quadir MA, Hammond PT, Grodzinsky AJ. Charge based intra-cartilage delivery of single dose dexamethasone using Avidin nano-carriers suppresses cytokine-induced catabolism long term. Osteoarthr Cartil. 2016;49:48–56.

118. Bajpayee AG, Grodzinsky AJ. Cartilage-targeting drug delivery: Can electrostatic interactions help? Nat Rev Rheumatol. 2017;13:183–93.

119. Krishnan Y, Rees HA, Rossitto CP, Kim SE, Hung HHK, Frank EH, et al. Green fluorescent proteins engineered for cartilage-targeted drug delivery: Insights for transport into highly charged avascular tissues. Biomaterials. 2018;183:218–33.

120. Formica FA, Barreto G, Zenobi-Wong M. Cartilage-targeting dexamethasone prodrugs increase the efficacy of dexamethasone. J Control Release. 2019;295:118–29.

121. Geiger BC, Wang S, Padera RF, Grodzinsky AJ, Hammond PT. Cartilage-penetrating nanocarriers improve delivery and efficacy of growth factor treatment of osteoarthritis. Sci Transl Med. 2018;10.

122. Stefani RM, Lee AJ, Tan AR, Halder SS, Hu Y, Guo XE, et al. Sustained low-dose dexamethasone delivery via a PLGA microsphere-embedded agarose implant for enhanced osteochondral repair. Acta Biomater. 2020;102:326–40.

123. Di Francesco M, Bedingfield SK, Di Francesco V, Colazo JM, Yu F, Ceseracciu L, et al. Shape-defined microPlates for the sustained intra-articular release of dexamethasone in the management of overload-induced osteoarthritis. ACS Appl Mater Interfaces. 2021;13:31379–92.

124. Holyoak DT, Wheeler TA, Van Der Meulen MCH, Singh A. Injectable mechanical pillows for attenuation of load-induced post-traumatic osteoarthritis. Regen Biomater. 2019;6:211–9.

125. Zhao Y, Wei C, Chen X, Liu J, Yu Q, Liu Y, et al. Drug delivery system based on near-infrared light-responsive molybdenum disulfide nanosheets controls the high-efficiency release of dexamethasone to inhibit inflammation and treat osteoarthritis. ACS Appl Mater Interfaces. 2019;11:11587–601.

126. Wang Q-S, Xu B-X, Fan K-J, Fan Y-S, Teng H, Wang T-Y. Dexamethasone-loaded thermo-sensitive hydrogel

attenuates osteoarthritis by protecting cartilage and providing effective pain relief. Ann Transl Med. 2021;9:1120–1120.

127. Hu Y, Chen X, Wang S, Jing Y, Su J. Subchondral bone microenvironment in osteoarthritis and pain. Bone Res. Springer US; 2021;9:1–13.

128. Subramanian A, Tamayo P, Mootha VK, Mukherjee S, Ebert BL, Gillette MA, et al. Gene set enrichment analysis: A knowledge-based approach for interpreting genome-wide expression profiles. Proc Natl Acad Sci U S A. 2005;102:15545–50.

129. Black R, Grodzinsky AJ. Dexamethasone: Chondroprotective corticosteroid or catabolic killer? Eur Cells Mater. 2019;38:246–63.

130. Wang Y, Li Y, Khabut A, Chubinskaya S, Grodzinsky AJ, Önnerfjord P. Quantitative proteomics analysis of cartilage response to mechanical injury and cytokine treatment. Matrix Biol. 2017;63:11–22.

131. Li Y, Frank E, Wang Y, Chubinskaya S, Huang H-H, Grodzinsky AJ. Moderate dynamic compression inhibits pro-catabolic response of cartilage to mechancial injury, TNF-alpha and IL-6, but accentuates degradation above a strain threshold. Osteoarthr Cartil. 2013;21:1–17.

132. Ritchie ME, Phipson B, Wu D, Hu Y, Law CW, Shi W, et al. Limma powers differential expression analyses for RNA-sequencing and microarray studies. Nucleic Acids Res. 2015;43:e47.

133. Altschul SF, Madden TL, Schäffer AA, Zhang J, Zhang Z, Miller W, et al. Gapped BLAST and PSI-BLAST: a new generation of protein database search programs. Nucleic Acids Res. 1997;25:3389–402.

134. The Gene Ontology Consortium. Gene Ontology : tool for the unification of biology. Nat Genet. 2000;25:25–9.

135. The Gene Ontology Consortium. The Gene Ontology Resource: 20 years and still GOing strong. Nucleic Acids Res. Oxford University Press; 2019;47:D330–8.

136. Szklarczyk D, Gable AL, Lyon D, Junge A, Wyder S, Huerta-Cepas J, et al. STRING v11: Protein-protein association networks with increased coverage, supporting functional discovery in genome-wide experimental datasets. Nucleic Acids Res. Oxford University Press; 2019;47:D607–13.

137. Bateman A. UniProt: A worldwide hub of protein knowledge. Nucleic Acids Res. Oxford University Press; 2019;47:D506–15.

138. Good PI. Resampling methods: a practical guide to data analysis. second ed. Boston: Birkhäuser; 2001.

139. Farndale RW, Buttle DJ, Barrett AJ. Improved quantitation and discrimination of sulphated glycosaminoglycans by use of dimethylmethylene blue. Biochim Biophys Acta. 1986;883:173–7.

140. Struglics A, Larsson S, Pratta MA, Kumar S, Lark MW, Lohmander LS. Human osteoarthritis synovial fluid and joint cartilage contain both aggrecanase- and matrix metalloproteinase-generated aggrecan fragments. Osteoarthr Cartil. 2006;14:101–13.

141. Struglics A, Larsson S. A comparison of different purification methods of aggrecan fragments from human articular cartilage and synovial fluid. Matrix Biol. Elsevier B.V.; 2010;29:74–83.

142. Pratta MA, Su JL, Leesnitzer MA, Struglics A, Larsson S, Lohmander LS, et al. Development and characterization of a highly specific and sensitive sandwich ELISA for detection of aggrecanase-generated aggrecan fragments. Osteoarthr Cartil. 2006;14:702–13.

143. Struglics A, Hansson M, Lohmander LS. Human aggrecanase generated synovial fluid fragment levels are elevated directly after knee injuries due to proteolysis both in the inter globular and chondroitin sulfate domains. Osteoarthr Cartil. Elsevier Ltd; 2011;19:1047–57.

144. Laemmli UK. Cleavage of structural proteins during the assembly of the head of bacteriophage T4. Nature. 1970;227:680–5.

145. Hedbom E, Antonsson P, Hjerpe A, Aeschlimann D, Paulsson M, Rosa-Pimentel E, et al. Cartilage matrix

proteins. An acidic oligomeric protein (COMP) detected only in cartilage. J Biol Chem. 1992;267:6132–6.

146. Perez-Riverol Y, Csordas A, Bai J, Bernal-Llinares M, Hewapathirana S, Kundu DJ, et al. The PRIDE database and related tools and resources in 2019: Improving support for quantification data. Nucleic Acids Res. 2019;47:D442–50.

147. Said Ahmed MA, Saweeres ES, Abdelkader NA, Abdelmajeed SF, Fares AR. Improved pain and function in knee osteoarthritis with dexamethasone phonophoresis: a randomized controlled trial. Indian J Orthop. 2019;53:700–7.

148. Hajialilo M, Ghorbanihaghjo A, Valaee L, Kolahi S, Rashtchizadeh N, Amirkhiz MB, et al. A double-blind randomized comparative study of triamcinolone hexacetonide and dexamethasone intra-articular injection for the treatment of knee joint arthritis in rheumatoid arthritis. Clin Rheumatol. Clinical Rheumatology; 2016;35:2887–91.

149. Bajpayee AG, De la Vega RE, Scheu M, Varady NH, Yannatos IA, Brown LA, et al. Sustained intra-cartilage delivery of low dose dexamethasone using a cationic carrier for treatment of post traumatic osteoarthritis. Eur Cell Mater. 2017;34:341–64.

150. Evans CH, Kraus VB, Setton LA. Progress in intra-articular therapy. Nat Rev Rheumatol. 2014;10:11–22.

151. Anderson DD, Chubinskaya S, Guilak F, Martin JA, Oegema TR, Olson SA, et al. Post-traumatic osteoarthritis: Improved understanding and opportunities for early intervention. J Orthop Res. 2011;29:802–9.

152. Wang Y, Grodzinsky AJ. The response of cartilage to injury. Post-Traumatic Arthritis Pathog Diagnosis Manag. 2015;121–33.

153. Carbone A, Rodeo S. Review of current understanding of post-traumatic osteoarthritis resulting from sports injuries. J Orthop Res. 2017;35:397–405.

154. Rose BJ, Kooyman DL. A tale of two joints: the role of matrix metalloproteases in cartilage biology. Dis Markers. 2016;

155. Kadler KE, Hill A, Canty-Laird EG. Collagen fibrillogenesis: fibronectin, integrins, and minor collagens as organizers and nucleators. Curr Opin Cell Biol. 2008;20:495–501.

156. Eyre DR, Weis MA, Wu JJ. Advances in collagen cross-link analysis. Methods. 2008;45:65–74.

157. Farjanel J, Sève S, Borel A, Sommer P, Hulmes JS. Inhibition of lysyl oxidase activity can delay phenotypic modulation of chondrocytes in two-dimensional culture. Osteoarthr Cartil. 2005;13:120–8.

158. Sanchez C, Bay-Jensen AC, Pap T, Dvir-Ginzberg M, Quasnichka H, Barrett-Jolley R, et al. Chondrocyte secretome: a source of novel insights and exploratory biomarkers of osteoarthritis. Osteoarthr Cartil. Elsevier Ltd; 2017;25:1199–209.

159. Nakayama N, Han CYE, Cam L, Lee JI, Pretorius J, Fisher S, et al. A novel chordin-like BMP inhibitor, CHL2, expressed preferentially in chondrocytes of developing cartilage and osteoarthritic joint cartilage. Development. 2004;131:229–40.

160. Aki T, Hashimoto K, Ogasawara M, Itoi E. A whole-genome transcriptome analysis of articular chondrocytes in secondary osteoarthritis of the hip. PLoS One. 2018;13.

161. Zhang Q, Yin ZS, Zhang FW, Cao K, Sun HY. CTHRC1 mediates il-1β-induced apoptosis in chondrocytes via JNK1/2 signaling. Int J Mol Med. 2018;41:2270–8.

162. Durmus T, LeClair RJ, Park KS, Terzic A, Yoon JK, Lindner V. Expression analysis of the novel gene collagen triple helix repeat containing-1 (Cthrc1). Gene Expr Patterns. 2006;6:935–40.

163. Baud'huin M, Duplomb L, Teletchea S, Ruiz-Velasco C, Maillasson M, Redini F, et al. Osteoprotegerin: multiple partners for multiple functions. Cytokine Growth Factor Rev. 2013;24:401–9.

164. Simonet WS, Lacey DL, Dunstan CR, Kelley M, Chang MS, Lüthy R, et al. Osteoprotegerin: A novel secreted protein involved in the regulation of bone density. Cell. 1997;89:309–19.

165. Blanco FJ, Ruiz-Romero C. New targets for disease modifying osteoarthritis drugs: chondrogenesis and Runx1. Ann Rheum Dis. 2013;72:631–4.

166. Taylor DK, Meganck JA, Terkhorn S, Rajani R, Naik A, O'Keefe RJ, et al. Thrombospondin-2 influences the proportion of cartilage and bone during fracture healing. J Bone Miner Res. 2009;24:1043–54.

167. Poole CA, Ayad S, Schofield JR. Chondrons from articular cartilage: I. Immunolocalization of type VI collagen in the pericellular capsule of isolated canine tibial chondrons. J Cell Sci. 1988;90:635–43.

168. Tang X, Muhammad H, McLean C, Miotla-Zarebska J, Fleming J, Didangelos A, et al. Connective tissue growth factor contributes to joint homeostasis and osteoarthritis severity by controlling the matrix sequestration and activation of latent TGFβ. Ann Rheum Dis. 2018;77:1372–80.

169. Okada H, Kikuta T, Inoue T, Kanno Y, Ban S, Sugaya T, et al. Dexamethasone induces connective tissue growth factor expression in renal tubular epithelial cells in a mouse strain-specific manner. Am J Pathol. 2006;168:737–47.

170. Hausser HJ, Decking R, Brenner RE. Testican-1, an inhibitor of pro-MMP-2 activation, is expressed in cartilage. Osteoarthr Cartil. 2004;12:870–7.

171. Grimstein C, Choi YK, Wasserfall CH, Satoh M, Atkinson MA, Brantly ML, et al. Alpha-1 antitrypsin protein and gene therapies decrease autoimmunity and delay arthritis development in mouse model. J Transl Med. 2011;9.

172. Swärd P, Wang Y, Hansson M, Lohmander LS, Grodzinsky AJ, Struglics A. Coculture of bovine cartilage with synovium and fibrous joint capsule increases aggrecanase and matrix metalloproteinase activity. Arthritis Res Ther. 2017;19:1–12.

173. Thomas AC, Hubbard-Turner T, Wikstrom EA, Palmieri-Smith RM. Epidemiology of posttraumatic osteoarthritis. J Athl Train. 2017;52:491–6.

174. Black RM, Wang Y, Struglics A, Lorenzo P, Tillgren V, Rydén M, et al. Proteomic analysis reveals dexamethasone rescues matrix breakdown but not anabolic dysregulation in a cartilage injury model. Osteoarthr Cartil Open. 2020;2:100099.

175. Bodker AM, Latterman C, Chubinskaya S. Biomarkers in Early and Post-Traumatic Osteoarthritis. In: Cole BJ, Harris JD, editors. Biologic Knee Reconstruction: A Surgeon's Guide. Slack Incorporated; 2015. p. 41–5.

176. Neuman P, Dahlberg LE, Englund M, Struglics A. Concentrations of synovial fluid biomarkers and the prediction of knee osteoarthritis 16 years after anterior cruciate ligament injury. Osteoarthr Cartil. Elsevier Ltd; 2017;25:492–8.

177. Muehleman C, Bareither D, Huch K, Cole AA, Kuettner KE. Prevalence of degenerative morphological changes in the joints of the lower extremity. Osteoarthr Cartil. 1997;5:23–37.

178. Lazar C, Gatto L, Ferro M, Bruley C, Burger T. Accounting for the multiple natures of missing values in label-free quantitative proteomics data sets to compare imputation strategies. J Proteome Res. 2016;15:1116–25.

179. Heinegård D. Proteoglycans and more - from molecules to biology. Int J Exp Pathol. 2009;90:575–86.

180. Swärd P, Frobell R, Englund M, Roos H, Struglics A. Cartilage and bone markers and inflammatory cytokines are increased in synovial fluid in the acute phase of knee injury (hemarthrosis) - a cross-sectional analysis. Osteoarthr Cartil. Elsevier Ltd; 2012;20:1302–8.

181. Swärd P, Struglics A, Englund M, Roos HP, Frobell RB. Soft tissue knee injury with concomitant osteochondral fracture is associated with higher degree of acute joint inflammation. Am J Sports Med. 2014;42:1096–102.

182. Åhrman E, Lorenzo P, Holmgren K, Grodzinsky AJ, Dahlberg LE, Saxne T, et al. Novel cartilage oligomeric matrix protein (COMP) neoepitopes identified in synovial fluids from patients with joint diseases using affinity chromatography and mass spectrometry. J Biol Chem. 2014;289:20908–16.

183. Struglics A, Okroj M, Swärd P, Frobell R, Saxne T, Lohmander LS, et al. The complement system is activated in synovial fluid from subjects with knee injury and from patients with osteoarthritis. Arthritis Res Ther. Arthritis Research & Therapy; 2016;18:1–11.

184. Kumahashi N, Swärd P, Larsson S, Lohmander LS, Frobell R, Struglics A. Type II collagen C2C epitope in human synovial fluid and serum after knee injury - associations with molecular and structural markers of injury. Osteoarthritis and Cartilage. 2015. p. 1506–12.

185. Frobell RB, Roos HP, Roos EM, Hellio Le Graverand MP, Buck R, Tamez-Pena J, et al. The acutely ACL injured knee assessed by MRI: are large volume traumatic bone marrow lesions a sign of severe compression injury? Osteoarthr Cartil. 2008;16:829–36.

186. Cheng C, Gao S, Lei G. Association of osteopontin with osteoarthritis. Rheumatol Int. 2014;34:1627–31.

187. Mobasheri A, Bay-Jensen AC, van Spil WE, Larkin J, Levesque MC. Osteoarthritis year in review 2016: biomarkers (biochemical markers). Osteoarthr Cartil. Elsevier Ltd; 2017;25:199–208.

188. Lohmander LS, Atley LM, Pietka TA, Eyre DR. The release of crosslinked peptides from type II collagen into human synovial fluid is increased soon after joint injury and in osteoarthritis. Arthritis Rheum. 2003;48:3130–9.

189. Ritter SY, Collins J, Krastins B, Sarracino D, Lopez M, Losina E, et al. Mass spectrometry assays of plasma biomarkers to predict radiographic progression of knee osteoarthritis. Arthritis Res Ther. 2014;16:456.

190. Haraden CA, Huebner JL, Hsueh MF, Li YJ, Kraus VB. Synovial fluid biomarkers associated with osteoarthritis severity reflect macrophage and neutrophil related inflammation. Arthritis Res Ther. 2019;21:146.

191. Agere SA, Akhtar N, Watson JM, Ahmed S. RANTES/CCL5 induces collagen degradation by activating MMP-1 and MMP-13 expression in human rheumatoid arthritis synovial fibroblasts. Front Immunol. 2017;8:55–67.

192. Sharma A, Khan R, Gupta N, Sharma A, Zaheer MS, Abbas M, et al. Acute phase reactant, Pentraxin 3, as a novel marker for the diagnosis of rheumatoid arthritis. Clin Chim Acta. 2018;480:65–70.

193. Alaaeddine N, Antoniou J, Moussa M, Hilal G, Kreichaty G, Ghanem I, et al. The chemokine CCL20 induces proinflammatory and matrix degradative responses in cartilage. Inflamm Res. Springer Basel; 2015;64:721–31.

194. Guan J, Li Y, Ding L Bin, Liu GY, Zheng XF, Xue W, et al. Relationship between serum and synovial fluid CCL20 concentrations with disease severity in primary knee osteoarthritis. J Musculoskelet Neuronal Interact. 2019;19:326–32.

195. Ben-Aderet L, Merquiol E, Fahham D, Kumar A, Reich E, Ben-Nun Y, et al. Detecting cathepsin activity in human osteoarthritis via activity-based probes. Arthritis Res Ther. 2015;17.

196. Yasuda Y, Kaleta J, Brömme D. The role of cathepsins in osteoporosis and arthritis: Rationale for the design of new therapeutics. Adv Drug Deliv Rev. 2005;57:973–93.

197. Kiapour AM, Sieker JT, Proffen BL, Lam TKT, Fleming BC, Murray MM. Synovial fluid proteome changes in ACL injury-induced posttraumatic osteoarthritis: Proteomics analysis of porcine knee synovial fluid. PLoS One. 2019;14:1–19.

198. Brophy RH, Cai L, Duan X, Zhang Q, Townsend RR, Nunley RM, et al. Proteomic analysis of synovial fluid identifies periostin as a biomarker for anterior cruciate ligament injury. Osteoarthr Cartil. 2019;27:1778–89.

199. Timur UT, Jahr H, Anderson J, Green DC, Emans PJ, Smagul A, et al. Identification of tissue-dependent proteins in knee OA synovial fluid. Osteoarthr Cartil. 2021;29:124–33.

200. Pratta MA, Yao W, Decicco C, Tortorella MD, Liu RQ, Copeland RA, et al. Aggrecan protects cartilage collagen from proteolytic cleavage. J Biol Chem. 2003;278:45539–45.

201. Fabricant PD, Kocher MS. Management of ACL injuries in children and adolescents. J Bone Jt Surg - Am Vol. 2017;99:600–12.

202. Wieland HA, Michaelis M, Kirschbaum BJ, Rudolphi KA. Osteoarthritis — an untreatable disease? Nat Rev

Drug Discov. Nature Publishing Group; 2005;4:331.

203. Oo WM, Little C, Duong V, Hunter DJ. The development of disease-modifying therapies for osteoarthritis (DMOADs): The evidence to date. Drug Des Devel Ther. 2021;15:2921–45.

204. Ghouri A, Conaghan PG. Update on novel pharmacological therapies for osteoarthritis. Ther Adv Musculoskelet Dis. 2019;11:1759720X1986449.

205. Vincent TL. Of mice and men: converging on a common molecular understanding of osteoarthritis. Lancet Rheumatol. 2020;2:e633–45.

206. Jiang A, Xu P, Sun S, Zhao Z, Tan Q, Li W, et al. Cellular alterations and crosstalk in the osteochondral joint in osteoarthritis and promising therapeutic strategies. Connect Tissue Res. 2021;62:709–19.

207. Siddappa R, Licht R, van Blitterswijk C, de Boer J. Donor variation and loss of multipotency during in vitro expansion of human mesenchymal stem cells for bone tissue engineering. J Orthop Res. 2007;25:1029–41.

208. Weinstein RS. Glucocorticoid-induced csteoporosis and csteonecrosis. Endocrinol Metab Clin North Am. 2012;41:595–611.

209. Delco ML, Kennedy JG, Bonassar LJ, Fortier LA. Post-traumatic osteoarthritis of the ankle: A distinct clinical entity requiring new research approaches. J Orthop Res. 2017;35:440–53.

210. Hsueh MF, Khabut A, Kjellström S, Önnerfjord P, Kraus VB. Elucidating the molecular composition of cartilage by proteomics. J Proteome Res. 2016;15:374–88.

211. Daly MJ, Patterson N, Mesirov JP, Golub TR, Tamayo P, Spiegelman B. PGC-1α-responsive genes involved in oxidative phosphorylation are coordinately downregulated in human diabetes. Nat Genet. 2003;34:267–73.

212. Mi H, Ebert D, Muruganujan A, Mills C, Albou LP, Mushayamaha T, et al. PANTHER version 16: A revised family classification, tree-based classification tool, enhancer regions and extensive API. Nucleic Acids Res. 2021;49:D394–403.

213. Geurts J, Jurić D, Müller M, Schären S, Netzer C. Novel ex vivo human osteochondral explant model of knee and spine osteoarthritis enables assessment of inflammatory and drug treatment responses. Int J Mol Sci. 2018;19:1314.

214. Patwari P, Kurz B, Sandy JD, Grodzinsky AJ. Mannosamine inhibits aggrecanase-mediated changes in the physical properties and biochemical composition of articular cartilage. Arch Biochem Biophys. 2000;374:79–85.

215. Kraus VB, Karsdal MA. Osteoarthritis: Current molecular biomarkers and the way forward. Calcif Tissue Int. Springer US; 2021;109:329–38.

216. Zappia J, Van der Cruyssen R, Sanchez C, Lausberg C, Lambert C, Florin A, et al. Osteomodulin impacts positively the bone remodeling process in osteoarthritis. Bone Reports. 2021;14:100904.

217. Lin W, Zhu X, Gao L, Mao M, Gao D, Huang Z. Osteomodulin positively regulates osteogenesis through interaction with BMP2. Cell Death Dis. 2021;12.

218. Chang JC, Christiansen BA, Murugesh DK, Sebastian A, Hum NR, Collette NM, et al. SOST/Sclerostin improves posttraumatic osteoarthritis and inhibits MMP2/3 expression after injury. J Bone Miner Res. 2018;33:1105–13.

219. Eastell R, Hannon RA. Biochemical markers of bone turnover. In: Lobo RA, editor. Treatment of the Postmenopausal Woman (Third Edition): Basic and Clinical Aspects. Academic Press; 2007. p. 337–49.

220. Park HM, Lee JH, Lee YJ. Positive association of serum alkaline phosphatase level with severe knee osteoarthritis: A nationwide population-based study. Diagnostics. 2020;10:1016.

221. Nakamura S, Kamihagi K, Satakeda H, Katayama M, Pan H, Okamoto H, et al. Enhancement of SPARC (osteonectin) synthesis in arthritic cartilage: Increased levels in synovial fluids from patients with rheumatoid arthritis and regulation by growth factors and cytokines in chondrocyte cultures. Arthritis Rheum. 1996;39:539–51.

222. Nanba Y, Nishida K, Yoshikawa T, Sato T, Inoue H, Kuboki Y. Expression of osteonectin in articular cartilage of osteoarthritic knees. Acta Med Okayama. 1997;51:239–43.

223. Liu Y, Chen Y, Zhao H, Zhong L, Wu L, Cui L. Effects of different doses of dexamethasone on bone qualities in rats. J Biomed Eng. 2011;28:737–43.

224. Huebner KD, Shrive NG, Frank CB. Dexamethasone inhibits inflammation and cartilage damage in a new model of post-traumatic osteoarthritis. J Orthop Res. 2014;32:566–72.

225. De Seny D, Cobraiville G, Charlier E, Neuville S, Lutteri L, Goff C Le, et al. Apolipoprotein-A1 as a damage-associated molecular patterns protein in osteoarthritis: Ex vivo and in vitro pro-inflammatory properties. PLoS One. 2015;10:1–17.

226. Lee JY, Kang MJ, Choi JY, Park JS, Park JK, Lee EY, et al. Apolipoprotein B binds to enolase-1 and aggravates inflammation in rheumatoid arthritis. Ann Rheum Dis. 2018;77:1480–9.

227. Zhang H, Wu LM, Wu J. Cross-talk between apolipoprotein E and cytokines. Mediators Inflamm. 2011;1–10.

228. Cho NH, Seong SY. Apolipoproteins inhibit the innate immunity activated by necrotic cells or bacterial endotoxin. Immunology. 2009;128:479–86.

229. Majetschak M, Perez M, Sorell LT, Lam J, Maldonado ME, Hoffman RW. Circulating 20S proteasome levels in patients with mixed connective tissue disease and systemic lupus erythematosus. Clin Vaccine Immunol. 2008;15:1489–93.

230. Verbrugge EE, Scheper RJ, Lems WF, de Gruijl TD, Jansen G. Proteasome inhibitors as experimental therapeutics of autoimmune diseases. Arthritis Res Ther. 2015;17:1–10.

231. Webb RJ, Mazidi M, Lip GYH, Kengne AP, Banach M, Davies IG. The role of adiposity, diet and inflammation on the discordance between LDL-C and apolipoprotein B. Nutr Metab Cardiovasc Dis. 2022;32:605–15.

232. Hsueh MF, Önnerfjord P, Bolognesi MP, Easley ME, Kraus VB. Analysis of “old” proteins unmasks dynamic gradient of cartilage turnover in human limbs. Sci Adv. 2019;5:1–10.

Appendix 1: Effects of Dexamethasone on Glucose Metabolism and Biosynthetic Pathways

Rebecca M. Black[1], Yang Wang[1], Pilar Lorenzo[2], Patrik Önnerfjord[2], and Alan J. Grodzinsky[1,3,4]

[1]Departments of Biological Engineering, [3]Mechanical Engineering, [4]Electrical Engineering and Computer Science, Massachusetts Institute of Technology, Cambridge, MA, USA
[2]Rheumatology, Department of Clinical Sciences Lund, Lund University, Lund, Sweden

Sections of this work were presented at the 2022 Orthopedic Research Society conference as "Metabolic Protein Release From Bovine Cartilage In PTOA Model Does Not Reflect Intracellular Synthesis", abstract #0626.

A1.1 Introduction

Glucose metabolism is critical to cartilage function and homeostasis during development as well as osteoarthritis (OA) pathogenesis [1]. Glucose can be broken down into lactate or pyruvate through glycolytic pathways that involve many reversible steps. The reversal of this process to synthesize glucose is called gluconeogenesis, which also utilizes the enzymes glucose-6-phosphatase (G6PC) and pyruvate carboxykinase (PEPCK) [2]. Cartilage is normally a highly glycolytic tissue, breaking down glucose to generate ATP mainly through anaerobic pathways, as mature cartilage has no vasculature, receiving its oxygen only from synovial fluid. During OA progression, glycolysis is upregulated as gluconeogenesis is downregulated to produce more ATP for anabolic processes [3,4]. Though this shift in metabolism produces more energy for protective reactions to disease stresses such as matrix synthesis, chondrocytes can be damaged due to the side effect of increased reactive oxygen species production from the mitochondrial electron transport chain. Many other systems-wide metabolic changes occur during OA progression, such as changes in lipid metabolism [3]. Metabolic biomarkers for OA progression related to these changes have been suggested, such as low serum levels of high-density lipoprotein cholesterol and the ratio between branch-chain amino acids and histidine [5,6].

Dexamethasone (Dex) is a corticosteroid that has shown promise as an anti-catabolic drug for the prevention of post-traumatic OA (PTOA), with many reports studying its effects against matrix degradation and inflammatory responses [7–9]. However, its effects are not limited to preventing matrix catabolism or reducing inflammation, as steroids also exert effects on the energy metabolism of tissues themselves [10]. 24 hours of treatment with 10 μM cortisol was shown to decrease glucose uptake by chondrocytes isolated from patients with OA, with or without

interleukin-1 beta (IL-1β) stimulation [11]. Dex modulates glucose levels systemically as well as locally within tissues by stimulating gluconeogenesis, though this effect has not been explored extensively in cartilage tissue [10,12]. As cartilage tissue can be damaged by oxidative stress produced by the shift towards glycolysis and increased ATP production in early OA, Dex may exert a protective effect and restore normal cartilage homeostasis by reversing the shift towards glycolysis. It is also of interest whether other metabolic pathways are affected by Dex to better understand the full scope of its effects on cartilage tissue.

The aim of this study is to observe the effect of Dex on cartilage energy metabolism via PCR, proteomic, and metabolomic analyses. We utilize bovine and human *ex vivo* models of PTOA to address the hypotheses that the induction of OA will increase glycolytic protein synthesis, while Dex will stimulate gluconeogenic gene synthesis. Using systems-level metabolomics analysis, we observe changes in metabolites associated with glycolysis and the tricarboxylic acid cycle, as well as other parts of energy metabolism, in cartilage treated with inflammatory cytokines and/or low doses of Dex.

A1.2 Materials and Methods

A1.2.1 Proteomic identification of metabolic enzymes

We utilized metabolic protein release from an existing proteomic data set of cytokine- and Dex-treated cartilage [8]. Cartilage disks (3 mm diameter x 1 mm height, including the intact superficial zone) were harvested from the femoropatellar grooves of 1-2-week-old bovines. After harvesting, explant disks were pre-equilibrated for two days. Four bovine explants were cultured per well, with one well per treatment condition for each of three animals. Explants were grouped into

untreated controls (N), continuous treatment with 100 nM Dex (D), continuous treatment with inflammatory cytokines (C = 10 ng/ml TNF-α, 20 ng/ml IL-6 and 100 ng/ml soluble IL-6 receptor (sIL-6R)), or cytokines plus 100 nM Dex (CD). Culture media was collected between the 48 and 96 hour timepoints and stored at -20°C. Proteomic identification and quantification using in-solution trypsin digestion followed by LC/MS/MS (Q-Exactive™) were performed for pooled culture medium samples using Proteome Discoverer 2.4 (Thermo). Statistical analyses were performed with the R package limma and empirical Bayes statistics [13].

A1.2.2 Bovine explant harvest and viability analysis

For quantitative real-time PCR (qRT-PCR) analysis, cartilage disks were harvested as above from separate bovine donors and treated for 72 hours with no treatment (N), 10 nM Dex, 100 nM Dex (D), 1 μM Dex, continuous culture with inflammatory cytokines (C = 25 ng/ml TNF-α, 50 ng/ml IL-6 and 250 ng/ml sIL-6R for qRT-PCR samples) and cytokines plus 100 nM Dex (CD). Cartilage explants were washed with phosphate buffered saline and snap-frozen in liquid nitrogen until analysis. Chondrocyte viability was assessed by staining 100-200 μm vertical slices cut from intact cartilage and stained with fluorescein diacetate and propidium iodide (Sigma) as previously described [14]. Tissue DNA content was determined using the Quanti-iT PicoGreen dsDNA kit (Thermo) according to manufacturer instructions.

A1.2.3 qRT-PCR for glycolytic and gluconeogenic genes

RNA was extracted from three bovine cartilage plugs per treatment condition and reverse transcribed to cDNA as previously described [15]. Genes of interest were those identified from proteomic analyses in culture media: triosephosphate isomerase 1 (TPI1), phosphoglycerate kinase

1 (PGK1), phosphoglycerate mutase 1 (PGAM1), and enolase 1 (ENO1). Glycolytic enzymes targeted for PCR analysis were glucose-6-phosphatase (G6PC) and cytosolic and mitochondrial phosphoenolpyruvate carboxykinase (PCK1 and -2, respectively). Primers used for qRT-PCR are listed in **Table A1.1**. Expression values were found by the ΔΔct method normalized to β-actin and pre-treatment cartilage. Statistical analysis was performed with the R package lme4, fitting the data to a linear mixed effects model with cow as a random variable and calculating *p* values with a least-squared means test.

A1.2.4 Human ankle cartilage explant harvest

Human osteochondral explants (3.5 mm diameter, full-thickness cartilage) were harvested from ankle talocrural joints of three human donors (48F, 60M, 47M, Collins grade 0-1) obtained postmortem through the Gift of Hope Organ and Tissue Donor Network (Itasca, IL). Explants were pre-equilibrated and cultured as described [8]. After pre-equilibration, osteochondral explants were treated for 48 hours with no treatment (N), with 100 nM Dex (D), continuous culture with inflammatory cytokines (C = 25 ng/ml TNF-α, 50 ng/ml IL-6 and 250 ng/ml sIL-6R for qRT-PCR samples) and cytokines plus Dex (CD). All donors provided both left and right ankles, and explants from both ankles were randomized within each treatment condition.

A1.2.5 Metabolite extraction and metabolomics analysis

Six human cartilage explants per treatment condition (day 0 untreated, and N, D, C, CD after 48 hours) were weighed and snap-frozen in liquid nitrogen. Frozen cartilage was pulverized and 25 uL/mg tissue 80% methanol in water with internal standards was added. Samples were homogenized for 30 seconds and then vortexed for one minute before centrifuging for 10 minutes

at maximum speed at 4ºC. 500 uL per sample was collected, avoiding the pellet, and dried in a lyophilizer overnight.

Metabolite profiling was conducted on a QExactive bench top orbitrap mass spectrometer equipped with an Ion Max source and a HESI II probe, which was coupled to a Dionex UltiMate 3000 HPLC system (Thermo Fisher Scientific, San Jose, CA). External mass calibration was performed using the standard calibration mixture every 7 days. Typically, samples were reconstituted in 50 uL water and 2 uL were injected onto a SeQuant® ZIC®-pHILIC 150 x 2.1 mm analytical column equipped with a 2.1 x 20 mm guard column (both 5 mm particle size; Millipore-Sigma). Buffer A was 20 mM ammonium carbonate, 0.1% ammonium hydroxide; Buffer B was acetonitrile. The column oven and autosampler tray were held at 25◦C and 4◦C, respectively. The chromatographic gradient was run at a flow rate of 0.150 mL/min as follows: 0-20 min: linear gradient from 80-20% B; 20-20.5 min: linear gradient form 20-80% B; 20.5-28 min: hold at 80% B. The mass spectrometer was operated in full-scan, polarity-switching mode, with the spray voltage set to 3.0 kV, the heated capillary held at 275◦C, and the HESI probe held at 350◦C. The sheath gas flow was set to 40 units, the auxiliary gas flow was set to 15 units, and the sweep gas flow was set to 1 unit. Mass spectrometry (MS) data acquisition was performed in a range of m/z = 70-1000, with the resolution set at 70,000, the AGC target at $1x10^6$, and the maximum injection time at 20 msec. Relative quantitation of polar metabolites was performed with TraceFinder™ 4.1 (Thermo Fisher Scientific) using a 5 ppm mass tolerance and referencing an in-house library of chemical standards. Data were filtered according to predetermined QC metrics: CV of pools <25%; R of linear dilution series <0.975.

Metabolomic data were filtered to remove exogenously added standards and metabolites with >50% missing values. For each standard, the ratio of each sample to the median quantity of that standard across all samples was calculated, and each sample normalized to the average of its standard ratios. Metabolite quantities were then normalized to the average DNA/wet weight content of each treatment condition for each donor, determined from three separate osteochondral explants. Statistical analyses were performed with the R package limma as above.

A1.3 Results

A1.3.1 Glycolytic enzymes experience increased release from diseased cartilage

Proteomic analysis of early conditioned culture medium identified several glycolytic enzymes (TPI1, PGK1, PGAM1, and ENO1) with increased release from juveline bovine cartilage with cytokine treatment after 96 hours (**Fig. A1.1**). These proteins all had increased release with cytokine and Dex treatment (C/N; CD/N), with a non-significant decrease compared to cytokines alone (CD/C). Dex alone had no significant effect on the release of these proteins.

A1.3.2 Bovine cartilage experienced no change in viability between experimental conditions

The increased release of intracellular metabolic proteins was hypothesized to be an indicator of cell death in the cytokine-treated conditions, so bovine cartilage explants were analyzed with FDA/PI fluorescent imaging (**Fig. A1.2**). After 72 hours, no treatment condition showed any visual difference in cell death compared to control (**Fig. A1.2A**), even with the addition of inflammatory cytokines (**Fig. A1.2C**).

A1.3.3 Glycolytic and gluconeogenic protein synthesis were not affected by Dex

To investigate the regulation of these genes related to glucose metabolism under disease and Dex stress, we performed qRT-PCR after 72 hours of (**Fig. A1.3**). All three tested doses of Dex had little to no effect on the genes, with 10 nM Dex slightly decreasing the synthesis of G6PC and PCK2, and 1 uM Dex decreasing G6PC synthesis (**Fig. A1.3E-G**). In cartilage explants from a separate batch of bovine calves, cytokine treatment decreased the synthesis all four glycolytic genes (**Fig. A1.4A-D**) with no effect on the three gluconeogenic genes. The combination of Dex and cytokine treatment had no effect compared to cytokines alone.

A1.3.4 Human cartilage tissue had minimal metabolomic changes after 48 hours of treatment

Metabolites in human ankle cartilage isolated from osteochondral plugs were identified using MS after 48 hours of treatment with or without cytokines and/or Dex. After filtering as above, 112 metabolites were quantified and compared across 3 donors and normalized to internal standards and DNA content per wet weight of cartilage from that donor with that treatment to adjust for different cartilage plug sizes and cellularity (**Fig. A1.5**). The low dose of 100 nM Dex (D/N) had little effect after 48 hours, only affecting cartilage levels of cystathionine. Cytokine treatment, however, had a significant effect on many more metabolites (C/N), causing increases in dihydroorotate, itaconic acid, citrulline, succinate, saccharopine, carbamoyl aspartate, and C5 carnitines. Many metabolites were decreased after cytokine treatment, including glucose, many amino acids, and cytosine. Dex did not have a strong effect on cytokine-treated explants (CD/N), though with the addition of Dex the levels of 2-aminoadipate, glucose-3-phosphate, NAD, and UDP-GlcNAC were increased.

A1.4 Discussion

The assessments of glycolysis and gluconeogenesis in this study in both bovine and human models of early PTOA do not fully support previous findings on the effect of disease on glucose metabolism within cartilage. We observed that the extracellular release of glycolytic proteins into culture medium in a bovine PTOA model was not indicative of changes in the expression of those genes intracellularly. This is suspected to be a stress response to cytokine treatment, likely a marker of or precursor to early cell death in this model. However, chondrocyte death was not visible via propidium iodide staining, though low levels of cell death might still increase media levels of low-abundant metabolic proteins above control levels even without noticeable changes to propidium iodide staining. Further studies using assays for terminal deoxynucleotidyl transferase (TdT)-mediated dUTP nick end labeling (TUNEL) staining or for caspase activity can confirm whether low levels of apoptosis or necrosis are occurring.

In juvenile bovine cartilage explants, Dex did not have an effect on gluconeogenic gene synthesis, contradicting our hypothesis that Dex exposure would increase gluconeogenesis by stimulating synthesis of G6PC and PEPCK [12]. If anything, Dex caused a slight decrease in the synthesis of these genes compared to control, though that effect was not consistent across different Dex doses. Dex also did not have any effect on the transcription of glycolytic genes, even at doses up to 1 μM. Higher doses of Dex for a longer duration of time might have had a stronger effect on gluconeogenic gene transcription, but when considering relevance to clinical treatment, it is desirable to reduce the dose and duration of Dex exposure to limit off-target effects. A lack of changes at the transcriptional level does not exclude changes to glucose processing via other

methods that regulate enzyme function such as phosphorylation, which has been shown for other proteins to be affected by Dex [16–18].

The one metabolite that Dex had an effect on in the presence or absence of cytokine stress was cystathionine, which is a product of H_2S synthesis and a precursor to glutathione [19,20]. H_2S is a mediator of inflammation and has been shown to be upregulated in the synovial fluid of patients with rheumatoid arthritis. The processing of cystathionine by cystathionine γ-lyase has also been shown to be important to reducing inflammation in synovial fibroblasts in a mouse model of rheumatoid arthritis. The processing of this metabolite is strongly suggested to be linked to how cartilage and the joint space mediate inflammatory stress, and targeted follow-up to this metabolic pathway should be performed to better understand the effect of Dex on the production and processing of cystathionine and how that relates to the anti-inflammatory properties of Dex in joint tissues. In a rat model studying hypertension, Dex reduced the levels of H_2S production in mesenteric beds and carotid arteries, which would suggest a corresponding decrease in cystathionine levels, opposite to what was seen in the current study, but there may be tissue-specific differences in metabolic responses to Dex [21]. The overall lack of Dex alone on the identified metabolites suggests a general lack of off-target effects on healthy cartilage within a 48-hour treatment window, supporting the safety of its use in early intervention for PTOA treatment.

Surprisingly, the expression of glycolytic genes was suppressed by cytokine exposure, suggesting that other mechanisms are responsible for the observed shift towards glycolysis in previous studies. This could be influenced by a broad, early suppression of protein synthesis within the first 48-72 hours of disease progression suggested by a decrease in many amino acids within the metabolomic

data. However, in that situation a decrease in gluconeogenic genes might be expected, but there was no change to their synthesis with cytokine treatment. In contrast to PCR results, the metabolomic data from adult human ankle cartilage suggest an increase in glycolytic activity with cytokine treatment. Cartilage levels of glucose were decreased, with a corresponding increase in succinate, an intermediate in the tricarboxylic acid cycle. Saccharopine and 2-aminoadipate were both increased with the combination of cytokine and Dex treatment compared to control, while cytokines alone did not have an effect on these metabolites. Saccharopine is converted to aminoadipic acid in a reversible reaction, and has been suggested to be a biomarker of type 2 diabetes risk and associated with glucose metabolism at the systems level, though the mechanisms behind this have not been explored [22–24]. The increase in this metabolite seen with Dex treatment and not without in an inflammatory context may suggest that Dex does modulate cartilage glucose metabolism if administered during early PTOA progression, and further insight into both this effect and what part of glucose metabolism are affected by or concurrent to increases in saccharopine levels is necessary to fully understand this effect.

Disease effects beyond glucose metabolism are also revealed with metabolomic analysis: citrulline, a byproduct of nitric oxide synthase (NOS) activity, was increased with cytokine treatment, and it is well-established that nitric oxide production is increased with cytokine treatment in human and animal models of PTOA [15,25,26]. The results on the effects of Dex can differ, however, as with juvenile bovine explants, human chondrocytes treated with IL-17, and human osteochondral explants treated with Dex had decreased NOS activity after 48 hours, whereas these results do not show an effect of Dex on the production of citrulline and inferred NOS activity [15,26,27]. Dihydroorotate and carbamoyl aspartate, a precursor to dihydroorotate,

were highly elevated in cytokine-treated cartilage, and inhibition of downstream processing of dihydroorotate in lymphocytes has been suggested as an anti-inflammatory mechanism of action for some rheumatoid arthritis therapeutics [28,29]. Itaconic acid and succinate were both found to be increased in cytokine-treated cartilage in this model, and both have been identified in rat models of rheumatoid arthritis as potential serum disease biomarkers [30]. Some protective effects can also be observed: C5 carnitine levels were also increased in cytokine-treated cartilage, and carnitine has been shown to exert a protective effect in OA models by promoting glycosaminoglycan and collagen II production, decreasing matrix metalloprotease synthesis, and maintaining overall histological joint health [31–33].

A1.4.1 Study limitations

Many differences between the metabolism of juvenile bovine and adult human cartilage are possible, but juvenile bovine cartilage was selected for PCR studies because of the consistency between donor cows and its high cellularity that yielded much higher quality cDNA after RNA extraction and reverse transcription. 72 hours was chosen as a timepoint for RNA extraction, in line with previous studies of juvenile bovine cartilage reactions to disease and Dex, and that number was adjusted to 48 hours for the metabolomics study to account for earlier events that might be missed as the cartilage metabolism adjusts to extended cytokine and Dex exposure. With current steroid treatment administered as intra-articular bolus injections, Dex is rapidly cleared from the joint, so short-term metabolic effects are of interest as well to understand its safety, given the much higher concentrations used clinically [34]. Future studies could expand these observations further into culture to observe later effects of Dex and inflammatory stress on the metabolism of cartilage in this osteochondral context, which is relevant to drug delivery systems

currently being developed to deliver sustained, low-dose therapeutics [35–37]. Further studies should also expand this model to an anaerobic system, as the current experiments were performed under normoxia, while the joint space is highly hypoxic, and glucose uptake is affected in chondrocytes under hypoxic conditions [38].

A1.5 Conclusions

These results from both juvenile bovine and human osteochondral models of PTOA allow insight into effects of Dex on cartilage glucose metabolism, a relatively underdeveloped aspect of the understanding of Dex action that is important to its use and effects. Overall, Dex had little effect on glucose metabolism and broad metabolic changes in both *ex vivo* tissue models, suggesting that in short durations at low dose, it does not have off-target effects on cartilage energy metabolism. With inflammatory cytokine treatment of bovine cartilage explants, extracellular levels of glycolytic genes increased while their synthesis decreased, highlighting that extracellular protein-level biomarkers do not always reflect changes in intracellular expression of these same proteins; thus, understanding of cartilage disease pathogenesis requires investigation of behaviors at all levels. Observing changes in the human cartilage metabolome broadly revealed suppression of amino acids and increases in many metabolites linked to rheumatoid arthritis progression, identifying potential therapeutic targets for PTOA intervention but requiring further follow-up with more donors in joint-relevant oxygen conditions for complete mechanistic understanding.

Acknowledgements

We thank Tenzin Kunchok and the Metabolite Profiling Core Facility at the Whitehead Institute for consultation, running metabolomics samples, and data analysis. We thank donors and donors' families, and the Gift of Hope donor bank (Itasca, IL). This work was supported by NIH/NCATS grant UG3/UH3 TR002186.

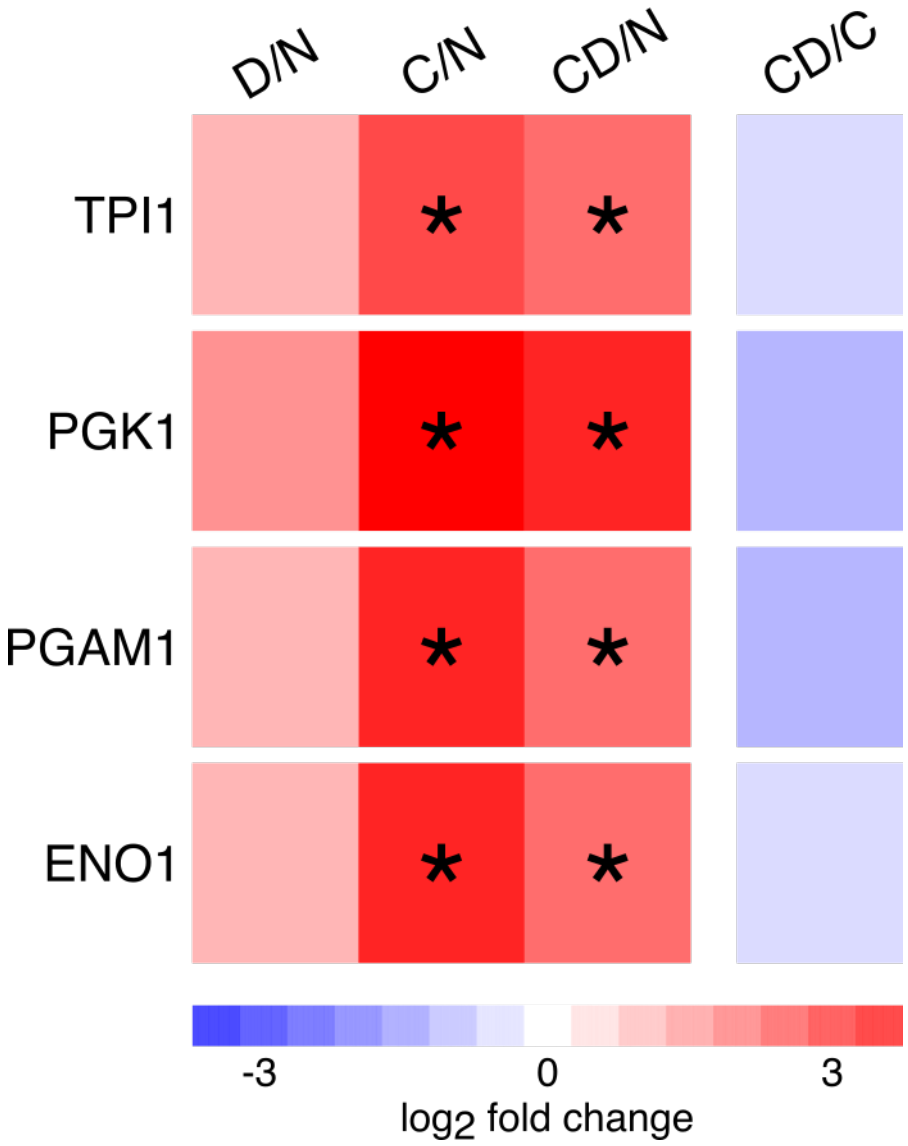

Figure A1.1. **Comparative log2 fold change of selected protein release between 48 and 96 hours from bovine cartilage explants.** Glycolytic proteins that showed a significant effect of treatment in a proteomic study using bovine cartilage explants are highlighted. TPI1: triosephosphate isomerase 1; PGK1: phosphoglycerate kinase 1; PGAM1: phosphoglycerate mutase 1; ENO1: enolase 1. N: no treatment. D: 100 nM Dex alone. C: inflammatory cytokine treatment. CD: cytokine and Dex treatment. *: $p < 0.05$.

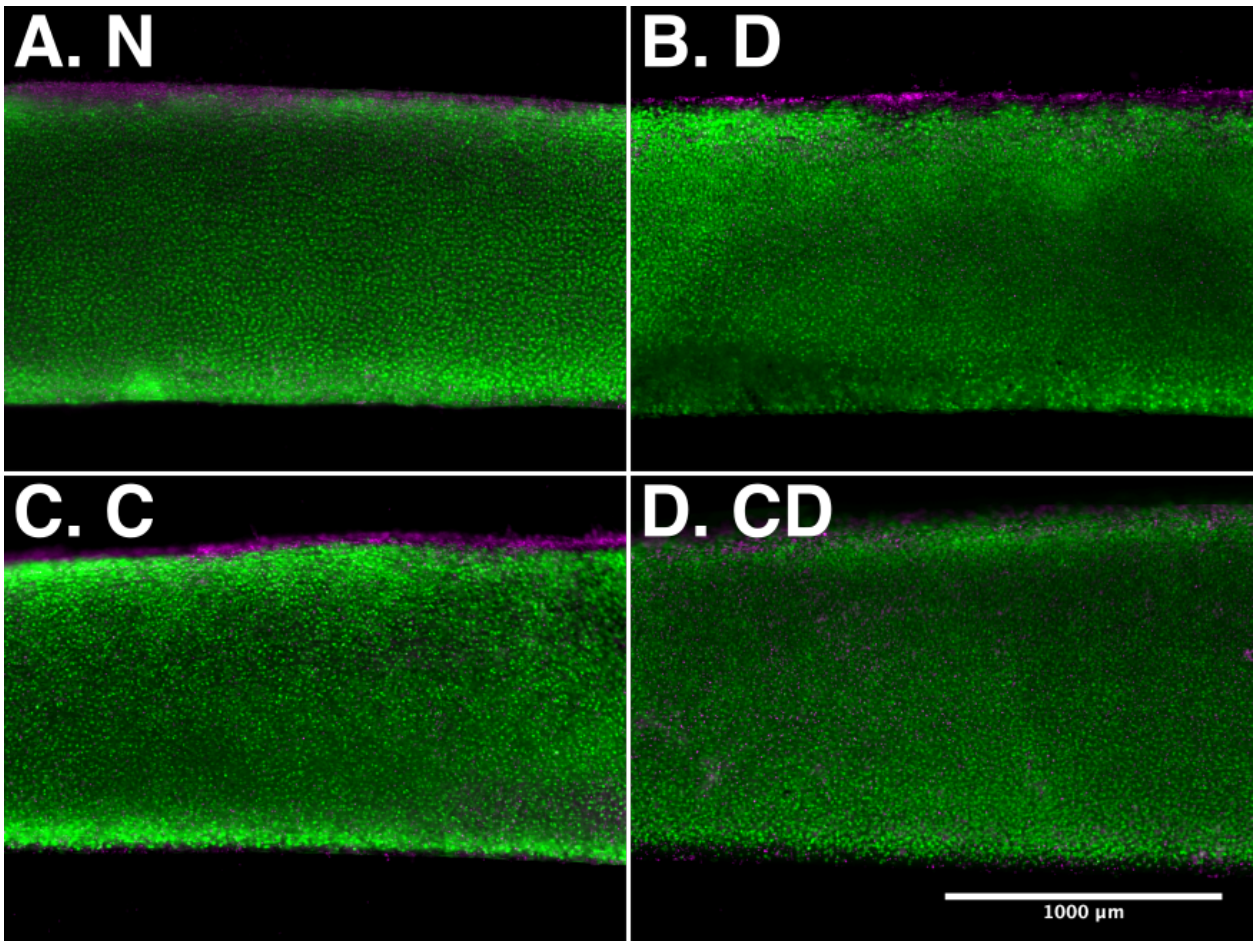

Figure A1.2: FDA/PI staining of bovine cartilage explants 72 hours post-treatment. Green: live cells. Magenta: dead cells. Scale bar: 1 mm.

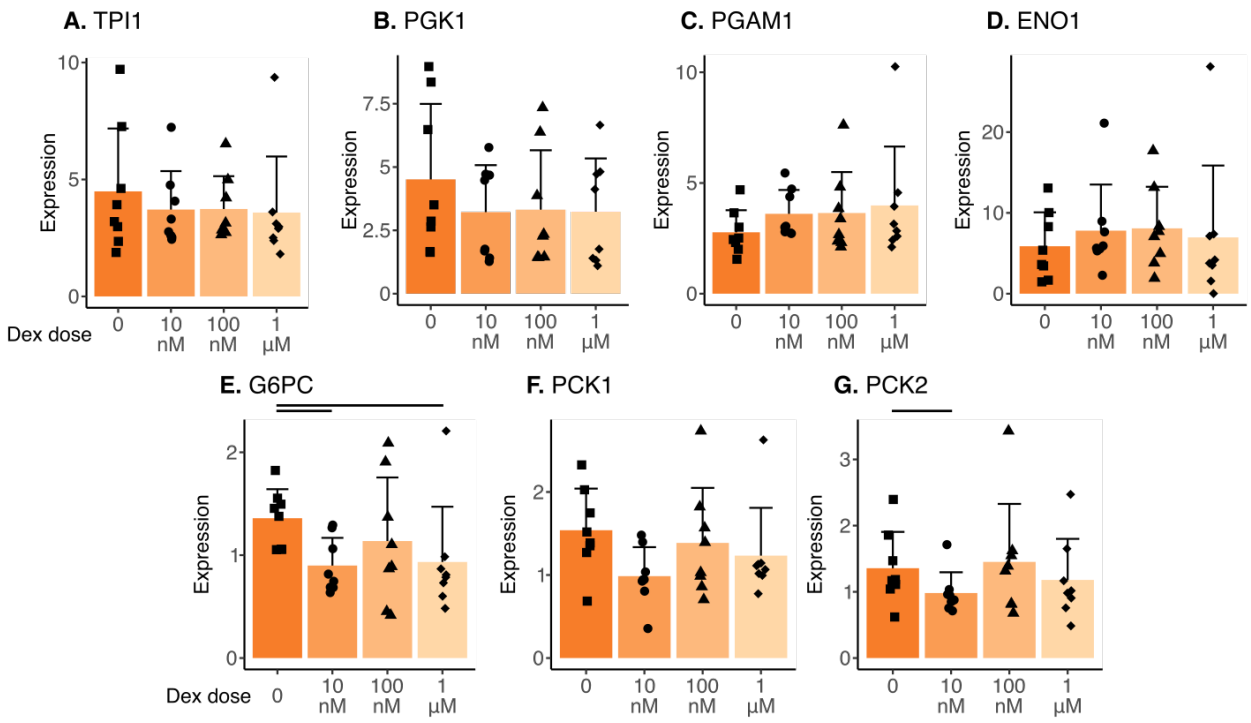

Figure A1.3: **Dex effects on gluconeogenic and glycolytic gene expression after 72 hours.** Expression levels determined from ΔΔct values normalized to β-actin and pre-treatment cartilage. Each point represents data from one biological (cow) replicate. TPI1: triosephosphate isomerase 1; PGK1: phosphoglycerate kinase 1; PGAM1: phosphoglycerate mutase 1; ENO1: enolase 1; G6PC: glucose-6-phosphatase; PCK1 and PCK2: cytosolic and mitochondrial phosphoenolpyruvate carboxykinase, respectively. Error bar: standard deviation. Bar: $p < 0.05$.

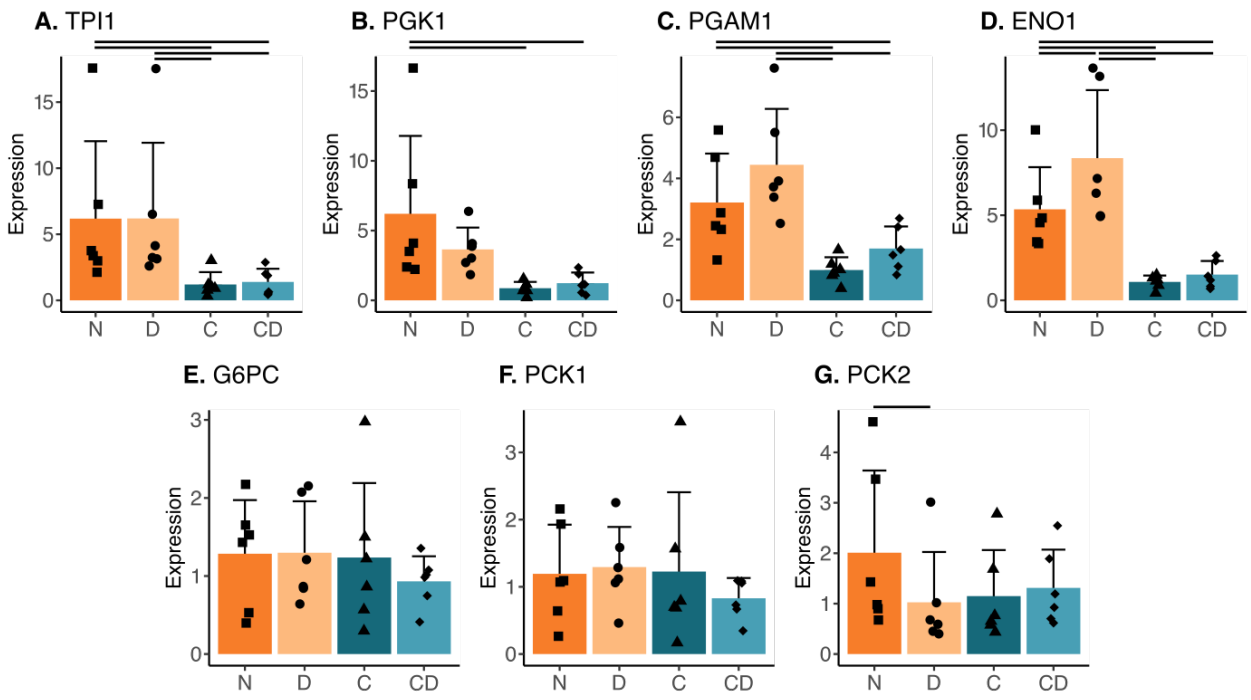

Figure A1.4. **Effects of cytokine treatment and Dex on gluconeogenic and glycolytic gene expression after 72 hours.** Expression levels determined from ΔΔct values normalized to β-actin and pre-treatment cartilage. Each point represents data from one biological (cow) replicate. N: no treatment. D: 100 nM Dex. C: inflammatory cytokine treatment. CD: cytokine and 100 nM Dex treatment. TPI1: triosephosphate isomerase 1; PGK1: phosphoglycerate kinase 1; PGAM1: phosphoglycerate mutase 1; ENO1: enolase 1; G6PC: glucose-6-phosphatase; PCK1 and PCK2: cytosolic and mitochondrial phosphoenolpyruvate carboxykinase, respectively. Error bar: standard deviation. Bar: $p < 0.05$.

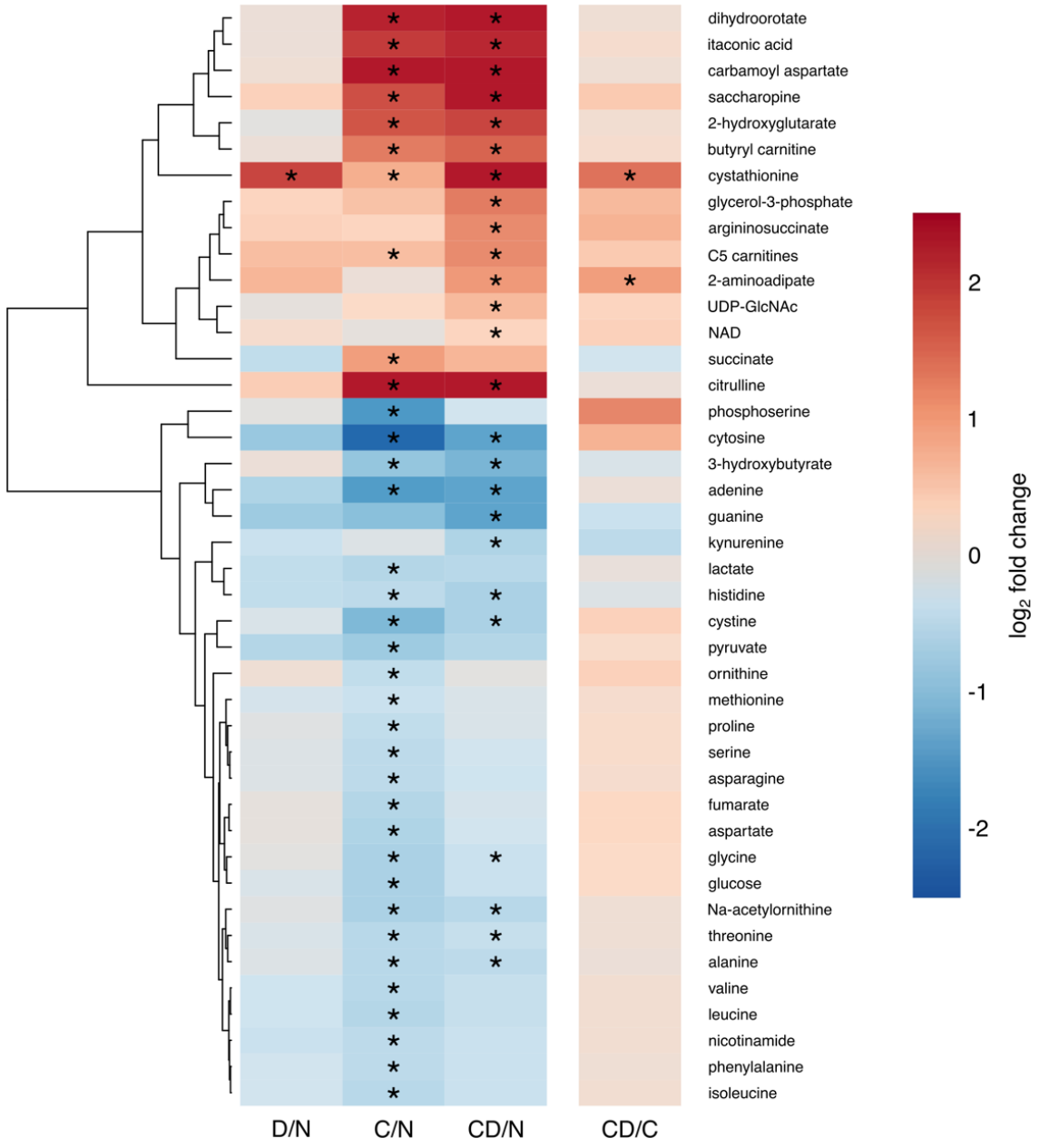

Figure A1.5. Metabolites with a significant effect of Dex, cytokine, or cytokine + Dex treatment after 48 hours in human ankle osteochondral explants. Metabolites with a significant of any treatment condition comparison are highlighted and clustered based on unsupervised hierarchical clustering. N: no treatment. D: 100 nM Dex alone. C: inflammatory cytokine treatment. CD: cytokine and Dex treatment. *: $p < 0.05$.

Gene	Forward sequence (5'-3')	Reverse sequence (5'-3')	Source
β-actin	GATCTGGCACCACACCTTCTAC	AGGCATACAGGGACAGCACA	Zhao *et al.*, 2016 [39]
ENO1	GGAGAAGATCGACAAGCTGATG	TACTTGCCCGACCTGTAGAA	-
G6PC	TGATGGACCAAGAAAGATCCAGGC	TATGGATTGACCTCACTGGCCCTCTT	Zhang et al., 2016 [40]
PCK1	GGATGGAAAGTAGAGTGTGTGG	CTTCTGGATGGTCTTGATGG	Ostrowska et al., 2013 [41]
PCK2	ACACCACCCAGTTGTTCTC	GAAGGCTCAGGTCACATTCT	-
PGAM1	CGGCTCCCAATTCCACATTA	CACGAACAGGCTCTTACTTCTC	-
PGK1	TGGTCCTGAGAGCAGTAAGA	CAGGAACCAGAAGGCAGAAA	-
TPI1	CAGAGGGACTTGGAGTGATTG	GCAGGAAGGGTAGTAGAGATAGA	-

Table A1.1. Primers used in bovine metabolic PCR study. A hyphen referring to the source of the sequence indicates original design. Original primers were designed using the IDT™ PrimerQuest tool. TPI1: triosephosphate isomerase 1; PGK1: phosphoglycerate kinase 1; PGAM1: phosphoglycerate mutase 1; ENO1: enolase 1; G6PC: glucose-6-phosphatase; PCK1 and PCK2: cytosolic and mitochondrial phosphoenolpyruvate carboxykinase, respectively.

References

1. Mobasheri A, Vannucci SJ, Bondy CA, Carter SD, Innes JF, Arteaga MF, et al. Glucose transport and metabolism in chondrocytes: A key to understanding chondrogenesis, skeletal development and cartilage degradation in osteoarthritis. Histol Histopathol. 2002;17:1239–67.

2. Hers HG, Hue L. Gluconeogenesis and related aspects of glycolysis. Annu Rev Biochem. 1983;Vol. 52:617–53.

3. Zhai G. Alteration of metabolic pathways in osteoarthritis. Metabolites. 2019;9.

4. Korostynski M, Malek N, Piechota M, Starowicz K. Cell-type-specific gene expression patterns in the knee cartilage in an osteoarthritis rat model. Funct Integr Genomics. Functional & Integrative Genomics; 2018;18:79–87.

5. Garcia-Gil M, Reyes C, Ramos R, Sanchez-Santos MT, Prieto-Alhambra D, Spector TD, et al. Serum lipid levels and risk of hand osteoarthritis: the chingford prospective cohort study. Sci Rep. 2017;7.

6. Zhai G, Wang-Sattler R, Hart DJ, Arden NK, Hakim AJ, Illig T, et al. Serum branched-chain amino acid to histidine ratio: a novel metabolomic biomarker of knee osteoarthritis. Ann Rheum Dis. 2010;69:1227–31.

7. Black R, Grodzinsky AJ. Dexamethasone: Chondroprotective corticosteroid or catabolic killer? Eur Cells Mater. 2019;38:246–63.

8. Black RM, Wang Y, Struglics A, Lorenzo P, Tillgren V, Rydén M, et al. Proteomic analysis reveals dexamethasone rescues matrix breakdown but not anabolic dysregulation in a cartilage injury model. Osteoarthr Cartil Open. 2020;2:100099.

9. Black RM, Wang Y, Struglics A, Lorenzo P, Chubinskaya S, Grodzinsky AJ, et al. Proteomic clustering reveals the kinetics of disease biomarkers in bovine and human models of post-traumatic osteoarthritis. Osteoarthr Cartil Open. 2021;3:100191.

10. Feliu JE, Hue L, Hers HG. Hormonal control of pyruvate kinase activity and of gluconeogenesis in isolated hepatocytes. Proc Natl Acad Sci U S A. 1976;73:2762–6.

11. Hernvann A, Jaffray P, Hilliquin P, Cazalet C, Menkes CJ, Ekindjian OG. Interleukin-1β-mediated glucose uptake by chondrocytes. Inhibition by cortisol. Osteoarthr Cartil. 1996;4:139–42.

12. Ma R, Zhang W, Tang K, Zhang H, Zhang Y, Li D, et al. Switch of glycolysis to gluconeogenesis by dexamethasone for treatment of hepatocarcinoma. Nat Commun. Nature Publishing Group; 2013;4:1–12.

13. Ritchie ME, Phipson B, Wu D, Hu Y, Law CW, Shi W, et al. Limma powers differential expression analyses for RNA-sequencing and microarray studies. Nucleic Acids Res. 2015;43:e47.

14. Li Y, Wang Y, Chubinskaya S, Schoeberl B, Florine E, Kopesky P, et al. Effects of insulin-like growth factor-1 and dexamethasone on cytokine-challenged cartilage: Relevance to post-traumatic osteoarthritis. Osteoarthr Cartil. 2015;23:266–74.

15. Lu YCS, Evans CH, Grodzinsky AJ. Effects of short-term glucocorticoid treatment on changes in cartilage matrix degradation and chondrocyte gene expression induced by mechanical injury and inflammatory cytokines. Arthritis Res Ther. 2011;13:R142.

16. Pan S, World CJ, Kovacs CJ, Berk BC. Glucose 6-phosphate dehydrogenase is regulated through c-Src-mediated tyrosine phosphorylation in endothelial cells. Arterioscler Thromb Vasc Biol. 2009;29:895–901.

17. Inoue E, Yamauchi J. AMP-activated protein kinase regulates PEPCK gene expression by direct phosphorylation of a novel zinc finger transcription factor. Biochem Biophys Res Commun. 2006;351:793–9.

18. Wang Y, Wan S, Drago J, White FM, Grodzinsky AJ. Phosphoproteomics analysis of signaling changes in human chondrocytes following treatment with Il-1, IGF-1 and dexamethasone. Osteoarthr Cartil. Elsevier; 2017;25:S165–6.

19. Robert K, Maurin N, Vayssettes C, Siauve N, Janel N. Cystathionine β synthase deficiency affects mouse

endochondral ossification. Anat Rec - Part A Discov Mol Cell Evol Biol. 2005;282:1–7.

20. Essouma M, Noubiap JJN. Therapeutic potential of folic acid supplementation for cardiovascular disease prevention through homocysteine lowering and blockade in rheumatoid arthritis patients. Biomark Res. 2015;3.

21. D'Emmanuele Di Villa Bianca R, Mitidieri E, Donnarumma E, Tramontano T, Brancaleone V, Cirino G, et al. Hydrogen sulfide is involved in dexamethasone-induced hypertension in rat. Nitric Oxide - Biol Chem. 2015;46:80–6.

22. Emery PW. Amino acids: Metabolism. In: Caballero B, editor. Encyclopedia of Human Nutrition. Elsevier Ltd; 2013. p. 72–8.

23. Jones EE, Bro, Quist HP. Saccharopine, an intermediate of the aminoadipic acid pathway of lysine. J Biol Chem. 1965;240:2531–6.

24. Wang TJ, Ngo D, Psychogios N, Dejam A, Larson MG, Vasan RS, et al. 2-Aminoadipic acid is a biomarker for diabetes risk. J Clin Invest. 2013;123:4309–17.

25. Keilhoff G, Reiser M, Stanarius A, Aoki E, Wolf G. Citrulline immunohistochemistry for demonstration of NOS activity in vivo and in vitro. Nitric Oxide - Biol Chem. 2000;4:343–53.

26. Szapary HJ, Flaman L, Frank E, Chubinskaya S, Dwivedi G, Grodzinsky AJ. Biomechanical and biochemical changes and responses to dynamic loading on cytokine-challenged osteochondral tissue with dexamethasone. J Biomech. 2022;In prep.

27. Shalom-Barak T, Quach J, Lotz M. Interleukin-17-induced gene expression in articular chondrocytes is associated with activation of mitogen-activated protein kinases and NF-κB. 1998;273:27467–73.

28. Porter TN, Li Y, Raushel FM. Mechanism of the dihydroorotase reaction. Biochemistry. 2004;43:16285–92.

29. Rückemann K, Fairbanks LD, Carrey EA, Hawrylowicz CM, Richards DF, Kirschbaum B, et al. Leflunomide inhibits pyrimidine de novo synthesis in mitogen-stimulated T-lymphocytes from healthy humans. J Biol Chem. 1998;273:21682–91.

30. Michopoulos F, Karagianni N, Whalley NM, Firth MA, Nikolaou C, Wilson ID, et al. Targeted metabolic profiling of the Tg197 mouse model reveals itaconic acid as a marker of rheumatoid arthritis. J Proteome Res. 2016;15:4579–90.

31. Stoppoloni D, Politi L, Dalla Vedova P, Messano M, Koverech A, Scandurra R, et al. L-Carnitine enhances extracellular matrix synthesis in human primary chondrocytes. Rheumatol Int. 2013;33:2399–403.

32. Malek Mahdavi A, Mahdavi R, Kolahi S. Effects of l-Carnitine Supplementation on Serum Inflammatory Factors and Matrix Metalloproteinase Enzymes in Females with Knee Osteoarthritis: A Randomized, Double-Blind, Placebo-Controlled Pilot Study. J Am Coll Nutr. 2016;35:597–603.

33. Bianchi E, Di Cesare Mannelli L, Menicacci C, Lorenzoni P, Aglianò M, Ghelardini C. Prophylactic role of acetyl-l-carnitine on knee lesions and associated pain in a rat model of osteoarthritis. Life Sci. 2014;106:32–9.

34. Evans CH, Kraus VB, Setton LA. Progress in intra-articular therapy. Nat Rev Rheumatol. 2014;10:11–22.

35. Krishnan Y, Rees HA, Rossitto CP, Kim SE, Hung HHK, Frank EH, et al. Green fluorescent proteins engineered for cartilage-targeted drug delivery: Insights for transport into highly charged avascular tissues. Biomaterials. 2018;183:218–33.

36. Geiger BC, Wang S, Padera RF, Grodzinsky AJ, Hammond PT. Cartilage-penetrating nanocarriers improve delivery and efficacy of growth factor treatment of osteoarthritis. Sci Transl Med. 2018;10.

37. Bajpayee AG, De la Vega RE, Scheu M, Varady NH, Yannatos IA, Brown LA, et al. Sustained intra-cartilage delivery of low dose dexamethasone using a cationic carrier for treatment of post traumatic osteoarthritis. Eur Cell Mater. 2017;34:341–64.

38. Peansukmanee S, Vaughan-thomas A, Carter SD, Clegg PD, Taylor S, Redmond C, et al. Effects of hypoxia on

glucose transport in primary equine chondrocytes in vitro and evidence of reduced GLUT1 gene expression in pathologic cartilage in vivo. 2009;529–35.

39. Zhao H, Liu J, Li Y, Yang C, Zhao S, Liu J, et al. Validation of reference genes for quantitative real-time PCR in bovine PBMCs transformed and non-transformed by Theileria annulata. Korean J Parasitol. 2016;54:39–46.

40. Zhang Q, Koser SL, Donkin SS. Propionate induces mRNA expression of gluconeogenic genes in bovine calf hepatocytes. J Dairy Sci. 2016;99:3908–15.

41. Ostrowska M, Górka P, Żelazowska B. Expression of PC, PCK1, PCK2, LDHB, FBP1 and G6PC genes in the liver of cows in the transition from pregnancy to lactation. Anim Sci Pap Reports. 2013;31:281–90.

Appendix 2: Dexamethasone and IGF-1 Effects in Cartilage/Bone/Synovium PTOA Model on Earth and in Space

Rebecca M. Black[1], Garima Dwivedi[1,2], Lisa L. Flaman[1], Karin Lindblom[2], Eliot H. Frank[1], Yamini Krishnan[1], Han-Hwa Hung[1], Susan Chubinskaya[3], Patrik Önnerfjord[2], and Alan J. Grodzinsky[1,4,5]

[1]Departments of Biological Engineering, [4]Mechanical Engineering, [5]Electrical Engineering and Computer Science, Massachusetts Institute of Technology, Cambridge, MA
[2]Rheumatology, Department of Clinical Sciences Lund, Lund University, Lund, Sweden
[3]Departments of Pediatrics, Orthopedic Surgery and Medicine (Section of Rheumatology), Rush University Medical Center, Chicago, IL, USA

This manuscript is currently in preparation for submission.

A2.1 Introduction

In the effort to understand disease mechanisms and find disease-modifying treatments, post-traumatic osteoarthritis (PTOA) has been studied using many different model systems. This degenerative disease can be modeled with surgical injuries to the joints of whole animals, with *ex vivo* cartilage explants, or with primary chondrocytes from healthy or injured animals [1–4]. Animal models, however, do not always produce results that are translatable to humans, and this is likely one reason why there is currently no disease-modifying drug for PTOA prevention. Human tissue models of PTOA have used primary chondrocytes and chondrocyte explants, and more recent studies have been performed with cartilage and bone co-culture [3,5]. These co-culture systems allow for crosstalk between different joint tissues, reflecting the complex signaling networks that regulate cartilage and bone homeostasis while still allowing control over the dose and duration of exposure to inflammatory cytokines used to induce cartilage breakdown. Using human cartilage and bone with exogenous cytokines does not capture the full scope of the chemokines released by other tissues such as the synovial joint capsule, which contains synoviocytes, macrophages, and other inflammatory cells that contribute to joint damage after an injury [6,7].

Models that include additional joint tissues are relevant to finding treatments for PTOA as well, as different tissues could respond to the same drug in different ways. Dexamethasone (Dex) is a corticosteroid that has promising anti-catabolic effects on cartilage in monoculture ex vivo human explant models, but concerns exist over its potential negative effects on bone [2,8,9]. In studies with monoculture *ex vivo* cartilage explants from healthy human knees, Dex prevented matrix breakdown but did not restore all anabolic processes back to control levels, assessed by proteomic

analysis or by observing overall biosynthesis [3,5]. The addition of pro-anabolic insulin-like growth factor 1 (IGF-1), however, rescued human ankle cartilage biosynthesis significantly towards control levels, and in knee cartilage still had a greater effect on maintaining biosynthesis than Dex alone. The combination of these two drugs is a promising treatment to combat both inflammation that Dex can counteract and stimulate anabolic processes. However, their combined signaling pathways are complex and multifaceted, requiring the treatment of multiple joint tissues to fully understand their effects on disease progression.

A multi-tissue *in vitro* model system of PTOA is desirable not only to study the effects of OA and potential treatments on Earth, but in space as well. As spaceflight becomes more common and the potential for extraterrestrial exploration becomes more of a reality, it is important to understand the risks of spaceflight on joint injuries and the development of diseases like PTOA. Astronauts stationed on mission on the International Space Station National Lab (ISS-NL) experience a number of joint injuries that can interrupt their activities, with up to three times as many musculoskeletal injuries while they are on the ISS compared to the overall average of their service [10–12]. The environment of space, with low gravity causing mechanical differences in joint loading and the exposure to high radiation outside of the atmosphere, is already understood to lead to musculoskeletal atrophy and an increase in osteonecrosis, with some studies linking back pain in astronauts to histological and structural changes within the intervertebral disk [13,14]. To combat some of the understood effects on muscle and bone health, astronauts perform rigorous exercise regimens aboard the ISS, increasing their risk of joint injuries [15,16]. However, it is not known what effect the environment of space has on osteoarthritis progression after a traumatic injury or how drug treatments are affected.

This study uses a multi-tissue model that incorporates cartilage, bone, and joint capsule synovium tissue to model PTOA progression and assess the ability of Dex and IGF-1 to rescue disease effects in the context of multiple joint tissues on Earth and on the ISS-NL. Tissue breakdown and signaling events are analyzed using mass spectrometry (MS) analysis to compare diseased and drug-treated conditions across several human donors. We aim to compare the effects of Dex and IGF-1 on disease progression in a system using synovial tissue to observe whether they demonstrate the same anti-catabolic and pro-anabolic effects seen in other studies that used exogenous cytokines, and whether low gravity and high radiation in space affect their ability to rescue disease effects.

A2.2 Materials and Methods

A2.2.1 Human osteochondral and synovium explant harvest

All procedures were approved by Rush University Medical Center Institutional Review Board and Committee on the use of Humans as Experimental Subjects at MIT. Osteochondral plugs (3.5 mm diameter with full-thickness cartilage and ~3 mm underlying bone) were harvested from the condyles and trochlear grooves of cadaveric distal femurs (Collins grade 1/2, 64-82 y.o.) A complete list of donors can be found in **Table A2.1**. Knee-matched whole synovial joint capsule tissues were collected and cultured in 50 mL conical tubes until being cut into individual explants at day 0 of treatment. Osteochondral samples were cultured in 4.5 g/L high glucose Dulbecco's Modified Eagle Medium (DMEM) supplemented with 1% ITS (insulin-transferrin-selenium at 10 µg/ml, 5.5 µg/ml, and 5 ng/ml, respectively; Sigma), 20 mM MOPS buffer, 0.1 mM nonessential amino acids, 0.4 mM proline, 20 µg/ml ascorbic acid, 100 U/ml penicillin G, 100 µg/ ml streptomycin, and 0.25 µg/ml amphotericin for two days after harvest before switching to low

glucose (1 g/L) DMEM. Media used for the spaceflight samples used CO_2 independent media (Thermo Fisher) to accommodate for culture conditions on the ISS.

A2.2.2 PTOA model and therapeutic treatments

Treatment groups shared between ground controls and spaceflight were: cartilage and bone control (CB), cartilage + bone explants injured with a single injurious unconfined compression (15 MPa/sec to peak stress of 5 MPa, held at 5MPa for 0.4 sec, then unloaded at 15 MPa/sec using an in-house incubator-housed compression apparatus [17,18]) co-cultured with 4-5 mm explants of synovium harvested from the synovial joint capsule of the same knee as a model of PTOA (CBS), and CBS samples with additional 100 nM Dex and 100 ng/mL IGF-1 (CBDSI). The synovial tissue explants were cut immediately before addition to wells containing osteochondral explants, which sufficiently created a disease-relevant inflamed state as they began to secrete inflammatory factors after being cut [19]. Ground controls additionally included CBS samples treated with only 100 nM Dex (CBSD) (**Table A2.1**). Donors 7 and 8 were used for spaceflight and included treatments with cartilage + bone with only Dex and IGF-1 without a disease challenge (DI) on Earth, and donor 8 in space as well (**Table A2.2**). Media from the first and second weeks of culture were pooled together across six replicates per treatment condition per donor and kept frozen at -20ºC until MS analysis.

A2.2.3 Spaceflight sample preparation and culture

Complete methods of spaceflight are in preparation for submission in a full manuscript describing this experiment. In brief, six osteochondral plugs were loaded into microfluidic culture chambers that contained 15 mL of culture media, held in place by a neoprene rubber sheet. Any

osteochondral plugs receiving CBS treatment received a mechanical impact injury prior to loading into the chamber. Six 6-7 mm diameter explants of synovial tissue were sutured onto the neoprene for samples with synovial co-culture. Culture chambers were mounted along with media bags into modules (designed by Techshot, Inc), and were maintained for 6-7 days at 15ºC to minimize metabolism during 1-2 days in the Dragon capsule before launch, subsequent launch, docking on ISS, and final module plug-in within Techshot carousels already onboard the ISS-NL.

Culture modules were launched to the ISS-NL on December 6, 2020 via a Dragon capsule on a SpaceX-21 Falcon 9 rocket from Kennedy Space Center, launch pad 39A. Once installed on the station, the 8 modules inside the 2 carousels (and thereby all the tissues within the culture chambers) were raised to 37ºC, accompanied by the first automated media change and collection of week-0 media. Every two days, 15 mL of fresh media were exchanged and the spent media was collected; after 3 media changes (every 6 days) the media sample collection bags and fresh media stock were replaced in each of the 8 modules. After 22 total days of culture, including 3 media bag swaps, media and tissue samples were frozen and stored before transportation back to earth. 6 media bags remained on the ISS due to logistical errors and remained in storage at -80 ºC until they were returned to MIT 6 months later.

A2.2.4 Mass spectrometry and analysis of media proteomes

Protein isolation and trypsinization from pooled week 1 and week 2 media samples, discovery MS, and protein quantification were performed as previously described (see **Chapter 4**). MS data were searched in two batches: all of the ground control samples, and then the space samples with their corresponding ground controls (donors 7 and 8) separately. For both the ground and space data

sets, proteins were filtered out if they were exogenous (e.g. from ITS media supplement) or not identified and quantified in at least 70% of samples, and missing values were imputed using the *k*-nearest neighbor method [5,20]. Individual peptide abundances for collagen I (COL1A1) and collagen II (COL2A1) were filtered and imputed via the same methods. Pairwise comparisons between treatments were performed using limma and MATLAB (MathWorks) [21]. Protein abundance data were $\log_2$-transformed and scaled, and principle component analysis (PCA) was performed using the "prcomp" function [2]. PCA protein loadings were ranked by their dot product and analyzed using Gene Set Enrichment Analysis (GSEA) c5 gene sets with the Human UniProt IDs chip and 1,000 repeats for enrichment score distributions [22,23]. For comparison of space and ground effects on the same proteins, proteins with a significant (adjusted p value < 0.05) effect of CBS treatment across all ground samples were selected. Within just Donor 7 and Donor 8, the $\log_2$ fold change of CBS versus CB samples were found for the proteins both identified in space samples and with a significant effect across all samples. Differences in space and ground responses were assessed by taking the square of the difference between the space fold change and ground fold change. Enrichment analysis for biological processes was performed using STRING analysis as previously described [2,24].

A2.3 Results

A2.3.1 Changes in media proteome on Earth in cartilage/bone/synovium system

MS analysis identified 2068 proteins with any abundance across all ground samples, with 1470 proteins remaining after filtering as above, and the search of the space group samples returned 1437 proteins, with 935 remaining after filtering. Pairwise comparisons were performed between treatment conditions for both week 1 and week 2 media proteomes across all ground samples. The

most prominent treatment effect was of CBS treatment versus CB: in week 1, collagens III, IV, V, VI, XIV, XV, and XVIII released to the media were increased, along with many proteasomes, cathepsins, matrix metalloproteinase-1 and -2 (MMP1 and -2), and many proteins associated with cytoskeleton organization, with similar results in the second week. Notably, media levels of aggrecan, collagen type I and II were decreased in the first week. Biomarkers of bone health alkaline phosphatase (ALPL), osteomodulin (OMD), osteonectin (SPARC), and sclerostin (SOST) were decreased with CBS treatment in both weeks, and osteopontin (SPP1) was also decreased in week 2. STRING analysis of proteins with increased release in both weeks (**Fig. A2.1**) showed clusters of proteins related to ECM organization, carbohydrate metabolism, and ribonucleoproteins.

A2.3.2 Dex and IGF-1 effects on ground samples

For the ground samples, Dex and IGF-1 had minimal effects, particularly in the first week. With the addition of only Dex to CBS cultures in week 1, MMP1, serpin family I member 1 (SERPINI1), and procollagen-lysine, 2-oxoglutarate 5-dioxygenase 2 (PLOD2) were decreased, along with a decrease in the release of some intracellular proteins such as annexin A3, translin-associated protein X, and 14-3-3 epsilon. The addition of IGF-1 as well as Dex also caused a decrease in the amount of MMP1 released, and caused an increase in the media levels of a mucin or mucin-like protein: mucin 5B with Dex alone, and mucin-like 1 with Dex and IGF-1. A larger number of proteins were affected in week 2, though no effect was seen on extracellular matrix components themselves. MMP1 and MMP13 were decreased in CBSD compared to CBS, and MMP9 and interleukin 8 (IL-8) was decreased with Dex and IGF-1 treatment compared to CBS. SERPINI1 was decreased with both drug regimens in week 1, as well as chordin-like 2. In the second week,

kininogen-1 (KNG1), complement C7, and metallothioneins such as metallothionein 1X, 2A, and 1E were increased with both Dex and the combination of Dex and IGF-1 compared to CBS alone.

A2.3.3 Comparison of media proteome changes on the ground versus in space

Principal component analysis (PCA, **Fig. A2.2**) was performed on the ground and space samples for week 1 (**A2.2A**, **A2.2C**) and week 2 (**A2.2B**, **A2.2D**) for donors 7 (**A2.2A**, **A2.2B**) and 8 (**A2.2C**, **A2.2D**). Across all four analyses, the most significant effect on sample variability was the separation of space versus ground samples, with the second largest contribution from injury and synovial co-culture versus samples with no treatment or only Dex and IGF-1 (DI). Dex and Dex+IGF-1 treated samples did not separate much from their untreated counterparts, particularly for donor 8. GSEA was performed on the ranked protein loadings from the first principal component for each data set to find which proteins were more associated with the space samples versus the ground samples. Culture on the ISS was consistently associated with proteins related to desmosomes such as cystatin A, desmocolins, desmoplakins, and plakophilin 1. Ground control samples were broadly associated with intracellular metabolic proteins such as protein disulfide isomerases, glucose-processing proteins, and those involved in endoplasmic reticulum function.

To compare whether changes on proteins in the ground control samples were recapitulated in space, we selected proteins with a significant effect of CBS treatment on the ground and filtered for proteins also identified in the space samples. The $\log_2$ fold change of CBS versus control within each of donor 7 and donor 8 for week 1 and week 2 were calculated for the ground and space samples, and ground and space fold changes plotted against each other (**Fig. A2.3**). Proteins were highlighted if the mean squared difference between the two was greater than 5, and the absolute

value of the fold changes for both space and ground were greater than 1 (i.e. a two-fold increase or decrease). Highlighted proteins are summarized in **Tables A2.3** and **A2.4**. Notable proteins for donor 7 that were not highlighted include IL-6, which had no change in the release in space in week 1 but a large increase in the ground samples, collagen II, which had a decrease with CBS treatment in the ground samples and a slight increase in space, and collagen VI (A1 and A2 chains), with a greater increase in space compared to ground. Donor 8 also had higher amounts of collagen II and collagen IV release in space for week 1 compared to decreases in their release in the ground samples. For both donors across both weeks, there were greater increases of SOST, OMD, and SPARC in the media compared to ground controls.

A2.3.4 Changes in collagen synthesis identified via analysis of peptide abundances

Collagen I and II synthesis was assessed in donors 7 and 8 via analysis of the individual peptides identified corresponding to those collagens. Comparing CBS treatments to CB alone, collagen II synthesis (assessed by changes in the N- and C-terminal peptides) was only increased in space and not on the ground over the first two weeks: in the first week for donor 7, and the second week for donor 8 (**Fig. A2.4**). Collagen I synthesis followed the same trend, with increases in N- and C-terminal peptides indicative of new synthesis only in space with CBS treatment.

A2.4 Discussion

The novel model of PTOA progression presented here incorporated three joint tissues from macroscopically healthy human joints, instead of arthroplasty discards that are common among human *ex vivo* studies [25]. This system allows for investigation of early PTOA events and the effects of intervention with therapeutics such as Dex and IGF-1, and by using native synovium

and fibrous joint capsule instead of exogenous inflammatory cytokines, captures the full scope of inflammation released by an injured joint. Over two weeks, the effects of co-culture with inflamed synovial tissue caused increases in the release of proteins associated with extracellular matrix organization and intracellular metabolic processes, similar to previous results using cartilage and bone explants [5] (see also **Chapter 4**). In the first week of culture, collagen-associated proteins and those found in the pericellular matrix such as collagen VI experienced increased release, and both collagen I and collagen II had decreased synthesis based on the release of their N- and C-terminal propeptides [26–28].

However, the extent to which the matrix broke down was lesser than in previous work, as only three MMPs showed an effect of disease treatment, aggrecan and cartilage oligomeric matrix protein (COMP) did not show increased release in either week, and the peptides in the core of collagen II that were shown to be increased after three weeks in a cartilage/bone co-culture model, indicating protein cleavage by proteases after injury and tumor necrosis factor alpha (TNF-α)/IL-6 treatment, were broadly decreased with CBS treatment in this study (**Fig. A2.4A-D**). This could be due to lower levels of inflammatory cytokines in the CBS model, as other studies use exogenous cytokines in the nanogram/mL range, while many cytokines identified in this model (but not all, particularly IL-6) were orders of magnitude lower, around picogram/mL concentrations [19]. Previous studies also applied continuous culture with cytokines during two to three weeks of culture, while this model has shown highly time-dependent release of cytokines from the synovial tissue, with highest release within the first few days that drops off rapidly over the course of the culture.

Across all ground control donors, there was a surprising lack of a Dex effect on CBS co-cultures. Dex has been shown in this model system to maintain chondrocyte viability, reduce glycosaminoglycan loss, and attenuate the release of inflammatory cytokines, but had little effect on the media proteome beyond reducing the levels of some MMPs and SERPINs [29]. Dex and IGF-1 did increase the release of metallothioneins, which are protective against oxidative stress [30]. It has been well-established that Dex treatment drives synthesis of metallothioneins, indicating a potential mechanism for therapeutic benefit, especially in the high-radiation environment of space [31]. These results suggest that the impact of early intervention with Dex and IGF-1 is to prevent matrix catabolism and cytotoxic events, without many off-target effects detectable in what was released to the media. It is notable that Dex increased the release of IGF binding protein 6, which could bind to IGF and decrease its activity [32].

To understand disease effects in space, for the sake of future space travel and astronauts that currently experience high rates of musculoskeletal injuries, cartilage, bone, and synovial explants from two human donors were co-cultured for three weeks on the ISS before shipment back to Earth for analysis. Culture in space had a significant effect on media proteome composition, with proteins associated with desmosomes prominent in space samples compared to those on the ground, across all treatment conditions. The increased presence of these proteins could be linked to the proliferation of cells in space: in previous studies of OA progression, increased cell number were found in cartilage lacunae, and desmocolin 3 was found at higher levels in plasma from RA patients [33,34]. The increase in desmosomal proteins is likely not only due to changes in the cartilage tissue: in cases of traumatic arthritis, more desmosomes have also observed between synovial cells [35]. Samples cultured on Earth were associated with higher release of intracellular

metabolic proteins, which are considered to be markers of necrotic cell death, particularly early in culture [5]. This suggests that early cell death events are not occurring in space, possibly because of the delayed timing of the induction of culture. Exposure to the conditions of space may cause proliferation and aggregation of cells together with corresponding increases in the amount of desmosomal junctions, which may replicate the behavior seen during OA progression. Future studies including histological sectioning of samples to observe cell behavior and cell number are needed to validate this hypothesis.

Depending on the duration of a mission, a traumatic joint injury in space might need immediate treatment or even pre-treatment before flight to attenuate any damage. However, with no gravity and the high radiation in space, the effects of therapeutics may be altered. Dex and IGF-1 had little effect on attenuating changes to the media proteome caused by disease progression, and PCA of space samples also showed little deviation between CBS and CBS + Dex and IGF-1 treatments.

The changes caused by CBS treatment on the ground could be compared within each donor that was cultured in space, as the majority of proteins with a significant effect across all donors on the ground had similar effects within just donors 7 and 8. These two donors experienced different effects of culture in space, which is unsurprising due to the high amount of donor variability possible due to differences in age, sex, and many other factors. Donor 7 experienced lower amounts of inflammatory mediators such as IL-8 and complement factors 1R and 1S, released with CBS treatment in space compared to the ground, but higher levels of peptides from the propeptide regions of collagen I, indicative of collagen I synthesis and bone osteoblast activity. The biomarkers of bone health OMD, SPARC, and SOST, all also had greater increases to the media

under disease stress in space than ground (for both donors), indicative of healthier bone metabolism [36–38]. In the second week, many intracellular proteins experienced a decrease in their release with CBS culture compared to an increase in their release with CBS treatment on the ground. This suggests less cell death and less of an inflammatory response to disease progression. Donor 8 experienced fewer differences between space and ground, but also experienced a lower level of IL-8 release with CBS treatment, as well as IL-6 and TNF-α induced protein 6 compared to ground. Collagens VI, XV, and XVIII, all pericellular matrix collagens, had a higher release in space in the second week for donor 8, suggesting either more of an anabolic response with new deposition of these proteins in response to disease progression in space or early catabolic breakdown events [39–41]. An increased anabolic response is supported by collagen II synthesis (**Fig. A2.4**), an important part of the cartilage reparative response to OA progression, not being decreased with CBS treatment in space as it was for ground for either donor, though these effects must be explored further [42].

A2.4.1 Study limitations

Compared to studies using exogenous cytokines, using synovial explants introduces more variability in cytokine release, as each donor will have different concentrations and different mixtures of cytokines that are released after the initial injury. This variability is disease-relevant, as different donors experience PTOA progression differently due to those changes in how the joints react to an injury, but for experimental studies it introduces noise into outcome measures of drug efficacy and disease effects. Using pooled conditioned media from synovial monoculture instead of individual synovial explants could introduce donor-specific inflammatory signaling in a more consistent manner across all replicates, but would lack the direct cell-cell crosstalk present by

having live synovial tissue present in the culture well. The synovial explants contained some adipose tissue, which could bind to Dex due to the lipophilicity of the drug and potentially affect its function [43,44]. However, Dex effects on viability, inflammatory mediators, and cartilage matrix catabolism in this model have already been assessed, indicating that it is biologically active on chondrocytes even with any changes to its transport. These considerations are important as drug delivery methods are optimized for disease-modifying drugs like Dex and IGF-1 that aim to target specific tissues but must pass through the phospholipid layers and highly charged molecules within the synovial fluid and cartilage matrix to reach their target cells [45–50]. Within a donor the amount of cartilage, bone, and synovial tissue could not be kept perfectly equal due to different thicknesses and cellularity of the tissue, and human error introduced by cutting synovial tissue and bone that do not cut cleanly or evenly. This was controlled for by pooling six replicates together: the media from six individual osteochondral plugs were pooled together at the end of the ground experiments, and six plugs per treatment condition were cultured together in one microfluidic chamber during culture on the ISS. Samples sent to the ISS-NL required one week of culture at 15ºC before the start of the experiment due to loading times and travel from Earth to the ISS, but being kept at this low temperature minimized cellular activity while still keeping the tissue alive to make the week-to-week comparisons between space and ground as translatable as possible. Increasing the number of donors in space would improve the ability to statistically assess the difference between ground and space samples, as well as to assess the donor variability in response to disease progression in space and should be considered for future repeats of these experiments.

A2.5 Conclusions

This multi-tissue primary human model of early PTOA is a clinically relevant model of early disease progression that demonstrates slower disease progression than other models that did not incorporate synovial joint capsule tissue, matching what is seen with patient disease pathology more closely. Low-dose Dex and IGF-1 decreased MMP release without effects on immune signaling that have been seen in other studies, a promising result for their anti-catabolic activity without off-target effects, though questions remain to be answered on the appropriate method of delivery and timing of drug intervention after an injury. Extensive work is ongoing to design delivery mechanisms, often using encapsulation or tethering to positively charged carriers to help direct delivery to specific tissues, reducing the effective concentration necessary in synovial fluid to further avoid off-target effects. This exploratory study of the effects in space revealed a less significant effect of disease progression over first two weeks, with lower cytokine levels and amount of ECM components released, and a maintenance of anabolic processes under disease stress. Dex and IGF-1 had little effect on the media proteome for samples cultured on the ISS-NL, suggesting no off-target effects, possibly due to milder effects of disease progression overall. This suggests that they may be considered for pre-treatment before a mission to counteract any catabolic effects that do occur after an injury on the ISS, but more experiments that cover a longer duration of disease progression with a higher number of human donors to capture the full scope of donor variability are necessary to fully understand their potential protective effects.

Acknowledgements

We thank donors and donors' families, and the donor banks Gift of Hope (Itasca, IL), National Disease Research Interchange (Philadelphia, PA), and LifeNet Health (Virginia Beach, VA). We

are grateful to Marc Giulianotti from CASIS-NASA for coordination on the SpaceX launch. We thank Jordan Fite, Chris Scherzer, Ken Barton, Brad Luyster, Eugene Boland, and Nathan Thomas from Techshot, Inc. We thank astronaut Kate Rubins for maintenance of the experiment on board the ISS-NL. This work was supported by grants NIH-NCATS UG3/UH3 TR002186 and CASIS (Center for the Advancement of Science in Space) GA-2021-9806.

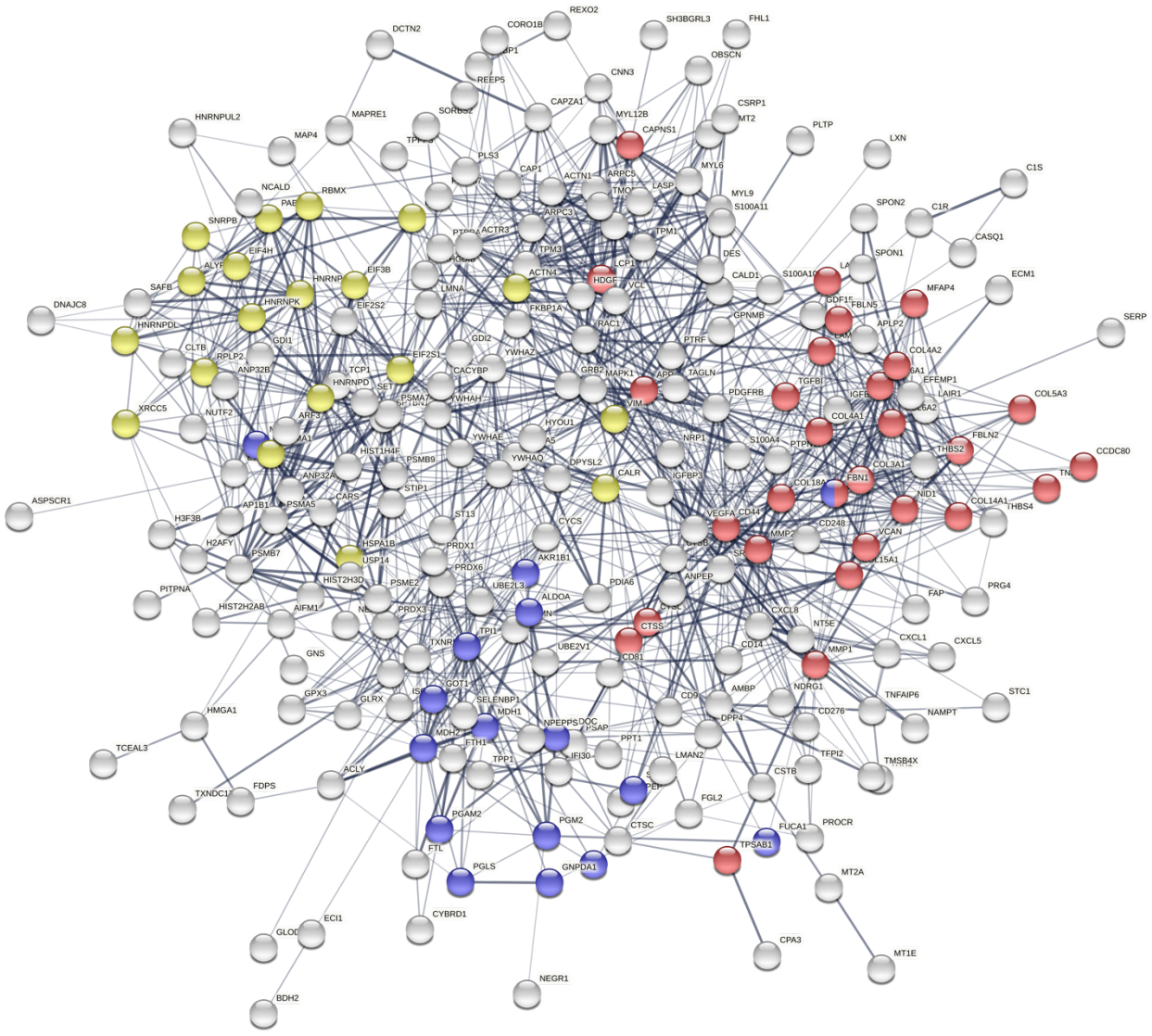

Figure A2.1: STRING network analysis of proteins increased in media with CBS treatment in ground samples on both week 1 and week 2. Coloring is based on biological process enrichment: ECM organization (red), carbohydrate metabolism (blue), and ribonucleoproteins (yellow).

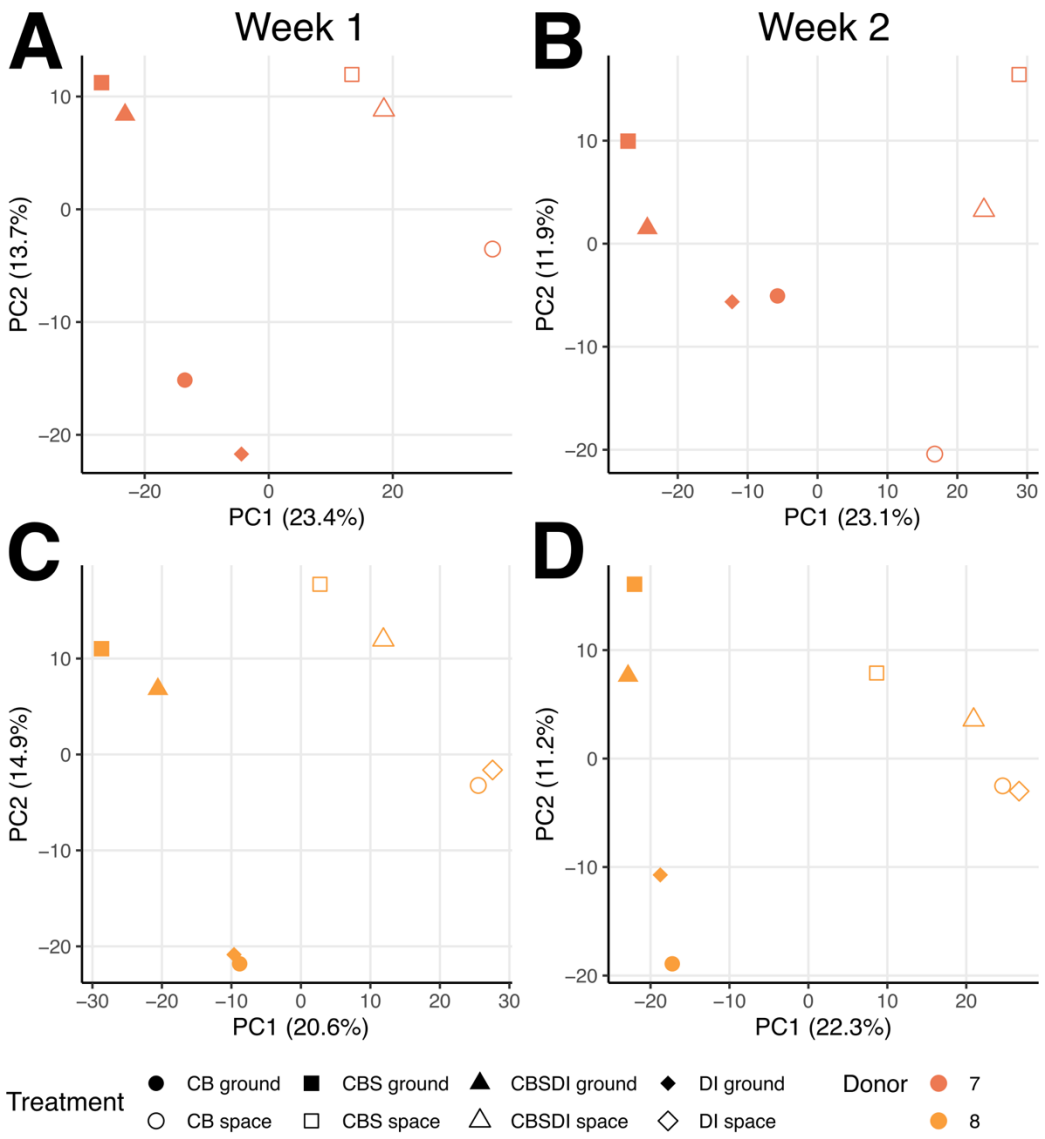

Figure A2.2. **Principal component analysis of space and ground samples.** Principle component analysis (PCA) was performed using abundance values from donors 7 (**A**, **B**) and 8 (**C**, **D**) for treatment conditions on both ground and space from the first or second week of treatment. Percentages on axes represent percent variance explained by that principal component. CB: cartilage and bone control. CBS: cartilage, bone, and synovial co-culture with mechanical injury. CBSDI: CBS treatment with the addition of Dex and IGF-1. DI: osteochondral explants treated with Dex and IGF-1.

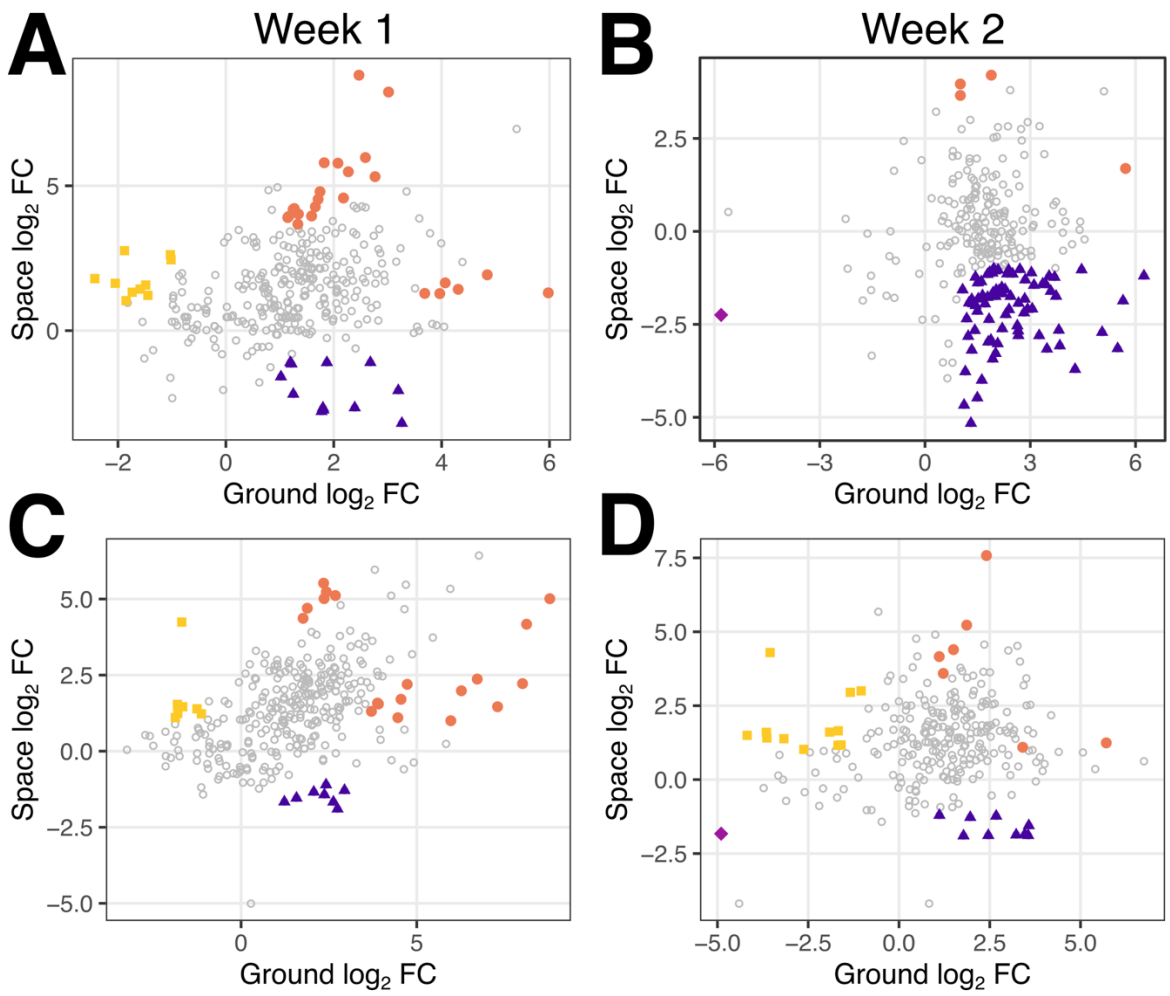

Figure A2.3: **Differences between space and ground culture on media abundances of proteins affected by disease progression in comparison to control.** Proteins with a significant effect of cartilage/bone/synovium co-culture (CBS) versus osteochondral controls (CB) on the ground were selected and filtered for proteins also identified in space samples. The $\log_2$ fold changes (FC) between CBS and CB were determined within just donors 7 (**A, B**) and 8 (**C, D**) on the ground and in space for each of week 1 (**A, C**) and week 2 (**B, D**). Each point represents an individual protein, and proteins are colored if their $\log_2$ FC for both ground and space were greater than 1 or less than -1, and the mean squared difference between space and ground were greater than 5, indicating a large difference between the behavior in ground and space as well as a noticeable change in both ground and space.

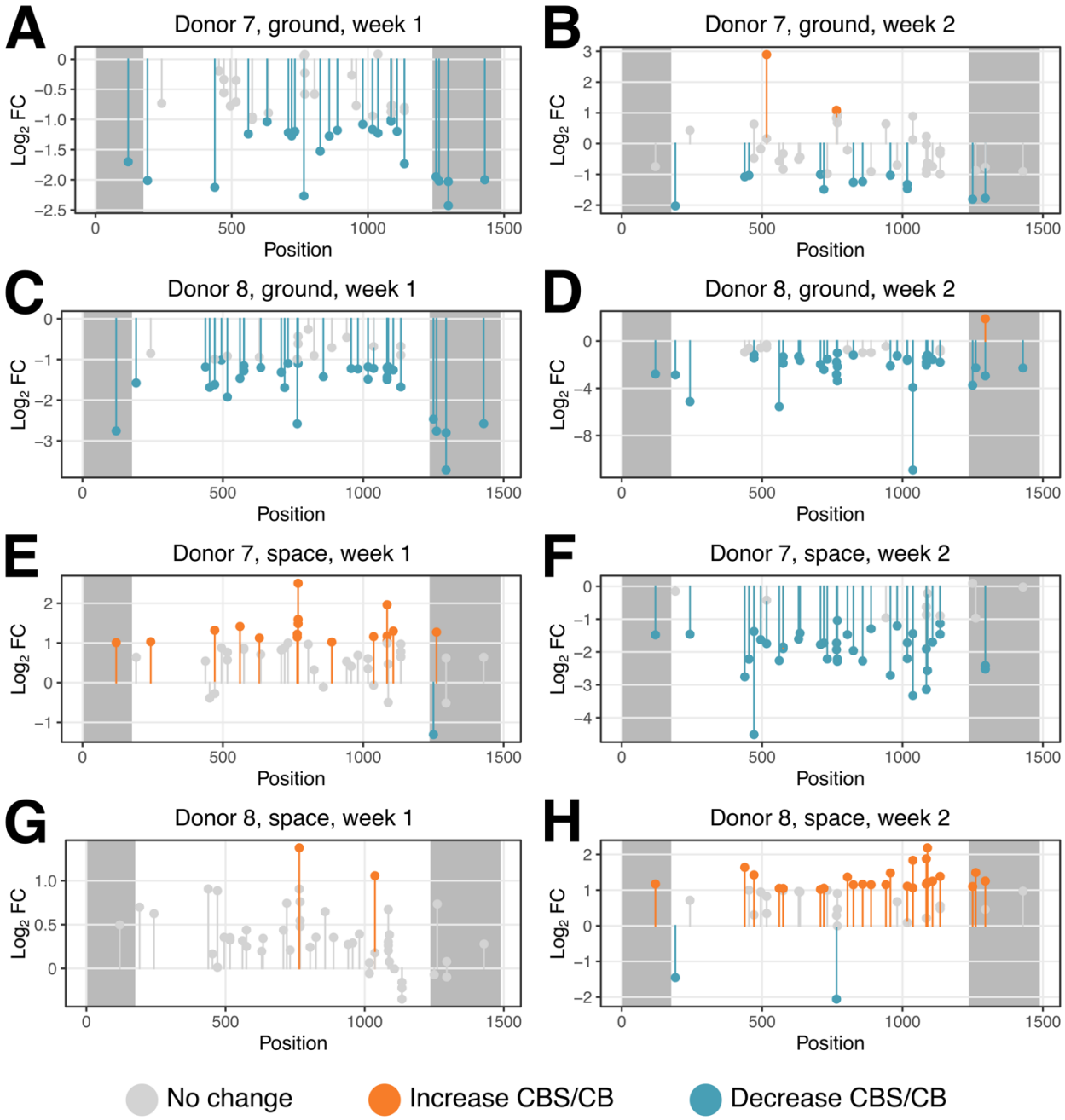

Figure A2.4: **Changes in media levels of collagen II peptides in CBS versus CB cultures on Earth and in space.** Log_2 fold change of cartilage/bone/synovium co-culture (CBS) treatment versus osteochondral control (CB) for peptides identified from collagen II. x-axis: residue position of first amino acid for each peptide. Orange: increase compared to control (log2 fold change > 1). Blue: decrease compared to control (log2 fold change < -1). Grey: no change compared to control. Positions of collagen II N- and C-terminal regions are highlighted in grey.

Donor	Age	Sex	Ground treatment			
			CB	CBS	CBSD	CBSDI
1	78	F	X	X	X	
2	34	M	X	X	X	
3	23	M	X	X	X	
4	66	F	X	X	X	X
5	49	F	X	X	X	X
6	69	F	X	X	X	X
7	31	M	X	X		X
8	47	F	X	X		X
9	34	F	X	X	X	X
10	49	M	X	X	X	X

Table A2.1. Donors used for ground control experiments. CB: cartilage and bone control. CBS: cartilage, bone, and synovial co-culture with mechanical injury. CBSD: CBS treatment with the addition of Dex only. CBSDI: CBS treatment with the addition of Dex and IGF-1.

Treatment	Location	Donor	
		7	8
CB	Ground	X	X
	Space	X	X
CBS	Ground	X	X
	Space	X	X
CBSDI	Ground	X	X
	Space	X	X
DI	Ground	X	X
	Space		X

Table A2.2. Experimental conditions for space versus ground comparisons. CB: cartilage and bone control. CBS: cartilage, bone, and synovial co-culture with mechanical injury. CBSDI: CBS treatment with the addition of Dex and IGF-1. DI: osteochondral explants treated with Dex and IGF-1. Issues with the microfluidic system for donor 7 treatment DI in space resulted in data not being collected for that treatment.

Donor	Week 1			Week 2				
	Up/ Up	Up/ Down	Down/ Up	Up/ Up	Up/ Down			Down/ Down
7	ACTN1	APP	AHSG	A1BG	ACTN1	ENO1	PDIA4	DLAT
	AMBP	CTSA	COL12A1	GLRX	AIFM1	ENO2	PDIA6	
	BASP1	CTTN	COL1A1	PFN1	AKR1A1	FKBP2	PEA15	
	COL15A1	DES	COL9A3	TNXB	AKR1B1	FSTL3	PGLS	
	COL18A1	DNPEP	HSPG2		ALDOA	GRB2	PPIA	
	CXCL8	FLNA	KLK9		ANXA6	GSTO1	PRG4	
	EFEMP1	GUSB	LOX		APOE	HDGF	PSAP	
	GNS	NID1	OMD		BPNT1	HMGA1	RBMX	
	GPX3	PABPC1	SCRG1		C1R	HNRNPA1	S100A10	
	ITIH1	PGM2	SPARC		C1S	HNRNPD	SEPTIN7	
	ITIH5	RRBP1			CAV1	HNRNPK	SIAE	
	MAP4	YWHAE			CCDC80	IGFBP3	SORBS2	
	MYL12B				CDV3	IGFBP4	SRSF1	
	NCL				CFD	LAMC1	SSBP1	
	NUCKS1				CLTB	LAMP2	STC1	
	PDIA6				CLTC	LXN	SUMO2	
	SORBS2				COL5A3	MAP1LC3A	TNFAIP6	
	SPAG9				COTL1	MARCKSL 1	TPI1	
	TAGLN				CSRP1	MDH2	TPM2	
	THBS4				CTSL	MFAP4	TPPP3	
	TNFAIP6				CXCL8	MYL12B	TXNDC5	
	TNXB				DES	MYL6	TXNRD1	
	TPPP3				EEF1G	NAMPT	YBX1	
	VCAN				EFEMP1	NENF	YWHAB	
					EIF4B	NUCKS1	YWHAE	
					EIF4H	PCBD1		

Table A2.3. Proteins with a large difference between the behavior in ground and space as well as a noticeable fold change from control with CBS treatment for donor 7. Proteins highlighted in **Figure A2.3** (panels **A** and **B**) are listed and categorized by their behavior on the ground versus the behavior in space (indicated by color and as "Ground/Space" behavior).

Donor	Week 1			Week 2			
	Up/ Up	Up/ Down	Down/ Up	Up/ Up	Up/ Down	Down/ Down	Down/ Up
8	BASP1	ALCAM	FBN1	CD9	CAPNS1	ALOX12B	BCAM
	COL14A1	ANXA11	LAMC1	COL15A1	CFD		CPE
	CXCL8	CFB	MVP	COL18A1	DLD		EEF1G
	DPYSL2	GUSB	PIP	COL6A2	GLRX		GNS
	EWSR1	PGM2	SCRG1	DPYSL2	LRP1		GRB2
	FBLN2	PSME2	SERPING1	GPX3	NUTF2		LAMC1
	FHL1	THBS2	XYLT1	NAMPT	PABPC1		LCP1
	GNPDA1	TPM1			SPTAN1		PTPA
	GPX3				SRI		SCRG1
	HNRNPU						TPM2
	IL6						UBE2L3
	MATN2						VCL
	NUCKS1						
	PCBD1						
	SORBS2						
	TAGLN						
	TNFAIP6						
	TPPP3						
	TPSAB1						

Table A2.4. Proteins with a large difference between the behavior in ground and space as well as a noticeable fold change from control with CBS treatment for donor 8. Proteins highlighted in **Figure A2.3** (panels **C** and **D**) are listed and categorized by their behavior on the ground versus the behavior in space (indicated by color and as "Ground/Space" behavior).

References

1. Black R, Grodzinsky AJ. Dexamethasone: Chondroprotective corticosteroid or catabolic killer? Eur Cells Mater. 2019;38:246–63.

2. Black RM, Wang Y, Struglics A, Lorenzo P, Tillgren V, Rydén M, et al. Proteomic analysis reveals dexamethasone rescues matrix breakdown but not anabolic dysregulation in a cartilage injury model. Osteoarthr Cartil Open. 2020;2:100099.

3. Li Y, Wang Y, Chubinskaya S, Schoeberl B, Florine E, Kopesky P, et al. Effects of insulin-like growth factor-1 and dexamethasone on cytokine-challenged cartilage: Relevance to post-traumatic osteoarthritis. Osteoarthr Cartil. 2015;23:266–74.

4. Chu CR, Andriacchi TP. Dance Between Biology, Mechanics, and Structure: A Systems- Based Approach to Developing Osteoarthritis Prevention Strategies. J Orthop Res. 2015;33:939–47.

5. Black RM, Wang Y, Struglics A, Lorenzo P, Chubinskaya S, Grodzinsky AJ, et al. Proteomic clustering reveals the kinetics of disease biomarkers in bovine and human models of post-traumatic osteoarthritis. Osteoarthr Cartil Open. 2021;3:100191.

6. Lieberthal J, Sambamurthy N, Scanzello CR. Inflammation in joint injury and post-traumatic osteoarthritis. Osteoarthritis and Cartilage. 2015. p. 1825–34.

7. Swärd P, Wang Y, Hansson M, Lohmander LS, Grodzinsky AJ, Struglics A. Coculture of bovine cartilage with synovium and fibrous joint capsule increases aggrecanase and matrix metalloproteinase activity. Arthritis Res Ther. 2017;19:1–12.

8. Weinstein RS. Glucocorticoid-induced csteoporosis and csteonecrosis. Endocrinol Metab Clin North Am. 2012;41:595–611.

9. Lu YCS, Evans CH, Grodzinsky AJ. Effects of short-term glucocorticoid treatment on changes in cartilage matrix degradation and chondrocyte gene expression induced by mechanical injury and inflammatory cytokines. Arthritis Res Ther. 2011;13:R142.

10. Injury Rate of Shuttle Astronauts. Longitud Study Astronaut Heal Newsl. NASA; 1999;8.

11. Ramachandran V, Dalal S, Scheuring RA, Jones JA. Musculoskeletal injuries in astronauts: Review of pre-flight, in-flight, post-flight, and extravehicular activity injuries. Curr Pathobiol Rep. 2018;6:149–58.

12. Scheuring RA, Mathers CH, Jones JA, Wear ML. Musculoskeletal injuries and minor trauma in space: Incidence and injury mechanisms in U.S. astronauts. Aviat Sp Environ Med. 2009;80:117–24.

13. Kandarpa K, Schneider V, Ganapathy K. Human health during space travel: An overview. Neurol India. 2019;67:S176–81.

14. Smith K, Mercuri J. Microgravity and radiation effects on astronaut intervertebral disc health. Aerosp Med Hum Perform. 2021;92:342–52.

15. Kerstman EL, Scheuring RA, Barnes MG, DeKorse TB, Saile LG. Space adaptation back pain: A retrospective study. Aviat Sp Environ Med. 2012;83:2–7.

16. Scheuring RA, Jones JA, Novak JD, Polk JD, Gillis DB, Schmid J, et al. The Apollo Medical Operations Project: Recommendations to improve crew health and performance for future exploration missions and lunar surface operations. Acta Astronaut. 2008;63:980–7.

17. Li Y, Frank E, Wang Y, Chubinskaya S, Huang H-H, Grodzinsky AJ. Moderate dynamic compression inhibits pro-catabolic response of cartilage to mechancial injury, TNF-alpha and IL-6, but accentuates degradation above a strain threshold. Osteoarthr Cartil. 2013;21:1–17.

18. Wang Y, Lorenzo P, Chubinskaya S, Grodzinsky AJ, Önnerfjord P. Dexamethasone treatment alters the response of human cartilage explants to inflammatory cytokines and mechanical injury as revealed by discovery

proteomics (Abstract). Osteoarthr Cartil. Elsevier; 2017;25:S381–2.

19. Dwivedi G, Flama L, Struglics A, Larsson S, Frank E, Chubinskaya S, et al. Markers of cartilage matrix degradation resulting from mechanical injury and inflammation were reduced with low dose dexamethasone treatment (Abstract). Trans 66th Orthopedic Research Society conference. Phoenix, AZ; 2020.

20. Lazar C, Gatto L, Ferro M, Bruley C, Burger T. Accounting for the multiple natures of missing values in label-free quantitative proteomics data sets to compare imputation strategies. J Proteome Res. 2016;15:1116–25.

21. Ritchie ME, Phipson B, Wu D, Hu Y, Law CW, Shi W, et al. Limma powers differential expression analyses for RNA-sequencing and microarray studies. Nucleic Acids Res. 2015;43:e47.

22. Subramanian A, Tamayo P, Mootha VK, Mukherjee S, Ebert BL, Gillette MA, et al. Gene set enrichment analysis: A knowledge-based approach for interpreting genome-wide expression profiles. Proc Natl Acad Sci U S A. 2005;102:15545–50.

23. Daly MJ, Patterson N, Mesirov JP, Golub TR, Tamayo P, Spiegelman B. PGC-1α-responsive genes involved in oxidative phosphorylation are coordinately downregulated in human diabetes. Nat Genet. 2003;34:267–73.

24. Szklarczyk D, Gable AL, Lyon D, Junge A, Wyder S, Huerta-Cepas J, et al. STRING v11: Protein-protein association networks with increased coverage, supporting functional discovery in genome-wide experimental datasets. Nucleic Acids Res. 2019;47:D607–13.

25. Chan MWY, Gomez-Aristizábal A, Mahomed N, Gandhi R, Viswanathan S. A tool for evaluating novel osteoarthritis therapies using multivariate analyses of human cartilage-synovium explant co-culture. Osteoarthr Cartil. 2022;30:147–59.

26. Kraus VB, Karsdal MA. Osteoarthritis: Current molecular biomarkers and the way forward. Calcif Tissue Int. Springer US; 2021;109:329–38.

27. Pollmann D, Siepmann S, Geppert R, Wernecke KD, Possinger K, Lüftner D. The amino-terminal propeptide (PINP) of type I collagen is a clinically valid indicator of bone turnover and extent of metastatic spread in osseous metastatic breast cancer. Anticancer Res. 2007;27:1853–62.

28. Seo WY, Kim JH, Baek DS, Kim SJ, Kang S, Yang WS, et al. Production of recombinant human procollagen type I C-terminal propeptide and establishment of a sandwich ELISA for quantification. Sci Rep. 2017;7.

29. Dwivedi G, Flaman L, Geischecke E, Rosen V, Chubinskaya S, Trippel SB, et al. Dexamethasone rescues chondrocyte viability and matrix degradation induced by injurious compression and exposure to inflammatory cytokines in a novel human cartilage-bone-synovium co-culture microphysiological system (Abstract). Trans 65th Orthopedic Research Society conference. Austin, TX; 2019.

30. Ruttkay-Nedecky B, Nejdl L, Gumulec J, Zitka O, Masarik M, Eckschlager T, et al. The role of metallothionein in oxidative stress. Int J Mol Sci. 2013;14:6044–66.

31. Karin M, Andersen RD, Slater E, Smith K, Herschman HR. Metallothionein mRNA induction in HeLa cells in response to zinc or dexamethasone is a primary induction response. Nature. 1980;286:295–7.

32. Tanaka N, Tsuno H, Ohashi S, Iwasawa M, Furukawa H, Kato T, et al. The attenuation of insulin-like growth factor signaling may be responsible for relative reduction in matrix synthesis in degenerated areas of osteoarthritic cartilage. BMC Musculoskelet Disord. 2021;22.

33. Lotz MK, Otsuki S, Grogan SP, Sah R, Terkeltaub R, D'Lima D. Cartilage cell clusters. Arthritis Rheum. 2010;62:2206–18.

34. Brink M, Lundquist A, Alexeyenko A, Lejon K, Rantapää-Dahlqvist S. Protein profiling and network enrichment analysis in individuals before and after the onset of rheumatoid arthritis. Arthritis Res Ther. 2019;21.

35. Ghadially FN, Lalonde JMA, Dick CE. A mechanism of formation of desmosome-like structures between synovial intimal cells. Experientia. 1978;34:1212–3.

36. Lin W, Zhu X, Gao L, Mao M, Gao D, Huang Z. Osteomodulin positively regulates osteogenesis through interaction with BMP2. Cell Death Dis. 2021;12.

37. Chang JC, Christiansen BA, Murugesh DK, Sebastian A, Hum NR, Collette NM, et al. SOST/Sclerostin improves posttraumatic osteoarthritis and inhibits MMP2/3 expression after injury. J Bone Miner Res. 2018;33:1105–13.

38. Eastell R, Hannon RA. Biochemical markers of bone turnover. In: Lobo RA, editor. Treatment of the Postmenopausal Woman (Third Edition): Basic and Clinical Aspects. Academic Press; 2007. p. 337–49.

39. Smeriglio P, Dhulipala L, Lai JH, Goodman SB, Dragoo JL, Smith RL, et al. Collagen VI enhances cartilage tissue generation by stimulating chondrocyte proliferation. Tissue Eng - Part A. 2015;21:840–9.

40. Bretaud S, Guillon E, Karppinen SM, Pihlajaniemi T, Ruggiero F. Collagen XV, a multifaceted multiplexin present across tissues and species. Matrix Biol Plus. 2020;6–7.

41. Pufe T, Petersen WJ, Miosge N, Goldring MB, Mentlein R, Varoga DJ, et al. Endostatin/collagen XVIII - an inhibitor of angiogenesis - is expressed in cartilage and fibrocartilage. Matrix Biol. 2004;23:267–76.

42. Sandell LJ, Aigner T. Articular cartilage and changes in arthritis: cell biology of osteoarthritis. Arthritis Res. 2001;3:107–13.

43. Jackson E, Shoemaker R, Larian N, Cassis L. Adipose tissue as a site of toxin accumulation. Compr Physiol. 2017;7:1085–135.

44. Thote AJ, Chappell JT, Gupta RB, Kumar R. Reduction in the initial-burst release by surface crosslinking of PLGA microparticles containing hydrophilic or hydrophobic drugs. Drug Dev Ind Pharm. 2005;31:43–57.

45. Pawlak Z, J. Kaldonski T, Gocman K, Kaldonski T, Yusuf K. Articular cartilage: hydrophilic and boundary layered lubrication mechanism with phospholipid - (lubricin, hyaluronan) participation. Clin Med Investig. 2019;5.

46. Tamer TM. Hyaluronan and synovial joint: function, distribution and healing. Interdiscip Toxicol. 2013;6:111–25.

47. Krishnan Y, Rees HA, Rossitto CP, Kim SE, Hung HHK, Frank EH, et al. Green fluorescent proteins engineered for cartilage-targeted drug delivery: Insights for transport into highly charged avascular tissues. Biomaterials. 2018;183:218–33.

48. Geiger BC, Wang S, Padera RF, Grodzinsky AJ, Hammond PT. Cartilage-penetrating nanocarriers improve delivery and efficacy of growth factor treatment of osteoarthritis. Sci Transl Med. 2018;10.

49. Bajpayee AG, Grodzinsky AJ. Cartilage-targeting drug delivery: Can electrostatic interactions help? Nat Rev Rheumatol. 2017;13:183–93.

50. Bajpayee AG, Scheu M, Grodzinsky AJ, Porter RM. A rabbit model demonstrates the influence of cartilage thickness on intra-articular drug delivery and retention within cartilage. J Orthop Res. 2015;33:660–7.